$$Specific\ productivity = 6.83 \cdot e^{-2.94 \cdot MN}$$

$$Specific\ activity = 46.58 \cdot K_{BDW}^{0.14}$$

Productivity

Predicting model — Influence

Influence — Predicting model

Morphology — Influence — Rheology

Predicting model

$$K_{BDW} = 4.12 \cdot 10^5 \cdot \left(2.5 \cdot 10^{-25}\right)^{MN}$$

# Cellular Morphology – A novel Process Parameter for the Cultivation of Eukaryotic Cells

## Thomas Wucherpfennig

**ibvt-Schriftenreihe**

Schriftenreihe des Institutes für Bioverfahrenstechnik
der Technischen Universität Braunschweig

Herausgegeben von Prof. Dr. Christoph Wittmann

**Band 70**

**Cuvillier-Verlag**
**Göttingen, Deutschland**

**Hinweis**: Obgleich alle Anstrengungen unternommen wurden, um richtige und aktuelle Angaben in diesem Werk zum Ausdruck zu bringen, übernehmen weder der Herausgeber, noch der Autor oder andere an der Arbeit beteiligten Personen eine Verantwortung für fehlerhafte Angaben oder deren Folgen. Eventuelle Berichtigungen können erst in der nächsten Auflage berücksichtigt werden.

# Cellular Morphology – A novel Process Parameter for the Cultivation of Eukaryotic Cells

Bei der Fakultät für Maschinenbau

der Technischen Universität Carolo-Wilhelmina zu Braunschweig

zur Erlangung der Würde

eines Doktor-Ingenieurs (Dr.-Ing.)

eingereichte Dissertation

von

Dipl.-Biotechnol. Thomas Wucherpfennig

aus

Erfurt

eingereicht am: 05.12.2012
mündliche Prüfung am: 15.02.2013

Prüfungsvorsitzender: Prof. Dr. Christoph Wittmann
1. Referent Prof. Dr. Rainer Krull
2. Referent Prof. Dr.-Ing. Arno Kwade

**2012**

All truths are easy to understand once they are discovered; the point is to discover them.

**Galileo Galilei**

Dedicated to my family

# Vorwort

Die vorliegende Arbeit entstand im Rahmen meiner Tätigkeit als wissenschaftlicher Mitarbeiter am Institut für Bioverfahrenstechnik der Technischen Universität Carolo-Wilhelmina zu Braunschweig im Teilprojekt B3 des Sonderforschungsbereiches SFB 578 „Integration gen- und verfahrenstechnischer Methoden zur Entwicklung biotechnologischer Prozesse – Vom Gen zum Produkt". Für meine Doktorarbeit bin ich sehr vielen Menschen einen herzlichen Dank schuldig. Besonders möchte ich mich bei meinem Doktorvater Prof. Rainer Krull bedanken, der mir sehr viel Vertrauen entgegen brachte und mich schon zu Studienzeiten unterstützt hat. Mit seiner Erfahrung, seinen fachspezifischen Fragen und Diskussionen über verschiedene Projekte hinaus trug er maßgeblich zum Gelingen dieser Arbeit bei.

Ein besonderes Wort des Dankes möchte ich auch an Herrn Prof. Christoph Wittmann richten, der mich freundlich am Institut aufgenommen hat und den Prüfungsvorsitz übernahm. Herrn Prof. a. D. Dr.-Ing. Dietmar C. Hempel danke ich für manch freundliche Diskussion im Zuge von diversen SFB 578 Zusammenkünften. Professor Arno Kwade danke ich für die Übernahme des Co-Referates.

Weiterhin möchte ich mich bei Kai Schütte, Matthias Pump und Dominik Sieblitz von der Phyton Biotech GmbH für die hervorragende Zusammenarbeit während des Projektes und der stets sehr freundlichen Aufnahme in Ahrensburg bedanken. Bei Dr. Gabriel Corkidi Blanco und Jaime Arturo Pimentel Cabrera möchte ich mich für die schöne Zeit an der UNAM in Mexico und die Hilfe bei der Entwicklung des Bildanalyseprogramms zur Viabilität von *Taxus* Zellen bedanken. Frau Dr.-Ing. Becky Sommer gebührt mein Dank für erste Arbeiten auf dem Gebiet der Viabilitätstests von Pflanzenzellen und die CLSM-Aufnahmen der *Taxus* Zellen.

Meinem Bürokollegen Dr.-Ing. Manely Eslahpazir danke ich für die tolle fortlaufende Unterstützung, die zahlreichen fachlichen, theoretischen Diskussionen und seine Freundschaft.

Jan-Hendrik Sachs danke ich für die erste gemeinsame Zeit am ibvt welche die Eingewöhnung deutlich erleichterte. Besonders die gemeinsame Übungsbetreuung, wo auch manchmal Rohre verlegt wurden, bleibt im Gedächtnis.

Bei Deborah Gernat möchte ich mich für erste Experimente zum Einfluss der Osmolalität auf die pilzliche Morphologie bedanken, welche im Zuge ihrer Bachelorarbeit entstanden.

Judith Mönch-Tegeder möchte ich für die wissenschaftlichen Arbeiten zum Zusammenhang zwischen Natrium/Kalium-Verhältnis im Medium und der *A. niger* Morphologie sowie die freundschaftliche Unterstützung während meiner gesamten Zeit in Braunschweig danken. Unvergessen bleibt unsere New York Reise mit Komplikationen.

Timo Hestler danke ich für die hervorragende Laborarbeit und die Unterstützung bei der Entwicklung der Morphologie Kennzahl. Antonia Lakowitz möchte ich für die herausragende Zusammenarbeit während Ihrer Bachelorarbeit, besonders beim Zusammenhang zwischen Sporenkonzentration und Morphologie, danken. Der Filmdreh kurz vor Weihnachten 2011 wird uns wohl für immer im Gedächtnis bleiben. Martin Kampa danke ich für seine tollen Arbeiten auf dem Gebiet der Bild-Akquisition und der Makro-Entwicklung.

Weiterhin möchte ich Jana Schilling und Annika Schulz danken, die durch ihre hervorragenden Bachelor und Masterarbeiten dem Phyton-Projekt wesentliche Anregungen, besonders auf dem Gebiet der Viabilitätsassays von Pflanzenzellen, geben konnten.

Meinen studentischen Mitarbeitern Oliver Schwich, Jan-Michael Blum, Felix Krujatz, Johannes Rebelein und Jakob Gabrielczyk danke ich herzlich für die tolle Unterstützung bei Labor- und Computerarbeit.

Allen Mitarbeitern des ibvts in Braunschweig danke ich für die sehr freundliche Aufnahme und die gute Zusammenarbeit während meiner gesamten Promotionszeit.

Mein großer und besonderer Dank gilt meinen Eltern, ohne die das Studium und die Doktorarbeit niemals möglich gewesen wären. Sie haben immer an mich geglaubt, mich fortwährend unterstützt und mich durch ihr großes Interesse an meiner Arbeit motiviert. Ohne die uneingeschränkte seelische und moralische Unterstützung meiner Frau Miriam hätte ich die Zeit und den Stress nicht überstehen können. Sie war immer für mich da und hat mir gemeinsam mit unserer Tochter Tabea Marie stets einen sicheren Rückhalt und ausreichende Ablenkung von der Wissenschaft gegeben.

# Publications

Partial results of this work have been published in advance. This was authorized by the Institute of Biochemical Engineering represented by Prof. Dr. Krull and Prof. Dr. Christoph Wittmann:

## Peer-reviewed Journals

**Wucherpfennig T**, Lakowitz A, Krull R (2013). Comprehension of viscous morphology - Evaluation of fractal and conventional parameters for rheological characterization of *Aspergillus niger* culture. J. Biotechnol. 163(2):124-32.

Krull R, **Wucherpfennig T**, Eslahpazir Esfandabadi M, Walisko R, Melzer G, Hempel DC, Kampen I, Kwade A, Wittmann C (2013). Characterization and control of fungal morphology for improved production performance in biotechnology. J. Biotechnol. 163(2):112-23.

Eslahpazir Esfandabadi M, **Wucherpfennig T**, and Krull R (2012). Agitation Induced Mechanical Stress in Stirred Tank Bioreactors-Linking CFD Simulations to Fungal Morphology. J. Chem. Eng. Jpn., 45(9): p. 742-748.

**Wucherpfennig T**, Lakowitz A, Driouch H, Krull R, Wittmann C (2013). Customization of *Aspergillus niger* Morphology Through Addition of Talc Micro Particles. J. Vis. Exp. 61.

**Wucherpfennig T**, Schilling JV, Sieblitz D, Pump M, Schütte K, Wittmann C, Krull R (2012). Improved assessment of aggregate size in *Taxus* plant cell suspension cultures using laser diffraction. Eng. Life Sci. 12:595-602.

Driouch H, Hänsch R, **Wucherpfennig T**, Krull R, Wittmann C (2011). Improved enzyme production by superior bio-pellets of *Aspergillus niger* - Targeted morphology engineering using titanate micro particles. Biotechnol. Bioeng. 109:462-471.

**Wucherpfennig T**, Hestler T, Krull R (2011). Morphology engineering – Osmolality and its effect on *Aspergillus niger* morphology and productivity. Microbial Cell Factories 10:58

## Books

**Wucherpfennig T**, Kiep K A, Driouch H, Wittmann C, Krull R (2010) Morphology and rheology in filamentous cultivations. In: Advances in Applied Microbiology, Vol. 72, Chapter 4, Laskin, A. I., Sariaslani, S., Gadd, G. M. (eds.), ISBN: 978-0-12-380989-6, Academic Press 72, 89-133, Elsevier

**Conference contributions**

**Wucherpfennig T**, Lakowitz A, Krull R (2012) Korrelation von Viskosität und Morphologie filamentöser Pilzkultivierungen mittels automatischer Bildanalyse, 30. DECHEMA-Jahrestagung der Biotechnologen und ProcessNet-Jahrestagung, 10.09.2012 - 13.09.2012 Karlsruhe (Poster)

Krull R, **Wucherpfennig T**, Eslahpazir M, Pump M, Sieblitz D, Schütte K, Wittmann C (2012) Produktion therapeutischer Wirkstoffe mit Pflanzenzellsuspensionskulturen Kopplung von Scherstress und Aggregatgröße zur Prozessoptimierung, GVC/DECHEMA Vortrags- und Diskussionstagung „Biopharmazeutische Produktion". 14.-16. May 2012. Freiburg (Presentation)

Eslahpazir M, **Wucherpfennig T**, Krull R (2012) Assessment of sliding grid interface in CFD-simulations of stirred tank bioreactors with multiple stirring systems. Jahrestreffen der Fachgruppen Mehrphasenströmungen und Mischvorgänge, Weimar, March 2012.

Eslahpazir M, **Wucherpfennig T** and Krull R (2011) A numerical approach on characterization of mechanical stress in stirred tank bioreactors. In: Fortschritt-Berichte VDI, Reihe 3 Verfahrenstechnik, Nr. 929, 6th International Berlin Workshop - IBW6 on Transport Phenomena with Moving Boundaries, Berlin, November 2011 (F.P. Schindler, M. Kraume (Eds.), VDI-Verlag, Düsseldorf 2012, 98 -108. (Presentation)

Eslahpazir M, **Wucherpfennig T**, Krull R (2011) Agitation induced mechanical stress in stirred tank bioreactors - linking CFD-simulations to fungal morphology 1st International Symposium on Multiscale Multiphase Process Engineering (MMPE), Proc. P39-1-5, Kanazawa, Japan, October 2011. (Poster)

**Wucherpfennig T**, Driouch H, Roth A, Dersch P, Wittmann C (2011) Systems Biotechnology for Production of Recombinant Proteins by *Aspergillus niger*. „1st European Congress of Applied Biotechnology-Together with DECHEMA's Biotechnology Annual Meeting''. 25. -29. September 2011. Berlin (Presentation)

**Wucherpfennig T**, Hestler T, Krull R (2011) Morphology engineering - customization of *Aspergillus niger* morphology by addition of sodium chloride. „1st European Congress of Applied Biotechnology-Together with DECHEMA's Biotechnology Annual Meeting''. 25. -29. September 2011. Berlin (Poster)

# Table of contents

12

# Abstract

In biotechnological processes the morphology of eukaryotic cells has been often recognized as being process relevant as it can be a determinant of productivity or provide information about cell age and viability. For morphologically very complex filamentous microorganisms, like *Aspergillus niger*, specific morphologic phenotypes have been revealed to correlate with maximum process performance. The complex morphology of this fungus comprises dense spherical pellets as well as viscous elongated filaments, depending on culture conditions. The exhibited morphology has tremendous effect on the overall process performance, making a precise understanding of fungal growth and morphology indispensable. Through the introduction of the versatile Morphology number (MN), this study provides the means for a desirable characterization of fungal morphology and makes it possible to quantify the interrelation between morphology, productivity and rheology in form of mathematical models. Thus, morphology as quantified by the Morphology number (MN) was demonstrated to be an important process parameter for the cultivation of *A. niger* SKAn 1015, because detailed morphologic information allowed the estimation of productivity and rheological properties of the cultivation broth. Moreover, fractal parameters were also found to enable a comprehensive description of fungal morphology. The presented fractal quotient ($D_{BM}/D_{BS}$) and lacunarity ($\Lambda$) were suitable tools for morphological characterization. A precise characterization, however, is only the first step towards a desired customization of fungal morphology. Besides micro particles, which were introduced just recently, osmolality was found in this study to be a useful parameter to adjust and customize *A. niger* morphology. Osmolality might provide a cheap and reliable approach to increase the productivity in industrial processes.

For the commercially established process of paclitaxel production with *Taxus* plant cell culture, the size of plant cell aggregates has been often acknowledged as an intangible parameter, which might be responsible for general variability in plant cell culture processes. In this study a novel method of aggregate size determination via laser diffraction was introduced and found to be exceptionally eligible for industrial application, since it provides a practicable, rapid, robust and reproducible way to sample large amounts of material. The Alamar Blue assay, newly introduced for *Taxus* cells, was found to be exceptional eligible for viability estimation in industrial processes. Moreover, aggregate coloration, as a morphologic attribute, could also be identified as a good indicator of viability. Generally, morphology was identified as an important parameter for both industrially relevant eukaryotic model processes.

# Zusammenfassung

In vielen biotechnologischen Prozessen mit eukaryotischen Zellen stellt die Morphologie einen Prozessparameter maßgeblicher Wichtigkeit dar, da er Rückschlüsse auf die Produktivität des Prozesses und die Viabilität des biologischen Systems erlaubt. In dieser Arbeit diente der filamentös wachsende Pilz *Aspergillus niger* als Modellorganismus, um den Einfluss der Morphologie auf die Produktivität des Kultivierungsprozesses quantitativ zu erfassen. Dieser Pilz ist einer der meistgenutzten Wirtsorganismen mit einer Vielzahl biotechnologischer Anwendungen. Im Gegensatz zu Hefen oder Säugerzellen weisen filamentös wachsende Pilzkulturen allerdings eine sehr komplexe Morphologie auf, die von kompakten Biopellets bis hin zu einem viskosen Hyphengeflecht, je nach eingestellten Kultivierungsbedingungen, reichen kann. In dieser Arbeit wurden Methoden der automatischen Bildanalyse entwickelt, um das gesamte Morphologiespektrum von *A. niger* zu charakterisieren. Parameter aus der Partikelformanalyse wurden zur dimensionslosen Morphologie-Kennzahl (MN) kombiniert. Weiterhin wurden nicht-euklidische Parameter wie der neu eingeführte Fraktal-Quotient und die Lakunarität erstmalig zur Morphologiecharakterisierung filamentöser Systeme angewandt. Mit Hilfe dieser Kennzahlen konnte ein eindeutiger mathematischer Zusammenhang zwischen der Morphologie des Pilzes und verschiedenen auf dem Ostwald-de Waele-Ansatz basierenden rheologischen Parametern abgeleitet werden. Weiterhin konnte gezeigt werden, dass die Produktion des homologen Enzyms Fructofuranosidase eindeutig mit seiner Morphologie korreliert. Um die optimale Morphologie für einen biotechnologischen Prozess einzustellen, wurde in dieser Arbeit, die Variation der Osmolalität des Kultivierungsmediums, ein neuartiger Prozessparameter zur maßgeschneiderten Morphologie-einstellung am Modellorganismus *A. niger* näher untersucht. Die Ergebnisse zeigen, dass die Erhöhung der Medienosmolalität eine geeignete und kostengünstige Methode darstellt, um die Produktivität vieler biotechnologischer Prozesse gezielt zu erhöhen.

Für einen zweiten Modellprozess, der kommerziell realisierten Pacliataxelherstellung mit *Taxus*-Kulturen, wurde die Größe der Pflanzenzellaggregate schon oft als wichtiger, aber schwer zu erfassender Parameter beschrieben. In dieser Studie wurde eine neue Methode entwickelt, um die Aggregatgröße mittels Laserbeugung online zu bestimmen. Diese Methode ist besonders für die industrielle Anwendung prädestiniert, da große Probenmengen in kurzer Zeit reproduzierbar vermessen werden können. Im Weiteren, wurde der „Almar Blue"-Viabilitätstest für die produktionsbegleitende Viabilitätsbestimmung von *Taxus*-Zellen etabliert. Hierbei wurde das morphologische Merkmal der Aggregatfärbung als zusätzlicher Indikator für die Lebensfähigkeit identifiziert.

# 1 Introduction

## 1.1 The concept of morphology and its use as a bioprocess parameter

The concept of morphology was first introduced by Johann Wolfgang von Goethe for description and differentiation of natural entities such as leaves [1]. The word originates from the Greek word "morphe" meaning *form* and "logos" translating to *word* or *research*. Transitional morphological forms were used by Goethe as a means of tracing identity, particularly in botany were morphologic appearance is most important for identification and naming [2]. Since then, morphology has been accepted as a general term for description of the outward appearance of an object and is considered to have two major aspects, shape and surface texture [3]. Color, pattern and size are also often used morphological characteristics. Shape is the expression of external morphology and for some is synonymous with form. However, these termini are regularly confused with each other [4]. Shape is a fundamental property of all objects, but it remains one of the most difficult to characterize and quantify for all but the very simplest of shapes [3]. Outward appearance can seldom be described by discrete morphological attributes; many of the morphological descriptors used routinely represent imprecise variables, such as long, short, large or irregular, which are often used in an ambiguous manner [5]. Techniques of geometric morphometrics, in contrast, are able to describe shapes accurately by mathematical geometry in terms of form, roundness, irregularity and sphericity. A more accurate characterization of shape also leads to more potential sources of morphological variation available for analysis [5].

In biotechnological processes the morphology of cells or microorganisms has been often recognized as being important, because general conditions of many organisms can be judged by their appearance. For mammalian cells, for example, cell size has been recognized as a major determinant of productivity [6]. For plant cells in suspension aggregate size has been acknowledged as an important process parameter [7], whereas the coloration of cells was shown to provide an indication on cell age and viability [8]. For morphologicalyl very complex filamentous microorganisms like *Aspergillus niger*, specific morphologic phenotypes have been revealed to correlate with maximum process performance [9]. Most data, however, is based on observation and appearance. Since an accurate quantification of morphology is mostly non-existent, it is hard to incorporate morphological data into existing process models. To be of value as a process parameter, an accurate quantification has to be established. Quantified morphological information can be used to build morphologically structured models of predictive value [9].

The use of computer-assisted automatic image analytic systems combined with geometric morphometrics has already been shown to be an invaluable tool for characterization of complex relationships between morphology and productivity. New models of morphology and process performance will lead to improved design and operation for eukaryotic cultivations, and will help to transfer laboratory models into industrial practice.

## 1.2 Objectives

One of the main aims of this thesis was to elucidate the relationship between morphology and process performance for two industrially relevant eukaryotic model processes: the production of fructofuranosidase with the filamentous fungus *Aspergillus niger* and the synthesis of paclitaxel with *Taxus chinensis* plant cell cultures. The first and foremost goal was the development and evaluation of novel methods for characterization and quantification of fungal morphology, based on microscopy and automatic image analytic techniques. A further objective was the assessment of additional tools for adjustment and customization of *A. niger* morphology, besides the already established method of micro particle supplementation [10-14].

Using established parameters for detailed morphologic description and new tools for morphologic adjustment, the investigation of the relationship between fungal morphology and productivity was a major focus. Furthermore, fungal morphology was to be correlated with rheological culture broth characteristics. All these findings were to be used to demonstrate the connection between morphology, rheology and productivity.

For the industrially established process of paclitaxel production by submerse cultivation of *Taxus chinensis* plant cells, a reliable and applicable way to measure aggregate size was to be determined and evaluated. Moreover, the connection between aggregate color and cell viability was an aspect for investigation. To achieve this goal, a reliable molecular assay for viability estimation had to be introduced first.

# 2 Theoretical Background

## 2.1 Cultivation of filamentous Mircoorganisms

Due to their metabolic diversity, high production capacity, secretion efficiency, and capability of carrying out post-translational modifications, filamentous fungi are widely exploited as efficient cell-factories in the production of metabolites, bioactive substances and native or heterologous proteins, respectively. The commercial use of fungal microorganisms is reported for multiple sectors such as detergent industry, food and beverage industry, and pharmaceutical industry [9, 15-17]. However, one of the outstanding, and unfortunately, often problematic characteristics of filamentous fungi is their morphology, which is much more complex than that of unicellular bacteria and yeasts in submerged culture [13]. Depending on the desired product, the optimal morphology for a given bioprocess varies [18]. Optimal productivity correlates with a specific morphological form [14, 19, 20].

### 2.1.1 Filamentous fungus Aspergillus niger *and the model product fructofuranosidase*

The filamentous fungus *Aspergillus niger,* the black mold, belongs to the division Ascomycota, defined by the ascus (from the greek word "sac"), which is formed as microscopical sexual structure by spores by some of its members. The Ascomycota are the largest phylum of fungi, with over 64,000 species, which may be either single-celled (yeasts), filamentous (hyphal) or both (dimorphic) [21]. Most ascomycetes grow as mycelia and can form conidospores; they are able to reproduce in sexual and non-sexual form. Some molds, like *A. niger,* can only reproduce asexually, do not have a sexual cycle, and do not form asci [21]. For *A. niger,* asexual reproduction occurs through the dispersal of conidia, produced from fruiting bodies termed conidiophores, the morphology of which can vary extensively from species to species [21].

The genus *Aspergillus* comprises about 250 species [22], including important industrially used species (*A. niger, A. oryzae, A. awamori, A. sojae, A. terreus*) and pathogenic and potentially harmful species (e.g. *A. fumigatus, A. parasiticus, A. flavus*) [23]. In their natural habitat, the soil, *Aspergilli* form a mycelial network of hyphae. They degrade an abundance of organic material, which is broken down into low-molecular-weight compounds which can be used as nutrients. The degradation is achieved by secretion of several hydrolytic enzymes, which are able to break down macromolecules like sucrose, starch, pectin, cellulose or even lignin [24].

*Aspergilli* can grow at a wide range of temperatures (10–50 °C), pH (2.0–11.0), and osmolarity (from nearly pure water up to 34% salt) [25], and are able to excrete large amounts of metabolites, e.g. up to 200 g L$^{-1}$ of citric acid into the culture medium [26]. As eukaryotic organisms, *Aspergilli* offer valuable advantages for enzyme secretion, such as facilitated proteolytic processing and protein folding as well as posttranslational modifications [16]. Furthermore, the genus can be used for solid-state or submerged fermentations and respective fermentation protocols have been established for large-scale industrial processes [23]. *Aspergilli* have been used for food production and beverage processes for more than 1,500 years [27]. *A. niger*, especially, stands out as a very attractive host for the biotechnology industry, partly due to its GRAS status (generally regarded as safe) issued by the American Food and Drug Administration (FDA). Industrial strains can secrete large quantities of many economically desired products, e.g. 25 g/L cephalosporin, 20 g/L glucoamylase, 40 g/L cellulase and 50 g/L penicillin [9, 28, 29]. Because of the progressing development of genetic engineering and efficient expression systems, *Aspergillus* species are also starting to receive attention as a host for the production of heterologous proteins [30].

In the current study the enzyme β-fructofuranosidase (EC 3.2.1.26) was produced. Fructofuranosidase is used industrially in the confectionery and food industry for the production of inverted sugar. The substrate sucrose is converted by specific cleavage of the β-1,2-glycosidic bond between the monosaccharaides glucose and fructose [31, 32]. The enzyme also has a fructosyltransferase function through which higher molecular sugars, so called fructooligosaccharides (FOS) can be formed [32-34]. All oligosaccharides from D-fructose molecules with β-(2-1)-glycosidic bonds and a terminal glucose residue are called FOS [34]. For the food industry, FOS are of interest mainly as nutritional supplements and alternative sweeteners [34, 35]. They are only a third as sweet as sucrose and cannot be digested by human digestive enzymes, making them calorie-free [34-36]. FOS also promote the growth and activity of symbiotic gut bacteria, reduce levels of cholesterol, phospholipids and triglycerides in the blood, strengthen the immune system and thus have a positive impact on general health [33-37]. Fructooligosaccharides have also been proven to reduce risk of colorectal cancer, thus a future application of FOS as a complementary strategy in the prevention and treatment of colorectal cancer is feasible [37-39]. These functional properties make FOS interesting for the pharmaceutical industry, as prebiotic food components, for the production of functional foods or as therapeutics [33, 35].

Currently, the market value of fructooligosaccharides is at U.S. $ 200 per kilogram, with applications in prebiotic products which are already commercially available, in the pharmaceutical

and diagnostic sector [35, 37, 40]. In the future, custom made FOSs might even increase the application potential. These could be enzymatically-produced sucrose analogues in which, for example in place of the glucose, the sugars mannose, galactose, or xylose are linked to fructose. The resulting novel, customized FOS may be of interest due to their properties for various industries and applications [37]. Compared to other strains, the *A. niger* strain SKAn 1015, used in this study, is sufficiently more productive to be interesting for industrial applications [37].

### 2.1.2 *Growth and morphology of* A. niger

In submerged cultivation two distinct growth forms of *A. niger* can be observed, the mycelial and the pelleted form [41-43]. Pellets are characterized by the mycelia developing into stable, spherical aggregates consisting of a more or less dense, branched and partially intertwined network of hyphae [43-45]. The morphological form which is adopted is a subject of considerable interest, due to the direct and indirect impact of morphology on produced metabolites [9, 46]. Moreover, process characteristics will often vary most significantly between the myriad morphological growth forms which are formed by the filamentous microorganism during submerged cultivation (**Figure 2.1**).
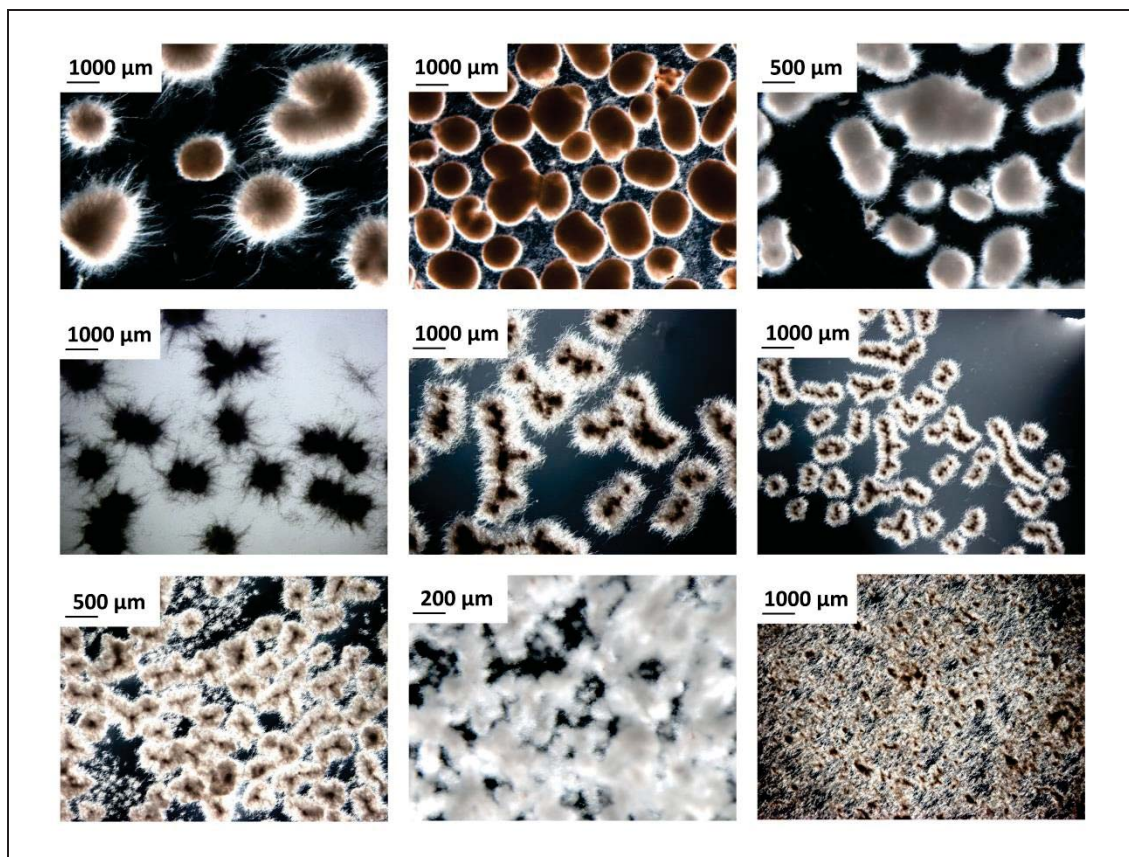


**Figure 2.1:** Morphologic diversity of filamentous fungus *A. niger* SKAn 1015 in submerged bioreactor cultivation.

At times, a pellet type of morphology is preferred in industrial cultivations and in downstream processing because of the non-viscous rheology of the broth [45, 47]. Pellet growth seems favourable for production of citric acid [9, 48], glucose oxidase [49], glucoamylase [50], or polygalacturonidase [51]. In these cultivations the mass transfer of oxygen and nutrients is considerably better, and the subsequent separation of the pellets from the cultivation broth is simpler than in mycelial cultivations [52]. Easy agitation and aeration ensure low operating costs, because much lower power input is needed [53]. Although the heat and mass transfer within the bioreactor is not limited, concentration gradients within the pellet result in a depletion of nutrients, especially oxygen, in the central region of the pellets [54]. However, the freely dispersed mycelium in submerged cultures of fungi has become very popular recently, due to the fact that this morphology enhances growth and production. The mycelial growth is preferred for the formation of fumaric acid or amylase [18].

Recently, studies have identified many interesting metabolites associated with mycelial growth exhibiting biological activities, including antitumour, anti-inflammatory and cytotoxicity to hepatoma cells [55]. Mycelial biomass can also be used for the biotransformation of steroids, where it facilitates downstream processing, the production of enzymes such as amylase, neo-fructosyltransferase and phytase [56], or penicillin [57].

In general mycelial growth as well as pellet growth increases the viscosity of the cultivation medium [58]. However, filamentous growth causes much higher viscosities than pelleted growth, which results in temperature and concentration gradients within the bioreactor as a result of transfer limitations [9, 59, 60]. Fungal morphology in general is of interest, because it influences not only the productivity of the process, but through its impact on rheology it also has an influence on mixing and mass transfer within the bioreactor. To ensure high protein secretion and at the same time a low viscosity of the cultivation broth, it is desired by the industry to tailor-make the morphology of filamentous fungi [46].

The morphological type and the related physiology strongly depend on environmental conditions in the bioreactor [60], which can be controlled by regulation of the process parameters. These variable environmental conditions are nowadays often summarized under the term environome, including parameters such as inoculum concentration and spore viability, pH value, temperature, dissolved oxygen concentration, as well as aeration and stirring induced mechanical stress [61].
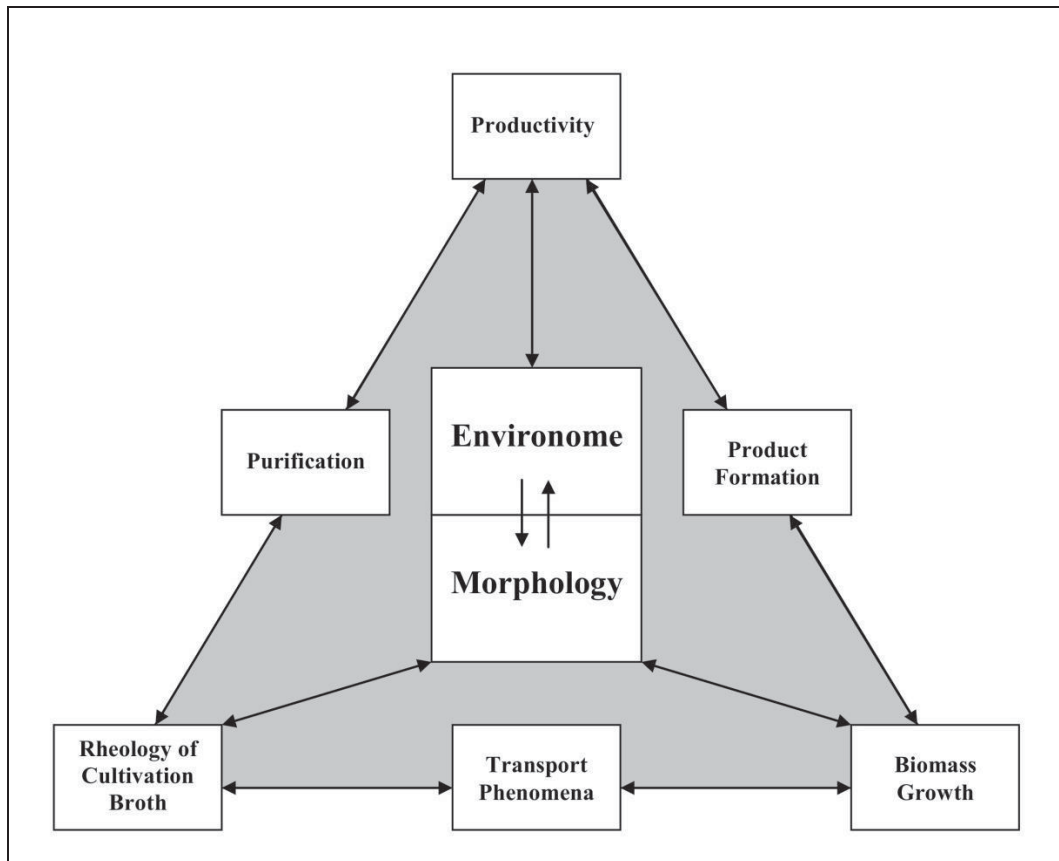
**Figure 2.2:** Schematic illustration of a biotechnological process, with the main parameters environome and morphology in the center, and the productivity, to be optimized, to the top of the triangle

**Figure 2.2** illustrates a biotechnological process of filamentous organisms, with the morphology of the biological system influenced by the environome. Morphology and environome as main process parameters are located in the centre of the triangle, as they have an influence on all environmental parameters. Productivity is placed on the top of the triangle, because it is the central parameter to be optimized. Broth rheology and biomass growth form the base, completing the triangle. All environmental parameters on the side of the equilateral triangle have an influence on each other. Broth rheology causes mixing problems, influencing transport phenomena, which in turn may lead to maintenance problems inhibiting cell growth. Product formation is closely related to biomass growth, as the product is thought to be mainly expressed at the tips of the hyphae. An optimized growth leads to an extensive product formation and therefore a high productivity. Furthermore, the rheology of the broth has an impact on the purification of the product, as high viscosities complicate the recovery. A laborious and expensive purification procedure in turn leads to an uneconomical overall production process.

The study of fungal morphology and the development of a thorough understanding of environmental variables which result in structural variation are therefore a key target in the optimization of cultivation processes with *A. niger* [21]. Growth of filamentous fungi can be

21

generally differentiated into micro- and macroscopic morphology [19]. In submerged cultivations, the observed macroscopic morphology of filamentous fungi varies from freely dispersed mycelium over loose mycelial clumps to dense pellets (**Figure 2.3**) [9, 62]

First approaches to describe fungal morphology from microscopic images have been made by Metz and Kossen [63]. Characterization of fungal microscopic morphology in the early phase of cultivation can be described by the average and total hyphal length, which is obtained by the sum of all hyphal length in a mycelium, the number of tips and the branching of individual hyphae [63, 64]. Depending on the strain properties and chosen cultivation conditions, i.e. inoculum properties, pH, mechanical stress, cultivation temperature, medium composition, osmolality or process mode the final macromorphology is determined [9, 52, 60, 62, 65].
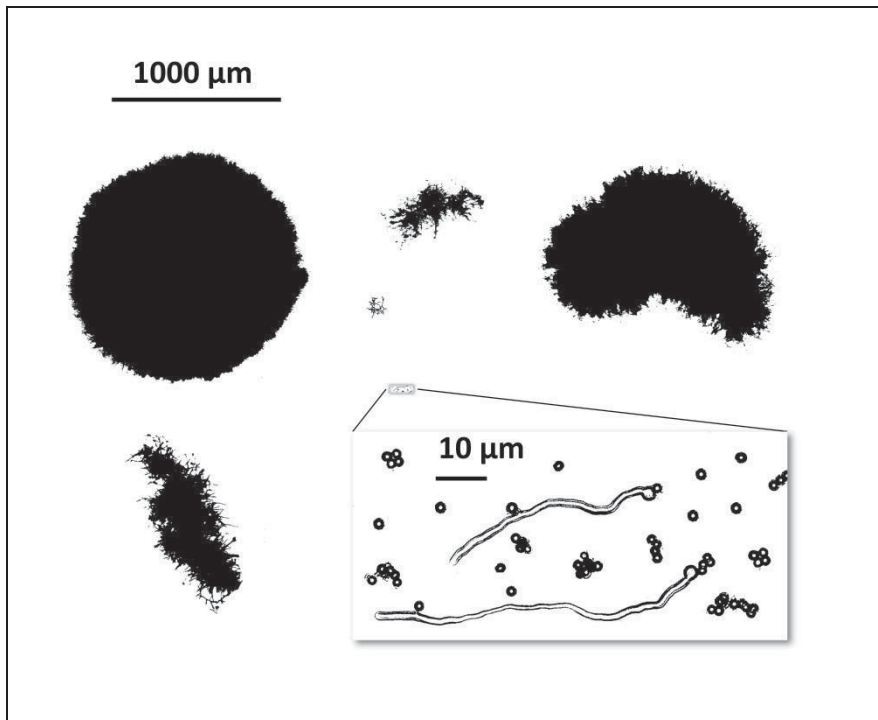


**Figure 2.3:** Different morphological growth forms with original dimension of *A. niger* SKAn 1015 found in submerged cultivation. Pellet structures originate from germinated spores and spore packages.

Fungal micromorphology covers events of fungal growth and development on a microscopic scale and involves cell wall structure of the hyphae, tip extension, septum formation and branching [59, 66]. Fungal growth begins with one or more spores which remain dormant until nutrients necessary for activation are supplied. Germination initiates by a swelling process during which lots of water is taken up, spores start to extend in an isotropic manner, and single germ-tube emerges [67-69]. Growth of the hyphae is polarized, with a linear extension rate at the hyphal apex. Along the length of the hypha, precursors for the cell wall as well as proteins, involved in cell wall synthesis, are transported in vesicles from the endoplasmatic reticulum (ER) to the hyphal tip. As a

result of its gradient distribution the ER network supports the directed transport of the vesicles to the tip [70, 71] where they accumulate as the so-called Spitzenkörper. The Spitzenkörper determines the tubular shape [72], as well as the growth rate and direction of the hyphal cell [46, 73].

After an initial acceleration phase the hyphae continues to grow with the maximal growth rate, while vesicle transport, with its constant velocity, is likely to be the limiting step of elongation [29, 74]. Septation of the hyphae is linked to further growth and nuclear division. In *Aspergillus nidulans* the first septum, dividing the hyphae into apical and subapical compartments, is formed when the germ tube contains eight nuclei due to several rounds of cell division [29, 75]. The apical compartment, located at the very hyphal tip, is able to exchange cytoplasm with the subapical compartment through the septum [76]. Subapical compartments are constant in length and contain three to four nuclei [77]. In contrast, the quantity of nuclei and length differs in apical compartments based on mitotic cycles and active growth [77]. With continued elongation, further septae are formed, and an apical compartment becomes a subapical one, while the subapical one transforms into a hyphal compartment [76]. Due to an accumulation and excess of transport vesicles, which cannot pass a septum, branching occurs in subapical compartments [74, 78], which then resume growth and nuclear division cycles [66, 77]. Farther away from the apex, hyphal compartments are highly vacuolized and not involved in growth [46, 77, 79]. These compartments contain larger vacuoles with further distance from the apex and display a different metabolism compared to the apical and subapical zones of the hyphae [76, 80].

With increasing cell age, vacuolization advances until, finally, autolysis occurs [81]. The differentiation of the hyphal cell in compartments with different metabolic activities leads to production of secondary metabolites in the growth-arrested parts of the cell, while growth-associated proteins are synthesized in the active compartments [46, 79, 80].

When a hyphal element has grown up to a certain length a branch is formed laterally to the parent [65]. The length of a hyphal element between two branching points is referred to as the hyphal growth unit (HGU) [82], which is approximately equal to the total hyphal length divided by the total number of tips [65]. Low values of the HGU indicate an increased number of growing tips in the mycelium [78]. This might be preferred in industrial production processes, as secretion is primarily related to the apical zone of the hypha at the sites of cell wall synthesis [23, 46, 83-87], which is assumed to contain larger pores due to plasticity of the cell wall [81]. However, other studies have found no correlation between the number of tips and protein secretion [88].

Micromorphologic growth, in general, can be characterized by the total average hyphal length (the sum of all single hyphal length in the mycelium), hyphal diameter, number of tips as well as tip extension, and branching rate of individual hyphae [59, 64, 66, 89, 90]. The overall mycelium exhibits exponential growth with a constant hyphal growth rate, as long as no substrate limitation occurs and hyphal density and diameter stay the same [78, 89]. Micromorphological parameters can be determined by microscopy and digital image analysis methods [62] to obtain information about culture performance and for establishment of structured models.

The apparent macromorphology, which is discernible by the size and structure of the growth form, ultimately results from micromorphological events. The formation of pellets or clumps can result from the aggregation of spores prior to germination, aggregation of spores and germ tubes, or aggregation of mycelia depending on the organism. Pellets can be described as stable spherical agglomerates composed of a branched network of hyphae. Their shape can vary from smooth and spherical to elongated and hairy. Different mechanisms of pellet formation have been reported [66, 90, 91]. The macroscopic growth of fungi to pellets is generally defined by the increase of the pellet radius and the so called "critical" radius. The "critical" radius indicates the point where diffusion limitations occur in the outer shell of the pellet [66]. The radius of a pellet can be in the range of 250 to 2,500 μm, dependent on culture conditions. Hairy or fluffy regions of the outer pellet consist of protruding hyphae in the range of 100 to 400 μm.

*A. niger* belongs to the coagulating type, which is characterized by aggregation of spores at the very beginning of the cultivation. Coagulating pellet formation has been reported for *A. niger* [92], *A. nidulans* [64], and *A. oryzae* [93]. Pellets are then formed by germination of just a fraction of the coagulated spores. The aggregation step has been previously shown to be influenced by pH value [93] and agitation [90]. Grimm et al. [92] characterized conidial inocula and seeding-cultures to assess the aggregation process by direct examination with an in-line particle size analyser. The pellet formation of coagulating spores is described as a two-step mechanism, which highly depends on the pH value and fluid dynamic conditions within the bioreactor [29].

Right in the beginning of the cultivation, just after inoculation, spores aggregate until a steady-state condition between aggregation and disintegration of conidia packages is reached. The steady state is disturbed by germination of conidia. Germination and hyphal growth of germtubes subsequently increase the hyphal surface area, where conidia attach to and trigger the second aggregation step [29]. This leads to an overall decrease in particle concentration and depends on the pH value as well as on agitation- and aeration-induced power input [92, 94]. Within the second

aggregation step, further spores attach to germinating conidia and hyphal elements of the aggregates, which finally form pellets in later cultivation stages [95].

One of the first introduced macromorphologic growth models is the cube-root law based on observations of Emerson (1950) on the growth of *Norcadia crassa* [96]. The cube-root law describes pellet growth as it occurs in the outer shell of constant width, which is well supplied with nutrients. Biomass in the inner core is substrate limited and does not participate in growth process. Assuming a homogenous pellet density along the radial coordinate, the pellet biomass concentration is proportional to the cultivation time to the power of 3. Pellets grow exponentially with a constant specific growth rate until the critical radius is reached, and mass transport limitations lead to a depletion of nutrients at the pellet core. The critical radius indicates the point where diffusion limitation occurs in the outer shell of the pellet; it is given as the quotient of nutrient supply due to diffusion and the substrate uptake [66]. Often, oxygen is the limited substrate, and the critical radius ranges from 50 to 200 µm depending on the density of the pellet [54, 66, 97].

With continued exponential and unlimited growth of the peripheral layer, the inner zone, in which the oxygen supply is limited, increases, until finally autolysis occurs and pellets with a hollow core can be observed [81, 83]. Different physiological zones within a pellet were quantified [98]. Based on staining with lactophenol blue, the active pellet region could be distinguished from non-growing zones. As a result, the production of lovastatin is linked to the growing outer zone of the pellets and pellet size. El-Enshasy et al. [99] visualized the zonal differentiation within fungal biomass by acridine orange staining and correlated the synthesis of glucose oxidase to the peripheral layer of pellets or the mycelial growth form.

Mass transfer in pellets of filamentous fungi in submerse cultivation can be broken down into three key processes, mass transfer from the bulk phase to the surface of the pellet and mass transport in the aggregate and turnover rates within the pellet. Every single process has the potential to limit the biomass productivity of the pellet. The penetration depth of substrate and thus, fraction of pellet biomass which contributes to turnover and production, is directly linked to mass transfer within these two regions [100]. Driouch and colleagues [10, 11] used a GFP-expressing *A. niger* strain to visualize active areas of pellets. Their studies revealed that GFP expression in large pellets (2 mm) was confined to a 200 µm surface layer. Through addition of microparticles this active layer could be increased up to 500 µm, resulting in an almost 10 fold increase in glucoamylase expression [10].

The majority of models of mass transport and turnover in fungal pellets depict mass transport as being purely diffusive, on the basis that advection and turbulence are negligible in submerged cultivations [101-103]. Following the assumption that diffusion is the dominating mass transport mechanism, the effective diffusion coefficient can be used as a parameter in equations for the description and calculation of mass transport and turnover [100]. Within pellets, the effective diffusion coefficient depends on the space available for transport, and is often expressed as a function of pellet porosity or biomass density. It has been shown that fungal pellet density varies over the radial coordinate [104] and changes with time of cultivation [49, 105]. Pellet morphology, which is a result of the environmental conditions and pellet age, has an important influence on the effective diffusion coefficient and the penetration depth of oxygen into the pellet [100, 101]. These properties have been studied with oxygen microelectrode measurements. Oxygen concentration profiles have been presented for pellets of different filamentous fungi [9, 54, 97, 100, 106, 107]. By considering porosity to be the only influential parameter, several authors have described mass transport in fungal pellets [101, 102, 108], where the effective diffusion coefficient is assumed to be directly proportional to the porosity. However, Hille et al. [100] found in their study, that diffusion is the sole transport mechanism within fungal biopellets, as long as laminar conditions are prevalent, the biopellet structures are very compact, and there is a laminar flow. Moreover, deformation of pellet structure was found to have a significant impact on penetration depth of substrates. Diffusion limitation of whole pellets was found to be mainly a function of size, with a pronounced influence of advection in the outer zone of pellets that is supplied with oxygen. It was concluded that the effective diffusion coefficient might not be sufficient for the description of mass transport within the pellet periphery for a broad range of realistic fluid dynamic conditions [100].

### 2.1.3  Impact of environomic parameters on fungal morphology and productivity

Several parameters have been described in literature to influence and even shape fungal morphology. Selected studies focused on variations in the environome, changing operating parameters such as inoculum level, pH value, power input due to agitation and aeration, temperature, and medium nutrients. Distinct environmental conditions result in different morphological forms, and thereby affect the production yields of native as well as heterologous proteins. The inoculum level, pH value, and power input due to agitation and aeration are generally recognized as the most important operating parameters on morphology formation and productivity in submerged processes.

The initial inoculums concentration of spores can have a significant influence on fungal morphology and productivity [9, 51, 57, 91-93, 98, 109-114]. Grimm et al. [92] investigated the influence of spore concentration on the aggregation velocity. As a result he found, that the aggregation velocity increased with an increasing number of conidia, until a maximum spore concentration of $3 \times 10^6$ mL$^{-1}$ was reached. In addition, spore germination hyphal growth rate was slowed down at higher conidia concentrations. Xu et al. [115] showed a decrease in pellet size with increasing conidia concentration. At values above $10^7$ mL$^{-1}$, freely dispersed mycelia occured. A maximum yield of heterologous protein in *A. niger* was observed with a spore concentration of $4 \times 10^6$ mL$^{-1}$ [115]. Bizukojc and Ledakowicz [98] proposed a linear relationship between the number of pellets and the initial spore concentration for *Aspergillus terreus*. A higher inoculum concentration led to more and considerably smaller pellets. Papagianni and Mattey [112] found similar results for *A. niger* and reported smaller, less compact pellets with a higher surface roughness with increasing inoculums concentration. A micromorphologic influence of initial conidia concentration was furthermore found by Johansen et al. [116]. These authors reported increased hyphal lengths and a higher degree of branching at low spore concentrations. Increased protein production was reported for cultures of *Trichoderma reesei* at high inoculums concentration. The higher protein levels were assumed to be related to the more mycelial morphology [110].

The pH of the medium is a cultivation parameter that is often kept constant, as it can significantly influence the performance of cultivation. However, pH can also affect the morphology and productivity most significantly [9, 57, 117-124]. Especially in the beginning of the cultivation, the chosen pH has an enormous strain effect on the aggregation of spores and therefore dictates the final morphology within submerged cultivations [29, 89, 93, 125]. Yet the exact morphologic response is strain dependent. Freely dispersed mycelium is linked to an acidic pH, compared to a distinct pellet morphology at higher pH values. Pirt and Callow [123] showed that a rise of the pH > 6 during cultivation is accompanied with an decrease of the hyphal length. A further increase above a pH value of 7 results in swollen hyphae, and pellet formation occured [123]. Dynesen and Nielsen [126] showed a reduced electrophoretic mobility of spores of *A. nidulans* with an increasing alkalinity of the medium, which resulted in an increased pellet formation. The hydrophobicity of conidiospores was found to be affected. Spore aggregation in liquid culture, as well as spore surface attachment, was shown by Priegnitz et al. [127] to be pH dependent for two strains of *A. niger*. In batch cultivations with *A. oryzae*, optimal α-amylase productivity was achieved at pH 6, as described by Carlsen et al. [119]. Vats et al. [124] have reported an increase in phytase production of *A. niger* in an acidic environment of pH 1.5 to 1.8.

The influence of the agitation intensity [30, 41, 49, 91, 94, 99, 101, 111, 122, 124, 128-135] as well as aeration [41, 101, 128, 136-138], and therefore varying mechanical power input [50, 139], on morphology and productivity has been an objective in several studies and reviews [18]. Mechanical agitation is generally required for the cultivation of filamentous fungi to guarantee sufficient mixing and mass transfer. The turbulent flows induced by the impeller can have a significant influence on fungal morphology. However, in many studies the description of mechanical power input is incomplete and insufficient, because power input is confused with stirrer speeds. For an impartial description of power input, the geometry and type of reactor is needed in addition to the agitation rate. Moreover, it is possible to use parameters like the volumetric power input, the turbulence kinetic energy, or kinetic energy dissipation to characterize the mechanical stress on filamentous systems. Lin et al. [50] described the alteration in pellet micromorphology (internal and surface structure) and macromorphology (pellet size and concentration) under different aeration and agitation intensities, although the total volumetric power input was kept constant. As a result of the increased share of aeration in the total power, the glucoamylase production was raised due to a high number of small and loosely structured pellets. Papagianni et al. [133] found an increase in the production of citric acid with higher agitation intensities, but they reported an reduced hyphal vacuolation as well. The authors revealed that the perimeter of mycelial clumps decreased with increasing agitation intensity, while citric acid production was amplified. The increased yield was presumed to be due to the morphological change [133]. However, in another study, high levels of agitation were also found to cause excessive levels of mycelial damage, impairing biomass yield and productivity [99]. Park et al. [140] also reported a reduction of pellet size of *Cordyceps militaris* at increased agitation intensity as the outer filamentous regions of the pellets were sheared off. The effect of shearing forces on pellet morphology was further investigated by Rodriguez-Porcel et al. [141] for cultivations of *A. terrereus*. The pellet diameter was successfully correlated with total volumetric power input. Power input led to an erosion of the pellet surface and a decline of the hairy outer regions of the pellets. El-Enshasy and colleagues [99], in agreement with the other studies, reported a decline of the pellet diameter with increasing agitation, resulting in more active biomass and thus increased metabolite production. The beneficial effect of greater power input on the active biomass available for metabolite production was also mentioned earlier by Paul et al. [142]. Besides declining pellet diameter and growth rate, Kelly and colleagues [129] reported a decrease in pellet concentration, which was proposed to be due to a higher aggregation rate.

In pioneering studies, the use of inorganic microparticles added to the culture was recently introduced to control fungal morphology development [13, 14]. As shown for *Caldariomyces*

28

*fumago*, the addition of microparticles consisting of aluminium oxide or hydrous magnesium silicate caused a dispersion of the cells up to the level of single hyphae and enhanced chloroperoxidase production [14]. The authors observed that microparticles influenced the morphology of other fungi as well, suggesting that intentional supplementation to the culture might generally stimulate growth of these organisms. Additionally, supplementation with silicate microparticles was used as novel approach to control the morphological development of *A. niger* in submerged culture. The authors demonstrated that, inoculated with spores, the morphology of *A. niger* can be precisely adjusted to a number of different distinct morphological forms by the addition of silicate microparticles [13]. Other microparticles led to an improved productivity as well, but produced slightly different morphological growth forms [10, 12]. Beyond previous findings, it was demonstrated that the use of microparticles not only enables free mycelium, but also a rather precise engineering of morphology through fine-tuned variation of particle size and concentration [143]. These findings could open new possibilities to use microparticles for tailor-made morphology design in biotechnological processes.

There is an abundance of literature on the effects of metal and other ions on fungal growth and metabolite production [9]. Only very few studies are devoted to the effect of so-called inert salts like sodium or potassium chloride, which are supposed to have no effect on metabolism. Allaway and Jennings [144, 145], for example, report a decrease of growth of the marine fungus *Dendryphiella salina* in the presence of 200 mM sodium and potassium chloride. Bobowicz-Lassociska et al. [146] were able to increase protein secretion of washed and filtered *A. niger* mycelia by addition of KCl. An enhanced membrane permeability due osmotic pressure was argued to be responsible for the significant increase in soluble protein. In addition, Fiedurek [147] was able to increase the activity of *A. niger*-expressed glucose oxidase 2.1 fold by adding 1.2 M NaCl to centrifuged mycelia, thus administering an osmotic shock to the fungus. It was further speculated that osmotic potential should be considered as a possible regulating factor in studies on the synthesis and secretion of microbial enzymes. In both studies fungal mycelia were administered an osmotic shock.

No work was done on the effect of osmolality of cultivation medium on fungal growth and productivity. In the field of mammalian cell cultivation [148-152] and plant cell cultivation [153-155], however, an increase in osmolality is a well-known tool to increase specific productivity and sometimes final product titer. Osmolality is generally dependent on the medium composition and changes during cultivation through accumulation of metabolic products and pH control, through addition of acid or base. Most culture media have an osmolality between 0.28 and 0.32 osmol kg$^{-1}$.

Further process parameters investigated were the temperature [119], the medium composition [49, 110, 111] and the cultivation type [156]. In other studies, the effect of biodegradable polymers added to the medium [110, 111, 157], or different carriers for immobilization [158] were tested.

### 2.1.4 Digital image analysis methods for characterization of fungal morphology

Image analysis has clear advantages for morphological characterization in terms of speed, precision, labor intensity and quantitative assessment [65]. From the beginning, morphological investigations have been undertaken to characterize hyphal growth and branching and quantify fungal morphology. The first attempts for quantitative description of fungal morphology were published in the 1950s by Dion et al. [159]. In the 1970s Fiddy and Trinci [160] and later Prosser and Trinci [74] investigated surface cultures of filamentous fungi, characterizing growth and branching. Back then, quantification was achieved by microscope and photography and direct measurement. In 1981 Metz et al. [161] described the first semiautomatic method for quantitative representation of mold morphology. With the help of a microscope, photographs of mycelial particles were made and projected on an electronic digitizing table attached to a computer, which determined the exact coordinates of any point touched by the cursor. This method for quantitative representation of hyphal morphology was found to be very accurate to control continuous cultivations. However, the reproducibility of the morphological data of batch cultures was poor [58, 161]. Although the image analysis was partly digitized, the process remained laborious and time consuming [59]. In 1988 an automated digital image analysis was developed [162], reducing the time needed for a single measurement. The method was still not completely automated, requiring manual intervention at times. Packer and Thomas [163] developed a software for fully automated image analysis, which was introduced in 1990. With sufficient automation and speed, whole distributions of hyphal parameters could be tested. Using this method, significant amounts of partly aggregated mycelial material could be identified within mycelial cultivation broths [9]. These so called clumps were agglomerates much less stable and dense than pellets. Tucker et al. [113] developed a method to measure clumps, presenting detailed geometrical information such as projected clump area, perimeter, compactness, roughness and circularity as well as the degree of branching. Clump projected area was found to give the best correlations with broth rheology [136]. Furthermore, this method was used by Amanullah et al. [94], to describe the dynamics of mycelial aggregation in batch and chemostat cultures of *Aspergillus oryzae*. Paul et al. [164, 165] quantified the structural complexity of the mycelium grown in dispersed form in submerged processes, using a fully automatic image analysis and differentiation method. This model allowed a quantitative

characterization of the biomass structure and therefore made it possible to develop a powerful structured model for the cultivation of *P. chrysogenum* [166].

Image analysis has also been used to describe pellet morphology. Reichl et al. [52] measured mean sizes, content and shape of pellets during a cultivation of *Streptomyces tendae* and introduced a shape factor specifying the form of a pellet, which was the first qualitative discrimination between pellets. Cox and Thomas [167] proposed image analysis methods to characterize pellets based on the presence of a central core. They further categorized pellets into smooth and hairy types using automatic image analysis. Many studies have quantified pellets in terms of their size and the extent of the filamentous region [168, 169], whereas others have focused on the high- throughput, low-resolution quantification of suspended pellets and aggregates [98, 170]. The choice depends on whether mechanistic insight about morphological development is sought, or image analysis is directed toward obtaining cultivation averages for process optimization.

Still, image analytic methods have to be further improved; online image acquisition, in particular, is desirable. A system capable of automatic dilution and subsequent imaging acquisition using a flow-through cell, permitting real-time analysis of cultivation was introduced by Treskatis and colleagues [171]. In situ image acquisition as applied in Galindo's study seems to be a promising approach [172]. Through such a method, all fungal particles could be researched in their native state. Further challenges will include 3D- image acquisition and incorporation of this data in appropriate models. The first 3D models for the simulation of fungal growth have already been introduced [103].

Image analysis has become a suitable tool for characterizing and developing mathematical models that describe morphology and growth of filamentous microorganisms, like characterization of pellet morphology, measurement and simulation of morphological development, and a mathematical model of apical growth, septation and branching [60]. Image analysis techniques permit the rapid and accurate measurement of simple cellular differentiation of fungi [9]. As of today, image analysis is state of the art for the characterization of morphology and simple differentiation of filamentous microorganisms, and is therefore of considerable significance for bioprocess control. The reduced cost of equipment, both hardware and software helped to make image analysis a routine laboratory tool [60]. A typical imaging system utilized for the quantification of fungal morphology might consist of a standard bright- field microscope onto which a digital camera is mounted. Once the image has been transferred to a PC, some form of image analysis application is required to extract the relevant data [65]. For this task commercial

systems such as Image-Pro Plus (Media Cybernetics, Rockville, USA), AxioVision (Carl Zeiss, Jena, Germany), Optimas (Meyer Instruments, Houston, USA), MetaMorph (Molecular Devices, Sunnyvale, USA) and Volocity (Perkin Elmer, Waltham, MA, USA) can be employed. Alternatively, often more powerful, open-source applications such as ImageJ (rsbweb.nih.gov/ij), Fiji (pacific.mpi-cbg.de) and OpenCV can be used, which can be freely customized by numerous plugins available [65].

### 2.1.5 Rheology of filamentous culture broths and its relation to morphology

Filamentous organisms such as *Aspergillus niger* can grow either in dense, spherical pellets with a near Newtonian flow behavior, or as disperse and viscous mycelia [19]. The exhibited morphology herby influences not only culture broth viscosity but also productivity, substrate diffusion and downstream processing [173]. The flow behavior of cultivation broths of filamentous organisms differs distinctly from broth of other microogranisms. Several studies show, that the complex morphology of filamentous fungi is responsible for highly viscous cultivation broths, characterized by shear-rate dependent viscosities and by yield stress [9, 42, 174-177]. Variations of the broth characteristics affect the bioreactor hydrodynamic properties which include mixing and mass transfer performances [178-180]. The efficiency and productivity of the entire cultivation process depends on these hydrodynamic properties [42]. An understanding of the flow behavior is necessary in order to develop design strategies that will help to overcome possible limitations in mass, momentum and heat transfer in bioreactors [9].

In general, mycelian growth, rather than pellet growth increases the viscosity of the medium [58]. Although pelleted cultivation broth may be Newtonian, of low viscosity, and more economical in the separation of the biomass. Problems might arise with the transport of nutrients into pellet cores, thus reducing productivity. The dispersed forms therefore predominate, in most industrial cultivations [53, 176]. Through creation of high-producing mycelial morphology, however, other problems with process performance present themselves. In such cultivations hyphal entanglement can result in significant changes in broth rheology [181]. Small increases in biomass concentration can lead to large increases in broth viscosity [63, 174, 176].

Filaments tend to grow uniquely to form three-dimensional networks by biomass accumulation at the growing tip of the hyphal network [182]. The resulting highly branched network exhibits several fluid dynamic interactions, thus changing the properties of the cultivation broth from the initially Newtonian character to a non-Newtonian one [183]. The increased culture broth viscosity

leads to heterogeneous, stagnant, non-mixed zone formations, which make the cultivation challenging and more expensive to operate [53, 90].

The strong negative influence of broth viscosity on oxygen transfer has been shown previously [179, 184]. Some of these problems can be increased when the process is scaled up, due to increased mixing times and generally lower agitation rates [176]. To control cultivation performance, it is essential to know how the operating conditions influence the rheological properties of the filamentous cultivation broth, as these depend on the morphology of the biological system. Consequently, the relationship between rheology and morphology is vitally important and has to be fully investigated [173]. Such knowledge can be very valuable in the optimization and design of common cultivation processes [9, 53].

Newton's law is the simplest of rheological models. Here, dynamic viscosity is defined as the relationship between the applied shear stress and the resulting movement of the fluid, defined as shear or strain rate

$$\eta \equiv \frac{\tau}{\dot{\gamma}} \qquad (2.1)$$

where $\eta$ is the dynamic viscosity [N·m$^{-2}$·s], $\tau$ is the shear stress [N·m$^{-2}$] and $\gamma$ is the shear rate [s$^{-1}$]. The viscosity of a Newtonian fluid is independent of the shear rate.

For non-Newtonian fluids this relationship is more complex. Mycelial cultivation broths generally have pronounced non-Newtonian rheological characteristics and show shear thinning or pseudoplastic behavior [175, 185]. Pseudoplastic fluids exhibit a decrease in viscosity with increasing shear rate. Non-Newtonian viscosity is usually characterized using the "apparent viscosity" [42, 186].

It is impossible to have a complete knowledge of shear stress/shear rate relations and elastic properties of inhomogeneous mixtures such as cultivation broths. Therefore several rheological models have been introduced, which may be regarded as an empirical fit to the experimental data [187]. Several authors used the Bingham model to describe the rheological properties of mould suspensions [185]. The Casson model is also occasionally used to describe filamentous cultivation broths at low shear rates [63, 177, 187, 188]. Most commonly, however, the Power law relationship of Ostwald–de Waele

$$\tau = K \cdot \dot{\gamma}^{n}, \qquad (2.2)$$

or the Herschel-Bulkley relationship

33

$$\tau = \tau_0 + K \cdot \dot{\gamma}^n \qquad\qquad (2.3)$$

are used as models for culture broth viscosity, where K is the consistency index, n the flow behavior index and $\tau_0$ the apparent yield stress. The Herschel-Bulkley model additionally includes the yield stress and is therefore preferred by some authors [186]. The existence of yield stress is important, because it will determine start-up power requirement in pumping through pipelines and mixers and the existence of dead regions in bioreactors [175, 189]. These relatively simple models were already demonstrated to be sufficient to describe the rheological properties of non-Newtonian cultivation broths [190, 191]. The fitting parameters K and n obtained by the Ostwald–de Waele model are most often used as the sole indicator of viscosity of filamentous cultivations [41, 43, 175, 176, 186, 190-195].

All models are understood to be empirical relationships and not physical laws [196]. Reuss et al. [191] compared the Casson, Herschel-Bulkley and the power law plots for the apparent viscosity of a suspension of *Penicillium chrysogenum*. The authors found that within the relatively small range of shear rates measureable, it was not possible to distinguish between these models. In another study it was shown that a two parameter model was sufficient for describing data measured in the shear rate ($\dot{\gamma}$) range between 2 to 650 s$^{-1}$. Through addition of a third parameter, the model fit to the data could not be significantly improved [190]. In some studies, the consistency index K, has been used as the sole indicator for the viscosity of filamentous cultivations [194, 197]. This seems to be a valid assumption, since the value of the flow index n is affected by the operational design to a much lesser extent than the value of K [190]. However, because n is an exponent, changes in n will have a larger effect on shear stress than a similar change in K, thus limiting the use of K-values as single indicator of fluid viscosity to data sets were n is approximately constant [175].

Rheology and morphology of filamentous fungi have been studied extensively, but often separately. Early studies examining the broth rheology simply published apparent viscosity measured at a single speed in the viscosimeter [198]. Other more detailed analyses, however, showed a variable flow rate of filamentous cultivation broths [174, 177, 198]. Comparatively few reports on correlations between morphological parameters and broth rheological properties exist. This is due to the large variability of mycelia growth in submerged cultures, which makes the characterization challenging [9, 63].

Until the early 1990s the appropriate instrumentation for making morphological measurements, not only on the micro morphological but also on macro morphological level was lacking [9].

Tucker and Thomas [113, 199, 200] were the first to use image analysis to investigate the separate influences of biomass concentration and mycelial morphology on broth rheology in the 1990s. The authors investigated the separate influences of biomass concentration and mycelial morphology on broth rheology, using an industrial strain of *Penicillium chrysogenum*. They proposed that the rheology of fungal cultivation broths should be related to clump properties, rather than to the morphology of small amounts of freely dispersed mycelia, and were able to investigate the effect of biomass concentration separately from that of morphology. The rheological parameter could be related to biomass concentration as dry cell weight (BDW)

$$RP = const. \; \cdot \; BDW^{\alpha} \tag{2.4}$$

where RP is the rheological parameter under examination and α is the exponent on biomass concentration (BDW) [176, 200].

Having established the effect of biomass concentration on rheology of filamentous cultivation broths, the effect of mycelial morphology could be investigated. Morphological parameters, as found in Paul and Thomas [62, 200], especially clump roughness (R) and compactness (C), proved to be significant, as they had a definite influence on broth rheology. With these findings the following correlation was proposed

$$RP = const. \; \cdot \; BDW^{\alpha} \; \cdot (R)^{\beta} \cdot (C)^{\gamma} \tag{2.5}$$

in which α, β and γ are the exponents for each the rheology affecting parameter [176].

The resulting correlations were highly successful at predicting broth rheology for filamentous batch cultivations [176, 200] (**Table 2.1**).

**Table 2.1:** Correlations for the prediction of rheology from biomass concentration and population averaged data from image analysis. This table was adapted from Wucherpfennig [173].

| Source | Correlation | Organism |
|---|---|---|
| Tucker and Thomas [200] | $K = BDW^{2.8} \times R^{0.7} \times C^{1.2} \times$ const.[a] | *P. chrysogenum* |
| Tucker [199] | $K = BDW^{2.3} \times R^{-0.96} \times C^{0.79} \times 6.6 \times 10^{-5}$ | *P. chrysogenum* |
| Olsvik et al. [193] | $K = -0.56 + 0.0018 \times R \times BDW^{1.7}$ | *A. niger – continuous* |
| Olsvik and Kristiansen [175] | $K = 0.38 + 4.8 \times 10^{-5} \times R \times BDW^{2.9}$ | *A. niger – fed batch* |
| Mohseni and Allen [201] | $\tau_y = 4.2 \times 10^{-6} \times BDW^{2.6} \times (L_l)^{2.2},$ $\tau_y = 7.2 \times 10^{-3} \times BDW^{2.2} \times (L_{HGU})^{0.65},$ $\tau_y = 4.8 \times 10^{-7} \times R^{3.2} \times BDW^{2.5}$ | *S. levoris* and *A. niger* |
| Riley et al. [176] | $K = BDW^{2} \times (5 \times 10^{-5} \times d -10^{-3})$ | *P. chrysogenum* |
| Riley et al. [195] | $K = BDW^{2} \times (4 \times 10^{-5} \times d - 9 \times 10^{-4})$ | *A. oryzae* and *A. niger* |

$K$ is he consistency index [Pa·s], $BDW$ is the biomass concentration as dry cell weight [g·L$^{-1}$], $R$ is the morphological parameter roughness, $C$ the morphological parameter compactness, $d$ is the mean maximum dimension, $L_l$ is the hyphal length, $L_{HGU}$ the mean length of hyphal growth unit [µm] and $a$ an arbitrary exponent.

35

Olsvik et al. [193] used the same image analysis method on *A. niger* broths from 7 L chemostats. They found that more than 89% of hyphae were in the form of clumps. Changes in biomass concentration and clump roughness led to different rheological properties of the broth, represented by the power law consistency index, which increased with the biomass. Olsvik and Kristiansen [175] proposed a similar correlation for batch and fed-batch cultivations. Mohseni and Allen [201] used image analysis to examine the influence of biomass concentration and particle morphology on the yielding properties of filamentous broth of *Streptomyces levoris* and *A. niger*. They found correlations with the freely dispersed form using the biomass concentration, the mean dimensionless length and the mean hyphal growth unit. Furthermore, the biomass in form of aggregates was correlated with yield stress, showing that clumps with greater roughness caused a greater yield stress, as shown by Olsvik et al. [193] and Olsvik and Kristiansen [175]. All studies reviewed thus far agree that clump morphology, particularly roughness, is important in determining fungal broth rheology [175, 193, 199-201]. Riley et al. [176] criticized earlier correlations based on clump morphology, stating that during later stages of cultivation, only 30 to 40% of biomass where in clumps. In this work, the authors found no clear relationship between the flow index and biomass concentration. The correlations identified for the consistency index were based on the biomass concentration, and the mycelial size represented by the mean maximum dimension of all the mycelia [176]. In all these correlations, the impact of biomass concentration varies, with an index from 1.7 to 2.9, while morphological parameters, such as maximum dimension, compactness or roughness have less importance with indices between 0.96 to 1.2 [186].

The measured morphological parameters were population averages based on selected samples and assumptions, with the drawback that much of the information from the image analysis data is lost by taking a population average, or excluding part of the population. A completely different approach for the prediction of rheological characteristics of filamentous cultivation broths was taken by Petersen et al. [186]. Using a PLSR (partial least squares regression) model, the authors were able to obtain reasonable predictions of apparent viscosity, yield stress, and consistency index, from the size distribution and biomass concentration.

## 2.2    Production of paclitaxel by submerse cultivation of *Taxus chinesis*

### 2.2.1  *Yew trees and discovery of paclitaxel*

The yew is one of the most fascinating trees, botanically notable, and culturally almost without comparison, with rich references in history, mythology, religion, folklore, medicine, and warfare [202]. The genus name *Taxus* originates from the greek word for bow "tóxo" [203], which gives an indication of the most common uses of this tree's timber. Because of the use of its wood in longbows and crossbows, the yew is predominantly associated with England [203]. The English longbow formed the basis for tactical system in medieval warfare [202]. The heavy use of yew wood for purposes of war soon led to a serious shortage. A vast network of trade relations for extraction and supply of yew wood was established all over Europe, to satisfy the high demand for this resource [202, 203]. As a result, the yew tree became almost extinct in central Europe and up to this date yew trees a scarce.

The toxicity of the yew tree has been long known. The yew was renowned as a death tree in Celtic, Greek, Germanic and Roman mythology and can up to this date be found on many graveyards [203]. Even Julius Caesar describes in his book "De Bello Gallico" a case were a local chieftain avoids capture through suicide by consumption of *Taxus* needles [204]. However, ingredients from the yew were not only used as poison, but also as medication. Historical literature shows that medieval physician Avicenna (980–1037) used a herbal drug extracted from *Taxus baccata* as a cardiac remedy [205]. Alkaloid mixtures (taxines) from yew trees were just recently demonstrated to possess calcium channel blocking activity. So, it is evident that Avicenna used a drug with calcium channel blocking activity much earlier than the arrival of commercial drugs belonging to the same pharmacological group [205]. In the Central Himalayas, the plant has been used as a treatment for breast and ovarian cancer for a very long time [206], and in most European countries, yew leaves had a popular use as an abortificient [205]. Additionally, extracts from *T. baccata* have been used in the treatment of asthma [207].

It was not until 1962 that *Taxus* samples were tested for their biological activity, by Barclay. By 1964, it was discovered that yew extract inhibited cancer cells [208]. The inhibiting substance was isolated, and the isolation of 0.5 g of pure paclitaxel from the pacific yew *Taxus brevifolia* took about 2 years [209].

Paclitaxel showed an extraordinarily broad spectrum of anti-tumor activity [208]. The molecular formula of the agent was determined to $C_{47}H_{51}NO_{14}$ [208]. The complicated structure of the diterpenoid paclitaxel was elucidated and published in 1971 [210]. In 1979, Horowitz explained

37

the mechanism of action of the drug on cancer cells [208]. Paclitaxel stabilizes microtubules, and thus blocks the necessary reorganization for mitosis [208, 211]. It prevents cell reproduction and works predominantly on quick dividing cells, like tumor cells [208]. In 1984, Paclitaxel was released by the Food and Drug Administration (FDA) for phase I tests [208]. It was approved for marketing as an anticancer agent in 1992 (Bristol- Myers Squibb), and by 1998 was the best-selling anticancer drug in history with $1 billion in commercial sales [212, 213]. Paclitaxel is used for the treatment of ovarian, breast and lung cancers as well as AIDS-related Kaposi's sarcoma [213]. 340,000 kg of *Taxus* bark, or 38,000 trees are required to meet the 25 kg per year demand for the anticancer drug paclitaxel [214]. The growing demand for the drug could potentially exceed 200–300 kg per year as applications are being developed for paclitaxel in the treatment of Alzheimer's and post-heart surgery patients [213, 215].

A serious obstacle to overcome is the generally low concentration (0.001–0.05%) of paclitaxel found even in the most productive species, and thus, considerable energy has been invested in trying to increase its extraction yield [216]. Extraction requires a complex system and specific purification techniques using advanced and expensive technology [216]. The harvest heavily depends upon seasonal variability and the slow growth rate of the tree, making it nearly impossible to keep up with demands [217]. Some effort has been undergone to establish ecologically sustainable harvesting protocols of yews in natural habitats in Canada [216, 218]. Likewise a plantation with 30 km$^2$ of yew trees has been established in the province of Yunan (China) by the company Yewcare, making it the largest yew tree producer in the world [216]. Since yew trees take over a hundred years to yield good amounts of paclitaxel [208], the planting of trees seems to be a far-fetched investment.

To prevent the extinction of *Taxus* species and decrease processing costs, alternative paclitaxel production methods were investigated [213]. Chemical synthesis is possible, but very complex, as it requires 40 synthesis steps with only 2 % yield [208, 219]. Chemical semisynthesis can be applied to use paclitaxel precursors which are present in amounts up to 0.1 % in *T. baccata* [220]. Semisynthesis requires 11 chemical transformations using 13 solvents and 13 organic reagents, making it expensive and environmentally unfavorable [221]. The cost of paclitaxel through semisynthetic means can be decreased to 25 % of that for natural harvest [222].

Nevertheless, an alternative and environmentally sustainable source of paclitaxel is the production in plant cell cultures. This methodology offers several advantages, not being subject to weather, season or contamination, and the material can be grown independently of its original, potentially remote location [216, 221]. Plant cell cultivation of *Taxus* cells is not only environmentally

38

sustainable, but also economically reasonable, as it reduces process costs to just 20% of that for natural harvest and is therefore even cheaper than semisynthesis of paclitaxel [222]. Currently, Phyton Biotech GmbH, Ahrensburg, Germany, is the largest producer of paclitaxel via plant cell cultivation.

### 2.2.2  Cultivation of plant cells in suspension – impact, issues and relevance

Higher plants can be an abundant source of bioactive and pharmaceutically important chemicals including drugs such as morphine, codeine, reserpine and several alkaloids and steroids [223]. The value of drugs containing phytochemicals prescribed in the United States in 2002 was valued at more than 30 billion US$, emphasizing the enormous market [224]. Over 60% of the anticancer drugs and 75% of drugs for infectious diseases currently used are made or extracted from natural sources [225]. The increasing demand for therapeutic molecules, produced by ecologically more sustainable processes, along with dramatic reductions in biodiversity, are driving efforts to find alternative ways to produce high-value plant-derived metabolites [226]. The development of plant cell cultures for biotechnological production of valuable secondary metabolites is an attractive alternative to the extraction of often very low-concentration substances from whole plant material. Furthermore, farming and harvesting of plants for their rare materials, has been shown before to be a risk to whole plant populations [227], making it ecological unsustainable. The ability of plant cells to grow in suspension in relatively inexpensive, chemicalyl defined media, their capacity for complex glycosylation and safety [228] are further advantages of plant cell cultures.

Haberlandt undertook the first to attempt to cultivate plant cells in 1902 and is recognized as the founder of plant cell cultures [229, 230]. In 1956, the first patent for submerged cultivation of numerous plant tissues isolated from several plant species, and the possibility of producing oxalic acid and coumarin from such cultures was filed [229]. Nowadays plant cell cultures can be created from virtually any plant through the isolation of plant tissue [213]. Extracts are sterilized using a chemical treatment, and plated on solid growth media containing growth hormones and nutrients necessary for proliferation [231]. Assuming an adequate medium composition, plant extract proliferates into a callus of dedifferentiated cells, which can be screened and transferred to liquid medium for the creation of suspension cultures [213]. Plant suspension cultures often produce similar concentrations of secondary metabolites as the native plant [232]. Hairy root cultures are an attractive alternative to regular plant cell cultures, as they can stably produce high levels of secondary metabolites and do not require growth hormones [233]. Hairy root cultures are created through infection of root cultures with *Agrobacterium rhizogenes* [213].

Commercial systems for cultivation of plant cells were established more than 25 years ago, still there has been little progress towards wide deployment and only a limited number of compounds are produced at a large scale. A more widespread application seems prevented by low metabolite yields, biochemical and genetic instabilities, low growth rates and difficulties associated with scale up [229, 234]. For plant cell culture, the transfer from shake flask to bioreactor is complicated [213]. A unique and often frustrating characteristic of plant cell cultures, in comparison to other microbial host systems, is their disposition to grow in aggregates rather than single cells. Plant cells often remain connected via a shared cell wall, and as a result, form aggregates ranging from few to several hundred cells [7]. Aggregates can therefore reach sizes up to several millimeters, leading to the formation of heterogeneities within the aggregates due to substrate and oxygen limitations [235]. Therefore, the size of plant aggregates was an issue in several studies. However, despite diffusion limitations, large aggregates were found to be favorable for the production of secondary metabolites by some authors [236-238]. Others reported a beneficial effect of larger aggregates up to a certain critical size [239, 240], or found large aggregates to be disadvantageous [7, 241, 242] for production of secondary metabolites. The optimal production of secondary metabolites by particular sizes of cell aggregates is apparently a characteristic of a species or a cell line [243]. The average aggregate size of a culture also varies over the culture period and can affect secondary metabolite accumulation. A current research focus is the elucidation of the link between aggregate size and secondary metabolite accumulation. A better understanding of this link and the associated heterogeneities, could allow product yields to be maximized by adjusting process conditions [213].

### 2.2.3  Particle size measurement of suspended plant cells and aggregates

Even if it remains unclear whether large aggregates or small plant cell aggregates are desirable for an optimal process, and this might very well depend on the scale, the cell line and the product, aggregate size, in general, seems to have a pronounced effect on secondary metabolite production. The analysis of aggregate size as a process variable seems therefore feasible, and was already discussed in a recent study [7]. However, particle size is not a bioprocess variable that can be measured easily, and while there are a handful of methods for particle size analysis only very few are applicable for plant cell aggregates.

Plant cell aggregate sizes have so far been often measured by mechanical sieving analysis [244]. While this method is considerably easier, it has the potential to alter the aggregate size distribution [245] and is prone to generating erroneous results. Another method recently used for plant cell

aggregate characterization is the application of the Coulter counter principle, based on the electrical resistance pulse seizing [234]. This method requires a heavy dilution and has a measuring range between 50 and 2,000 µm, and is therefore not suitable for measuring single cells within the culture broth. Further methods for plant cell aggregate analysis include image analysis and the focused beam reflectance measurement (FBRM). Image analysis techniques allow for the identification of aggregate size and have the advantage of enabling the identification of further morphologic parameters, like circularity, roughness or elongation, which might provide an on overall culture performance. The process of image analysis is mostly divided between sample dilution, image acquisition by microscope, and the more or less automated step of image analysis [242]. While providing a high resolution for single cells, estimation of means for the whole culture remains troublesome. Because of the usually very laborious process and exceptionally small throughput, it is hard to obtain statistically valid results by application of this method [234]. To cope with this disadvantage a minimum of analyzed objects based on a "running average" was suggested by Pearson and coworkers to achieve a statistical robustness [246].

The focused beam reflectance measurement system (FBRM), is another size-determining method previously used for plant cells [228, 247] or fungal systems [89]. FBRM is an optical technique based on the detection of backscattering laser light. The duration of reflectance of a particle passing a laser corresponds to the chord length of a particle. A photo detector converts the reflected light signal into an electronic signal, and the duration of backscattering, multiplied by the scan speed of the laser results in a chord length [248]. For non-transparent spherical particles, the chord length is equivalent to the object's diameter. For near transparent objects like plant cell aggregates, however, it is not as straight forward, as chord length is also a function of particle shape, opaqueness and surface properties. Here, chord length correlates with particle diameter, but is not equal to it [247].

A new method, so far not applied to plant cells, is laser diffraction, also known as Low Angle Laser Light Scattering (LALLS). This works on the basis of particles of a given refraction index interacting with a laser beam passing through an inverse Fourrier-type lens. The angle of the diffracted laser beam is hereby inversely and the intensity of the diffracted laser beam directly proportional to the particle size [249]. Laser diffraction can be used for the non-destructive analysis of wet or dry samples, and is generally the most used method for particle size analysis of inorganic matter like spray or powders [250]. Through continuous and non-destructive measurement the method has inherent advantages which make it preferable to other options for many different materials.

An employment of laser diffraction for microbial systems has been introduced only recently for size determination of fungal pellets [251], bacterial cell clumps [252] and measurement of germination time of *Aspergillus niger* conidia [253]. In association with plant cell systems, laser diffraction has been previously used to study the aggregation of rubber particles of *Hevea brasiliensis*, which are sized between 0.3 to 6.7 µm [254]. Because of the very broad measuring range of 0.02 to 2,000 µm, an application of this method for whole plant cell aggregates seemed feasible.

### 2.2.4 Shear sensitivity of plant cells and determination of viability

The effects of hydrodynamic stress on various kinds of living cells in suspension have been studied for a very long time [255, 256]. Plant cells have commonly been regarded as extraordinarily shear sensitive because of their relatively large size, their rigid cell wall, and their large vacuoles [255, 257]. The theory of isotropic turbulence by Kolmogorov provides an elucidation of why plant cells are more susceptible to shear stress introduced by the hydrodynamic environment than other cells [258, 259]. In this theory, the turbulent flow in the reactor is characterized by a large primary vortex. The eddies roughly correspond in size to the diameter of the stirrer in a stirred tank reactor and the diameter of the rising gas bubbles in a bubble column. The primary vortices are unstable and tend to fall apart. They transfer energy to smaller eddies [260]. The energy transfer takes place gradually, and the information with respect to the direction of the vortex is lost. The state when the movement of eddies and the transfer of kinetic energy in all directions at all points in the flow field of the reactor are equal is called isotropic turbulence. Thus, the energy transfer is statistically independent of the direction. The smallest eddies in a turbulent isotropic flow field are called Kolmogorov eddies. These micro vortices cannot break down to smaller eddies, but disintegrate into energy [259]. Plant cells in suspension, or any other cells, are strained when the diameter of the micro vortices is equal to or smaller than the diameter of the cell. Since plant cells, which often occur in aggregates, are relatively large structures, they can be easily attacked by Kolmogorov eddies. Therefore, plant cells are very sensitive to hydrodynamic stress [255, 261].

The effects of shear stress on plant cell culture can be both positive or negative [255]. A possible positive effect on plant cell production system is the stimulation of secondary metabolite production; furthermore, cell metabolism and gene expression can be promoted [255]. However, consequences of shear stress have been mostly regarded as negative for the survival of plant cells. Shear stress may have a negative impact on cell growth, metabolism, and cell-cell organization in aggregates. There are several symptoms that indicate cell damage. The most prominent is often a

42

change in cell morphology: for example by a reduction in aggregate size [262-265]. Moreover, shear stress can lead to the release of intracellular substances, which can lower the pH of the suspension [266]. Besides, changes in the metabolism and product yields are common [255, 267]. As a final symptom, a loss of viability is mentioned, which may lead to cell death. In many cases, the cells are, however, able to repair the damage [255]. With increasing hydrodynamic stress, the ability for regrowth [258], the cell membrane integrity [258, 261] as well as the respiratory activity [258, 266] decrease.

Between different plant cell lines, there are considerable differences in shear susceptibility [268]. Variations in the shear sensitivity in different cell lines are most likely due to the different morphological characteristics and general stability of the cell wall [258, 269]. The culture age, cultivation conditions, and the cultivation history have been identified as factors affecting shear sensitivity [262, 266]. In various experiments, it was found that cultures of the late exponential growth phase and early stationary phase are most susceptible to damage caused by hydrodynamic stress [255, 261]. The high shear sensitivity was argued to be related to the increase in aggregate size during this time [261].

Plant cells can, furthermore, adapt to hydrodynamic stress, and can develop a kind of robustness against hydrodynamic disorders [255]. Plant cells begin to adapt after they have been exposed to shear stress for a certain time [270]. A possible explanation for the shear tolerance is the ability of plant cells to repair cell wall damages through disposal of polysaccharides like callose [262]. Other cells have the ability to compensate for shear damage through increased growth [266].

One way to quantify shear damage inflicted upon plant cells is to determine the decrease in viability. The viability of cells or organisms reflects their capacity to live, which can be observed by their ability to grow [271, 272]. The measurement of growth is therefore the simplest way to determine the viability of the cells, for example through measurement of the fresh cell weight, or dry weight, as well as through the measurement of the increase in cell number [271, 273]. However, zero growth is not necessarily an indicator of poor viability, and since plant cells in suspension mainly stay connected after division and grow in aggregates, the determination of the number of cells is virtually impossible.

Further viability assays are based either on the physical properties or biochemical characteristics of the cells. The detection methods are based on the properties of the cells, such as endocytosis, enzymatic activity, the integrity of the cell membrane, or proliferation. There are generally different ways to measure the viability of cells. It is possible to obtain information on cell viability by observation of the cytoplasmic flow [272]. Another possibility is the determination of

membrane integrity by electrolyte flow, plasmolysis and dye exclusion or retention [271, 274, 275]. Furthermore, the biochemical activity can be measured as in protein synthesis [271], tetrazolium chloride reduction [272, 276], DNA and RNA synthesis [271] and fluorescien-di-acetate staining [275]. Microscopic measurements, based on the color of cells incubated with Evans Blue or Trypan Blue, are possible. Dead cells have a disrupted membrane, and can therefore take up the dye [277]. These days such tests are very popular for mammalian cell culture, as they allow easy automation. The absorbed substances may also have fluorescent properties, and thus can be determined fluorometrically. Another viability test using lactate dehydrogenase (LDH) measures the membrane integrity as a function of the amount of released cytoplasmic LDH into the medium. Luminometric or fluorometric viability assay are based on the metabolic activity of the cells; these tests are based on the uptake and metabolic conversion of a fluorescent or luminometric substance by cellular metabolism [278, 279].

A major breakthrough in the field biochemistry-based viability tests was achieved by the development of assays based on the activity of the electron transport chain [280]. Such assays, based on the water-soluble, colorless tetrazolium salts such as 3-((4,5-dimethylthiazol-2-yl)-2,5-diphenyl tetrazolium bromide (MTT) and 2,3,5-triphenyltetrazolium chloride (TTC) are very popular for mammalian and plant cell cultures. When entering a living cell, TTC is reduced by the dehydrogenase activity of the mitochondrial electron transport chain to form an insoluble red formazan product. Therefore, dead and living cells can be distinguished by color. For quantification, the red precipitate is extracted from the tissue with ethanol, and the absorbance of the extract can be determined spectrophotometrically [276]. Like the TTC test, the MTT assay is based on the dehydrogenase activity of the mitochondrial electron transport chain. Here, the yellow-colored tetrazole of MTT is converted to a water-insoluble purple formazan product. To dissolve the water-insoluble product, organic solvents such as DMSO or isopropanol are required. The intensity of the blue color can be directly placed in relation to the number of living cells [281]. The non-fluorescent, non-polar molecule fluorescein di-acetate (FDA), can also be used for viability determination. After entering the plant cell, FDA gets split by an esterase. The resulting fluorescent product (fluorescein) remains in the cell, since it cannot pass through the plasma membrane because of its polarity. Dead cells have a decreased esterase activity, and usually also leaky membranes; therefore, less fluorescein can accumulate within the cell [282].

Since most viability assays are based on metabolic studies of animal cultures, their validity for plant cell culture has to be ensured [271, 283]. Dyes which are used in animal cell cultures may not necessarily pass through the cell wall or react in plant cells.

# 3 Material and Methods

## 3.1 Microorganism and inoculum preparation for cultivation of *A. niger*

The recombinant strain *A. niger* SKAn1015 used in this study carried the suc1 (fructofuranosidase) gene to produce fructofuranosidase under the control of the constitutive pkiA (pyruvate kinase) promoter, and was obtained from the protease deficient mutant *A. niger* AB1.13 by transformation [37]. The organism was maintained as a frozen spore suspension at -80 °C in 50 % glycerol. To obtain spores, agar plates with the sporulation medium were plated out with spores from a frozen stock and incubated for five days at 30 °C. The sporulation medium for *A. niger* SKAn1015 contained 30 g L$^{-1}$ potato dextrose agar (Sigma–Aldrich) and 10 g L$^{-1}$ agar (Sigma–Aldrich).

After growth and sporulation, 30 mL sterile NaCl solution (0.9 % w/v) was added to each agar plate, which was scraped to release the aerial mycelium. The suspension was filtered through two layers of sterile Miracloth (pore size 22 to 25 μm, Merck) to prevent agar debris and conidiophores in the spore suspension. The optical density of the spore suspension was measured photometrically at 600 nm (SmartSpec$^{TM}$3000, BioRad). A conversion factor between the optical density and concentration of the spore suspension was determined beforehand using a microscope and a hemocytometer (Thoma new; 0.0025 mm$^2$, depth 0.1 mm; Blaubrand ®, Brand, Wertheim, Germany). The optical density of 1 at 600 nm equaled 1.16 · 10$^6$ spores mL$^{-1}$. This factor was then used to calculate the spore concentration of the inoculum from the measured OD600 values of the dilutions of the fresh spore stock solution.

## 3.2 Media and cultivation conditions

### 3.2.1 *Medium for cultivation of* A. niger

The cultivation medium of *A. niger* SKAn1015 contained per liter 20 g D-glucose as 20 mL salt solution (6 g L$^{-1}$ NaNO$_3$, 0.5 g L$^{-1}$ KCl, 1.5 g L$^{-1}$ KH$_2$PO$_4$, 0.5 g L$^{-1}$ MgSO$_4$·7H$_2$O) and 1 mL trace element solution (10 mg L$^{-1}$ EDTA, 4.4 mg L$^{-1}$ ZnSO$_4$·7H$_2$O, 1.01 mg L$^{-1}$ MnCl$_2$·4H$_2$O, 0.32 mg L$^{-1}$ CuSO$_4$·5H$_2$O, 1 mg L$^{-1}$ FeSO$_4$·7H$_2$O, 0.32 mg L$^{-1}$ CoCl$_2$·6H$_2$O, 1.47 mg L$^{-1}$ CaCl$_2$·2H$_2$O, and 0.22 mg L$^{-1}$ (NH$_4$)$_6$Mo$_7$O$_{24}$·4H$_2$O). Carbon source, salt, and trace element solutions were autoclaved separately at 121°C for 20 min and chilled to room temperature prior to mixing and use. The medium exhibited a standard osmolality of 350 mosmol kg$^{-1}$.

### 3.2.2 Cultivation conditions for bioreactor and shaking flask cultivations of A. niger

250 mL shaking flasks with 4 baffles containing 100 mL medium per flask were incubated for 72 h at $120\pm1$ min$^{-1}$ on a rotary shaker (Certomat BS-1/50mm, Sartorius, Göttingen, Germany). All cultivations were carried out at least in triplicate. The inoculation with a spore suspension was performed such, that spore concentration within the shaking flask was $10^6$ spores per milliliter. Growth temperature was $37 \pm 0 .1$ °C.

Batch cultivations were carried out in a 3-L stirred tank bioreactor (Applikon, Schiedam, The Netherlands) with two six-bladed disc turbine impellers. Bioreactors were inoculated with a suspension of freshly harvested conidia to give a spore concentration of $1 \cdot 10^6$ mL$^{-1}$ after inoculation. All bioreactor cultivations were carried out at least in triplicate. Growth temperature was $37\pm0.1$°C. Aeration rate (1.0 L min$^{-1}$), agitation speed (200 min$^{-1}$) and pH value (pH 5.0) were automatically kept constant.

### 3.3.3 Conditions for cultivation of Taxus chinensis

Gamborg B-5 Basal Medium as described by Gamborg and colleagues [284] was used for cultivation of *Taxus chinensis* CR1354r in 1L polycarbonate Erlenmeyer flasks with vent caps (Corning, USA), filled with 400 mL medium. Cultures were incubated for 240 hours at 120 min$^{-1}$ on a rotary shaker (Certomat BS-1/50mm, Sartorius, Göttingen, Germany). Cultivations were carried out in triplicate. The growth temperature was $25\pm0.1$°C.

## 3.3  Biomass concentration, osmolality, enzymatic assays and sampling

The biomass dry weight was measured gravimetrically by filtering (Nalgene 300-4000) a defined amount of biomass suspension through a pre-dried (48 h at 105°C) and pre-weighted suction filter (Filter Discs Grade 389, Sartorius). Prior to drying (48 h at 105°C), the filter was rinsed several times with deionized water to remove medium components from the biomass. The biomass dry weight concentration (g L$^{-1}$) was calculated as the difference between the weight of the filter with and without dried biomass divided by the sample volume.

In this work the unit osmolality (osmol kg$^{-1}$) instead of the more common osmolarity (osmol L$^{-1}$) was used, since osmolality, lacking a volumetric unit, is not as temperature sensitive as osmolarity. The osmolality of the standard medium was 350 mosmol kg$^{-1}$. To examine the effect of osmotic pressure, this standard osmolality was adjusted permanently to the desired value by addition of

sodium chloride. Osmolality was monitored regularly during cultivation. For determination of osmolality, 50 µl of bulk sample were analyzed by freezing-point depression using an Osmometer (Osmomant 030, Gonotec).

The specific activity of fructofuranosidase of bulk culture was quantified by filtration of 1.5 mL culture broth through a cellulose acetate filter (pore size 0,2 µm, Sartorius). The reaction mixture (220 µL) consisted of 200 µL 1.65M sucrose dissolved in 0.05M phosphate buffer (pH 5.4) and 20 µL sample. Reaction was initiated by addition of 200 µL sucrose to a 20 µL sample and incubated at 40°C for 20 min. The reaction was stopped by heating at 95°C for 10 min. After cooling, the reaction mixture was centrifuged at 13,000 g for 10 min at 4°C. Glucose formed from cleavage of sucrose by fructofuranosidase was then quantified using a GOD/POD assay (Sigma–Aldrich) [285], which was modified for high-throughput analysis in 96-well microtiter plates (MaxiSorp, Nunc, Langenselbold, Germany). For this assay an enzyme reagent solution was prepared by re-suspending 10.5 mg glucose oxidase (GOD) and 3 mg of peroxidase (POD) in 90 mL of 0.05M phosphate buffer (pH 7.0) and 10 mL of 95% ethanol containing 25 mg of o-dianosidine, respectively. Subsequently, the reagent solution was filtered through a cellulose acetate filter (pore size 20 mm, Sartorius) and immediately used for the assay. For this purpose, 2 µL sample was mixed with 200 µL of the reagent solution in a microtiter plate well. After 10 min incubation at room temperature, glucose was quantified indirectly through absorption measurement at 450nm using a 96-well Sunrise microplate reader (TECAN, Crailsheim, Germany) and the XFluor4 data retrieval software. To account for residual glucose in the culture broth, negative controls were carried out by using samples in which fructofuranosidase was inactivated by heating at 95°C for 10 min prior to incubation. All enzymatic assays were done in triplicate.

## 3.4   Microscopy and image analysis methods

### 3.4.1   Microscopic examination of A. niger and automatic image analysis

Fungal morphology was characterized using a semiautomatic system consisting of image acquisition by microscopy and a subsequent image analysis. For microscopy image acquisition, approximately 2 mL culture broth sample was taken and suspended in a petri dish containing cultivation medium. Throughout the cultivation culture, morphology was monitored offline using a stereo-microscope (Stemi 2000-C, ZEISS, Jena, Germany) with an AxioCamMRc5 camera (ZEISS, Jena, Germany) with a resolution of 2584 x 1936 pixels, or an all-inclusive all digital inverted microscope (EVOS xl, AMG, Bothell, WA, USA) containing a 3.1 mega pixel color sensor in the maximal resolution of 2048 x 1536 pixels (3.2 µm/pixel). Pictures were taken with 2

and 4x magnification, depending on the experiment. Between 50 and 100 pictures using the same magnification were made per cultivation, containing a minimum of 100 fungal particles, either pellet or mycelial.

Image analysis and characterization was carried out using the ImageJ 1.45 software that is available in the public domain (National Institute of Health, Bethesda, USA). ImageJ was chosen in this study for its robustness and versatility and the more than 400 plugins available to fit the program to personal needs [286]. Each image was converted into an 8-bit grey-scale image. Subsequently a grey-level threshold, calculated by ImageJ using the Otsu algorithm, was applied, resulting in a binary image which was later analyzed using the inbuilt analyze particles function. Only macro-morphologic parameters were considered for image analysis. The morphological parameters evaluated were projected area, perimeter, circularity, solidity, and aspect ratio for mycelial aggregates (clumps and pellets).

### 3.4.2 Fractal analysis and lacunarity

The box-counting method as described by Obert and colleagues [287] was used in this work to assess the fractal dimension of fungal morphology. A picture of the desired object is covered by a grid of the width $\varepsilon$. Subsequently, the number of boxes $N(\varepsilon)$ which overlap with the fungal particle is counted. The number of overlapping boxes $N(\varepsilon)$ changes with the width of the grid $\varepsilon$. For a given picture several grid widths $\varepsilon$ are tried out and related to $N(\varepsilon)$. $N(\varepsilon)$ is proportional to $\varepsilon^{-D}$, where D is the fractal dimension and C is the proportionality constant.

$$N(\varepsilon) = C \cdot \varepsilon^{-D} \ , \qquad\qquad (3.1)$$

Through sampling with various grid widths and grid positions an adequate number of $\varepsilon/N(\varepsilon)$ values can be determined to calculate the fractal dimension D [287-289]. Furthermore, there are boxes wholly contained by the fractal object and boxes which contain or adjoin at least one pixel of the object. $N(\varepsilon)$ is the total number of boxes intersected by the fractal object. Mycelial structures can be mass fractals, where the whole mass of the particle is fractal, or surface fractals, where just the surface of the object is fractal [287, 288].

The method using all boxes for the calculation of the fractal dimension is called box mass (BM) method and the gained fractal dimension is called box mass dimension $D_{BM}$ [288]. $D_{BM}$ describes the whole mass of the object, the space filling capacity and inner structure. The box surface dimension $D_{BS}$ is obtained by using only boxes covering the surface. $D_{BS}$ refers to the surface irregularity of an object. Objects for which $D_{BM}$ equals $D_{BS}$ are true mass fractals with a high

degree of self-similarity and can be described by a single fractal dimension [288]. If $D_{BM} > D_{BS}$, the object is a surface fractal and therefore not a true fractal [290]. Fractal dimensions can be applied for Euclidean figures as well. For a line applies $D_{BM} = D_{BS} = 1$, a circle or rectangle has a $D_{BM}$ of 2 and a $D_{BS}$ of 1 [287].

A fractal based value, which so far has not been used for characterization of fungal morphology, is the so called 'lacunarity'(from latin 'lacuna' for *lack*, *gap* or *hole*), although it has been recently applied for description of micro vascular systems, glia cells and identification of cancer cells [291, 292]. It describes heterogeneity of structure or the degree of structural variance within an object [293], which makes it an auspicious parameter for characterization of clump morphology. Box counting and lacunarity determination were conducted using the ImageJ plugin "Fractal Dimension and Lacunarity" [294]. Lacunarity ($\Lambda$) was determined based on data gathered during non-overlapping box counts using the following formula

$$\Lambda_{\varepsilon,g} = \left(\frac{\sigma_{\varepsilon,g}}{\mu_{\varepsilon,g}}\right)^2 \quad , \tag{3.2}$$

where $\sigma$ is the standard deviation of pixels per box, $\mu$ stands for mean pixels per box, the index $\varepsilon$ is the grid width and the index $g$ is the location of the box [294].

For determination of the surface fractal dimension, the outline function of ImageJ was used previous to analysis, which eliminates all pixels except for a halo of 1 pixel around the particle. Since self-similarity has its limitations for very large and very small objects [287] the grid width $\varepsilon$ was set to be no smaller than a single hyphae and not larger than a large fungal pellet [288].

### 3.4.3  *Microscopy and image analysis of* Taxus chinensis *samples*

Throughout the cultivation, culture morphology was monitored offline using an all-inclusive all-digital inverse-microscope (EVOS xl, AMG, Bothell, WA, USA). *Taxus* cell aggregates were diluted with sodium chloride solution as mentioned above. For picture generation plant cell aggregate solution was pumped (Pro-280 MCP, IDEX Health & Science SA, Switzerland) continuously through a specifically projected and designed flow-through cell (2 chambers, 45 · 8 mm), based on anti-corrosive aluminum and 24 · 60 mm cover slides (Roth, Karlsruhe, Germany). A similar approach was successfully tried and validated for *Streptomyces tendae* [171]. Approximately 50 pictures with a magnification of 10x were taken over a time span of 30 min, obtaining at the very least 400 analyzable single plant cell aggregates for statistical robustness. Image analysis and characterization was carried out using the ImageJ 1.45 software (National

Institute of Health, Bethesda, USA) that is available in the public domain. Each image was converted into an 8-bit grey-scale image. Subsequently, a dynamic threshold [295] was applied to ensure correct detection of partly opaque cells. The dynamic threshold was essential for the software to recognize the outlines of the near-opaque cells. The resulting binary images were later analyzed using the inbuilt Analyze Particles function of ImageJ.

For the purpose of viability estimation of *Taxus chinensis* aggregates, another procedure was used. Microscopic pictures with an even illumination were prepared. In the beginning of the image analysis process, a background flattening procedure (bright background, 40 pixels as typical feature size) was applied in order to obtain a homogeneous background. The intensity of the microscope illumination was kept unchanged for a whole set of slides containing the aggregates to be evaluated. A Gaussian filter (size 7, strength 10) was applied to the whole set of images in order to eliminate high frequency components which may produce small artifacts and rough aggregate contours. Two gray-level thresholds are then manually over a number of sample, one for the living regions within the aggregates ('LiveThres') and the other one for the dead ones ('DeadThres'). Then for the whole set of images, both thresholds were applied to the images to obtain the respective total areas in order to evaluate the viability ratio. **Figure 3.1** shows a typical processed image.
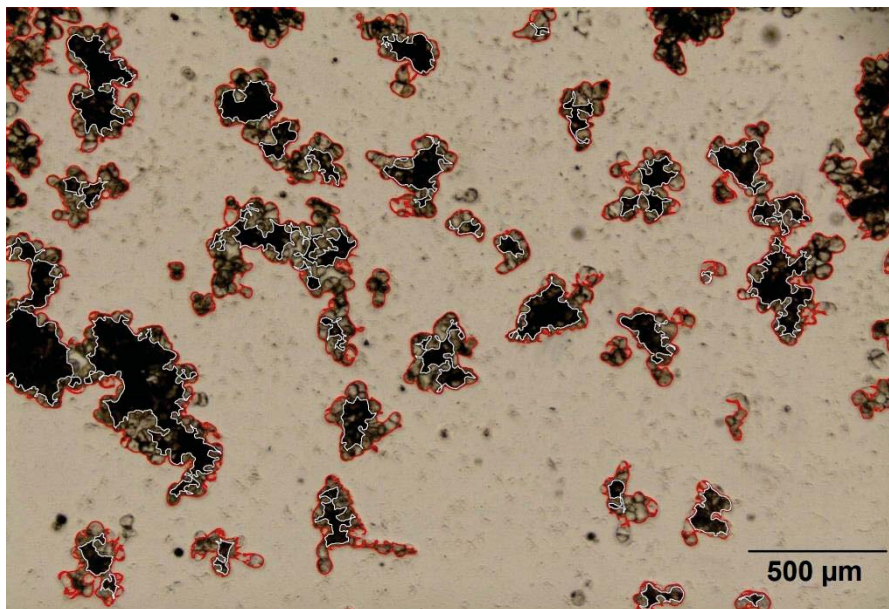


**Figure 3.1:** Evaluation of dark and grey area for estimation of viability. The healthy area is depicted in red, dead/unhealthy are dark with a white border.

## 3.5    Measurement of particle size by laser diffraction

The Mastersizer 2000 (Malvern Instruments, Worcesterchire, UK) was used for characterization of *A. niger* particles and *Taxus* aggregates by laser diffraction. The system is based on a helium-neon laser ($\lambda = 632.8$ nm) as a radiation source, which illuminates the dispersed aggregates in the measuring zone, and a series of detectors to measure the light pattern produced over a wide range of angles. The lower limit of the obscuration was set to 5%, which was high enough to achieve a good signal to noise ratio; the upper limit was 30%, which was below the limit defined by the detector dynamics and the algorithm treating multiple scattering. The dispersant cultivation medium approximated the optical properties of water. Both scattering angle and scattering intensity were dependent on the size of the measured particles. The diffraction of laser light on the dispersed aggregates resulted in a specific diffraction pattern, which was collected by the detectors and recorded by the software (Mastersizer 2000 software, version 5.60, Worcesterchire, UK). By applying an appropriate optical model (Fraunhofer Approximation) to calculate the scattering pattern and a mathematical de-convolution procedure, the volumetric particle size distribution that best matched the measured scattering pattern was calculated. There was no need to determine the exact optical properties of the biological sample, because for particles $> 50$ μm, like *Taxus* cells or most fungal particles the Fraunhofer Approximation can be used to calculate particle size distributions without knowledge of the optical properties [296, 297].

Plant cell aggregates or fungal particles were diluted in sodium chloride solution with the same osmolality as the culture medium. Dilution was prepared to reach a specific particle concentration required for the measurement. Sample measurement time was 15 seconds, resulting in a total of 15,000 snaps to be averaged, with an interval of 60 seconds between measurements. Five measurements were made for each sample and an average was taken.
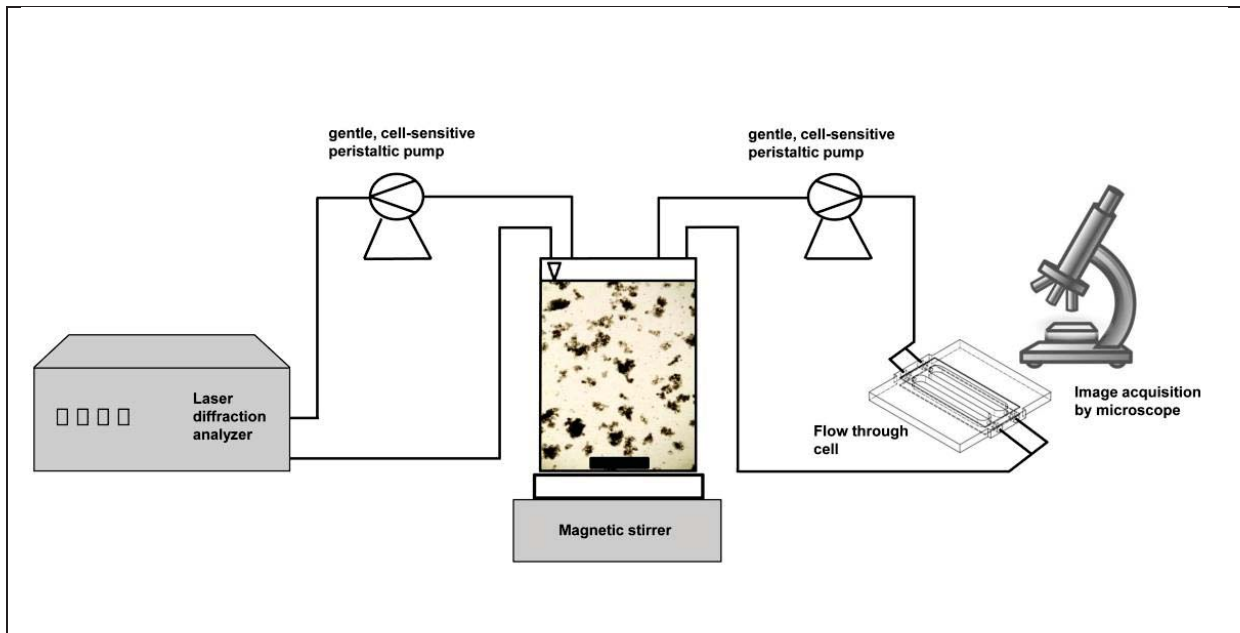
51

**Figure 3.2:** Set-up of equipment for continuous measurement of plant cell aggregate size. The flow through cell for microscopic image acquisition is made of two chambers 45 · 8 mm with a 2 mm orifice. The cavities are covered by two removable 24 · 60 mm microscopic cover slides.

Laser diffraction is a system mainly used for particle size analysis of inorganic material. To measure organic material which is usually very shear sensitive, the experimental set up had to be adjusted. For measurement of particle size, culture broth was pumped permanently to and from a 500 mL measurement beaker through the Mastersizer measuring cell. A peristaltic pump specifically designed for gentle pumping (Pro-280 MCP, IDEX Health & Science SA, Switzerland) was used to transfer the sample from a bioreactor or measurement beaker (**Figure 3.2**), instead of the original Hydro$^{TM}$ sample dispenser provided by the manufacturer.

This set up enabled a continuous operation and a shear stress-reduced environment. Several different kinds of pumps were tested for their influence on aggregate integrity. Gear pumps and conventional peristaltic pumps led to a comminution of biological aggregates up to 20 % (data not shown). Only the Pro-280 MCP manufactured by IDEX Health & Science SA showed no quantifiable impact on *Taxus* aggregate stability over a measurement period of 5 hours (**Figure 3.3**). Because of the large size of *Taxus* cells and aggregates, which were not smaller than 60 μm, the Fraunhofer Approximation, valid for this size range, was used to calculate the size distributions from scattering data [296, 297].
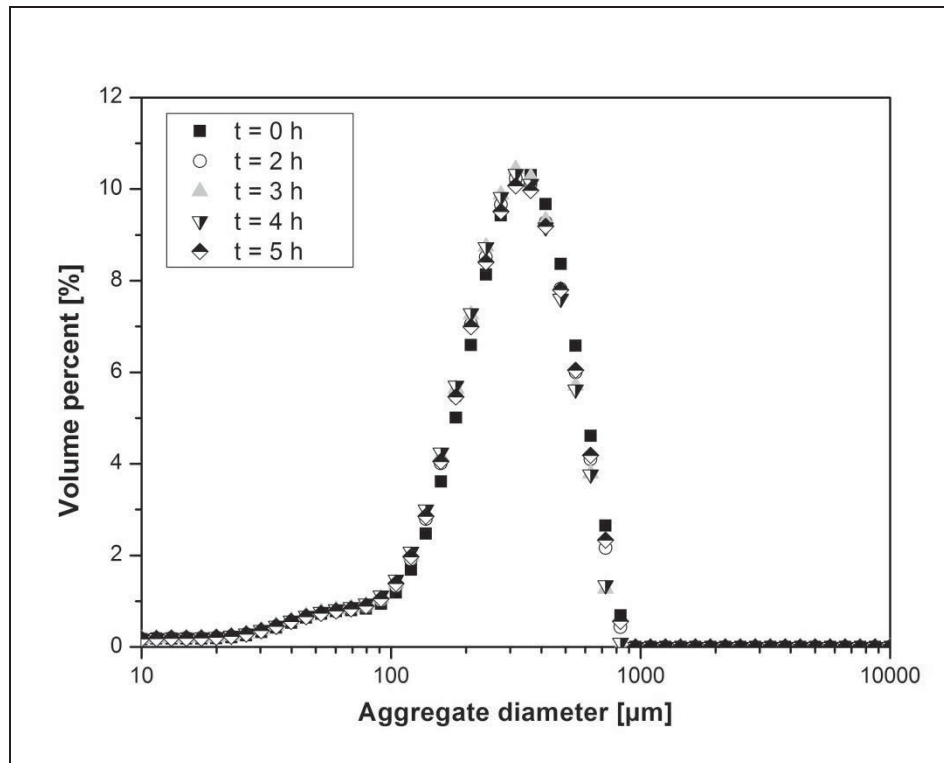
**Figure 3.3:** Measurement of *Taxus* aggregate size during 5 h of continuous operation.

## 3.6    Analysis of culture broth viscosity of *A. niger* cultivation broth

The estimation of suspension viscosity is a difficult and complex task, as it is related to mixing and mass transfer, including the Reynolds number and correlations for volumetric mass transfer coefficient $k_La$ [186]. Culture broth rheology is mostly determined by offline viscosity measurements. However, the appropriate instrument, the method of measurement, and representative sampling should be considered with utmost care, because viscosity is an intrinsic property of the fluid and should not be influenced by the measuring technique [175]. When dealing with heterogeneous and particulate solutions such as filamentous culture broths, special care should be taken. Common methods, such as the cone and plate or plate and plate systems for rotational viscometers, cannot be applied, as the culture is too inhomogeneous. Clumps and pellets are usually so large that a compliance with good rotational rheological measurement practice [298] is virtually impossible and results are hence not reproducible. Cone and plate systems were used in some studies, however, mostly with very unconventional gap sizes of up to 2 mm [186].

Rheological measurements in this work were performed using a rotational viscosimeter (Bohlin CS10, Malvern Instruments, UK), which works according to the principle of Searle. Numerous measurement systems and techniques were tried out. A double gap system was usable only up to a biomass concentration of 7 g L$^{-1}$. Furthermore, results tended to get unreliable as soon as a certain

53

maximal pellet dimension of around 1000 μm was reached. Only a four bladed vane tool (V25 Vane Tool, Malvern Instruments, UK) led to a reproducible resilient results and was therefore selected for further experimentzt. 100 mL sample was measured while the temperature was maintained at 37 °C. Because of differing biomass concentrations in the samples, the range of shear rates retaining laminar conditions changed. Rheology was accordingly measured at a shear rate range of 10 to 400 s$^{-1}$. Below a shear rate of 10 s$^{-1}$ some settling was observed: beyond 400 s$^{-1}$ conditions became turbulent, preventing reliable measurements. A measurement incorporated 25 data points and took 5 min, including 30 s of pre-shearing at 50 s$^{-1}$ to counter sedimentation issues. As in most studies [43, 175, 176, 182, 192, 195, 289, 299], the power law of Ostwald-de Waele was used to describe the rheological behavior of the cultivation broth. The Herschel-Bulkley relationship preferred by some authors [186] did not lead to a significant better fitting and was therefore not applied.

## 3.7 Calculation of specific productivity

Cultivation performance was, in general, judged by the activity of the produced enzyme fructofuranosidase. As units, the yield per volume of cultivation broth (U mL$^{-1}$) and specific yield per biomass cell weight U mg$^{-1}$ were measured at the end of cultivation. For determination of specific productivity, the growth curve of the microorganism, using biomass dry weight (BDW) as biomass was integrated, yielding the biomass dry weight integral (BDWI).

$$Biomass\ Dry\ Weight\ Integral\ (BDWI) = \int_{t1}^{t2} BDW \cdot dt \tag{3.3}$$

The BDWI was therefore calculated by:

$$BDWI_{t2} = BDWI_{t1} + \left[ \frac{(BDW_{t1} + BDW_{t2})}{2} \cdot (t_2 - t_1) \right] \tag{3.4}$$

Subsequently, the specific productivity (U mg$^{-1}$ h$^{-1}$) was obtained by plotting the enzymatic activity of the enzyme over the BDWI, providing an approximate linear relationship with the slope being equal to the specific productivity of the process

$$Specific\ productivity = \frac{dU}{dBDWI} \tag{3.5}$$

## 3.8 Statistical analysis

To test for statistically significant differences between samples, the Monte Carlo method was applied [300]. Sample data, within the standard error previously determined by experimentation, was evaluated using Matlab (MathWorks, United States). The data sets were used in a paired t-test ($p < 0.05$) conducted with Origin (Originlab, USA) to test for statistical difference between experiments.

# 4 Results and Discussion

## 4.1 Morphology – a sensitive process parameter in filamentous cultivations

### 4.1.1 Morphological quantification by image analytic methods

The accurate characterization of fungal morphology remains a key target for industrial biotechnology and image analysis methods are central for achieving this goal [21]. There have been many attempts to link the product yield of an expressed product to the specific morphological growth form of an organism [9]. In industrial processes, performance is often related to morphological appearance; however, information is mostly based on the experience of attending personnel and an accurate quantification method is essentially lacking. Early morphological investigations incorporated a laborious manual measurement of morphological traits per microscope. These studies generated lots of data, but only for a very limited amount of examined particles. Only 3 to 5 particles, for example, were studied during kinetic investigations of fungal growth conducted by Trinci et al. [21, 64], which involved printing of a microscopic picture and manual measurement. Since the proliferation of computer hardware and software, such data collection has become much easier. The software-assisted automatic image analysis allows the collection of detailed measurement of various morphological forms of filamentous fungi [62, 80] and a quantitative characterization of the relationship between fungal morphology and productivity [133]. Structured models based on singular image analysis parameters were used to describe growth of filamentous fungi [79]. Fungal morphology is usually characterized in terms of macromorphology, which is basically the process of pellet, clump or mycelia formation, or micromorphology, specifying properties of these growth forms like branching frequency, hyphal dimensions, the number of tips, and segregation [173]. Despite these advances, automated morphological quantification is still underrepresented or missing in too many recent studies [301-304]. Other authors use only qualitative morphologic descriptions, which heavily depend on the observer [305-307].

Since mycelial morphology as investigated was mostly in the form of clumps or pellets, parameters of particle size and shape, like projected area, perimeter, circularity, solidity and aspect ratio were considered in the present study. Because of greater industrial applicability and easy reproducibility mainly macro morphologic parameters were considered for morphologic description. Micromorphology was not taken into account for reasons of practicability, since an easy reproducible method to characterize fungal morphology with statistical significance was preferred over a laborious collection of micro morphological data from a few pellets.

56

Circularity is a parameter to quantify the closeness of an object to a perfect circle (**Table 4.1**), with a value of 1.0 indicating a perfect circle and an irregular object having a value closer to 0. Solidity is a measure of the surface of a particle, also known as roughness. It is calculated by dividing the projected area through the convex area. The convex area being the area enveloped by the convex hull perimeter, which can be illustrated as an elastic band placed around the particle; it is essentially a perimeter of an object with all the concavities filled. A smooth shape has a solidity of 1.0. Irregular objects tend to have a much lower value for solidity. Solidity is a good approximation of the surface area of the fungal pellet being available for mass transport. Aspect ratio is defined as major axis divided by minor axis, and is a measure of elongation of a particle. A shape symmetrical in all axes, such as a circle or square, will have an elongation value of 1.0, whereas elongated particles will possess considerably larger values. A complete review of sample preparation, image analysis techniques and definitions was given by Paul and Thomas [62] in their review on characterization of mycelial morphology using image analysis.

**Table 4.1:** Image analytical parameters used for morphological description of fungal particles

| Parameter | Formula | Description |
|---|---|---|
| Aspect ratio | $E = \dfrac{[Major\ axis]}{[Minor\ axis]}$ | Parameter describing the elongation of an particle |
| Circularity | $C = 4\pi \cdot \dfrac{A}{P^2}$ | Deviation of the object from a perfect circle |
| Ferret's Diameter | $D_F$ | The longest distance between any two points along the particle boundary |
| Perimeter | P | The length of an objects boundary |
| Projected area | A | Two dimensional area of an particle, sum of all pixel representing the object |
| Solidity | $S = \dfrac{A}{[Convex\ area]}$ | Measure of the surface properties of a particle like roughness, Convex area is the area of an object with all concavities filled |

In early experiments, susceptibility of *A. niger* SKAn 1015 morphology towards culture broth osmolality was discovered. This dependency was used to create several 2 L batches with a variable morphology, ranging from dense pellets to homogenous mycelia. The culture broth from these batches which gave a nice overview of *A. niger* morphology, was used to test the applicability of the introduced image analytic parameters for quantitative description of *A. niger* SKAn 1015 morphology (**Figure 4.1**). Although numerous parameters have been introduced, irregular structures of mycelial particles and structures lying between the two extreme forms of pellet and mycelial morphology are still difficult to be described by using only a single parameter [288],

which is also evident from  Figure 4.1, where the change of particle shape parameters is depicted for various morphological forms of *A. niger* SKAn 1015.
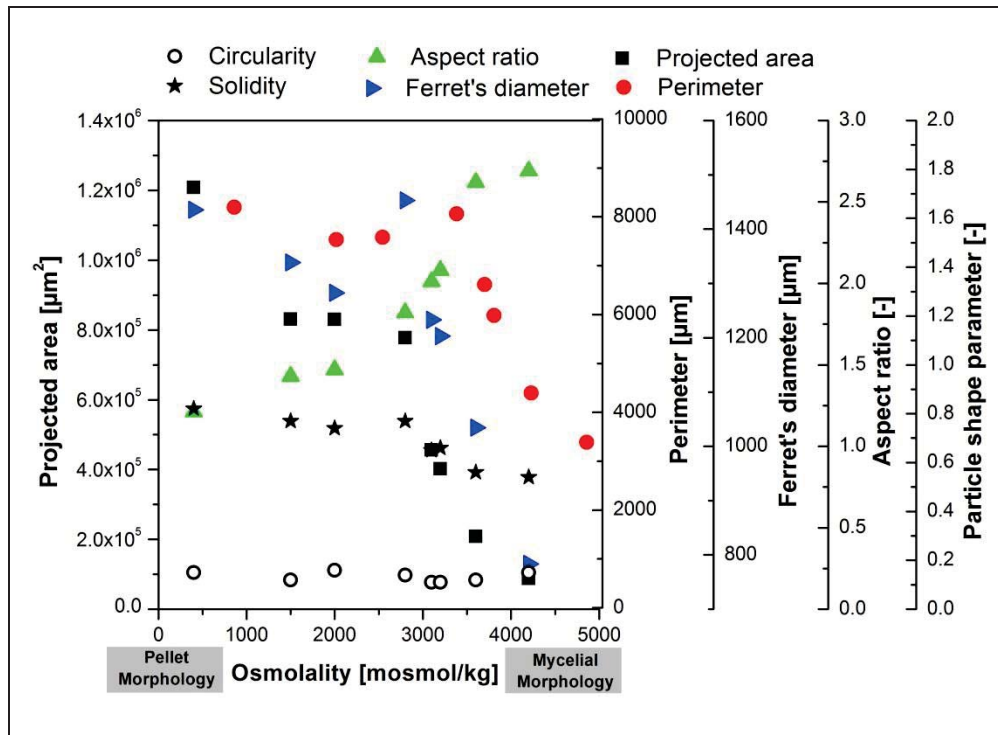


**Figure 4.1:** Development of image analytic parameters for 2 L cultivations of *A. niger* SKAn 1015 with variable morphology

Except for circularity, all parameters change significantly when different morphological growth forms are compared. However, the number of parameters which have to be considered make a quick quantification of fungal morphology troublesome. This phenomenon is known from chemical engineering issues, where correlating parameters are typically combined with dimensionless numbers like the Reynolds number, because application of all relevant parameters doesn't produce a curve, but something similar to a sky full of stars [308].

Therefore an effort was undertaken to combine relevant parameters from image analysis to a dimensionless Morphology Number (MN), which can be used for a holistic characterization of morphology. A similar approach was proposed by Blott and colleagues [3], who stated that no single quantitative measure could provide a full description of three-dimensional shape, and the use of several shape indices in combination provides the best method of grouping and discriminating between particles. Filamentous fungi can either grow as pellets or as mycelia. Between these extremes, there is a whole span of intermediates, like elongated irregular pellets or clumps. Accordingly, the following formula was introduced to combine the relevant morphological parameters observed:

58

$$Morphology\ Number\ (MN)\ \equiv \frac{2 \cdot \sqrt{A} \cdot S}{\sqrt{\pi} \cdot D_F \cdot E} \tag{4.1}$$

where A is the projected area, S is the image analysis parameter solidity, $D_F$ is the Feret's diameter of the pellet, and E is the elongation (aspect ratio) of the particle. Due to A and $D_F$, the magnitude of MN depends on the size of the pellets. Through the parameter E, the general shape of fungal particles is considered. Moreover, surface properties of the pellets are accounted for by the image analytic parameter S. Through introduction of the scaling factor $\frac{2}{\sqrt{\pi}}$, it is ensured that MN for true two-dimensional morphologic structures will have values between 0 and 1. Perfectly round and smooth pellets will in microscopic images appear as perfect circles. For such particles the MN has a value of 1, as the square root of the projected area ($\sqrt{\frac{\pi}{4}D^2}$) cancels itself out with the scaling factor and the Feret's diameter, aspect ratio and solidity will have values of 1. The smallest fragment of mycelial morphology can be simplified as a one-dimensional line or hyphae yielding a MN of zero. All intermediate morphological forms will therefore have values between 0 and 1, because the denominator will become significantly larger than the numerator. Fairly large particles will result in a high MN, elongated particles, or those with a large surface, in a low MN.
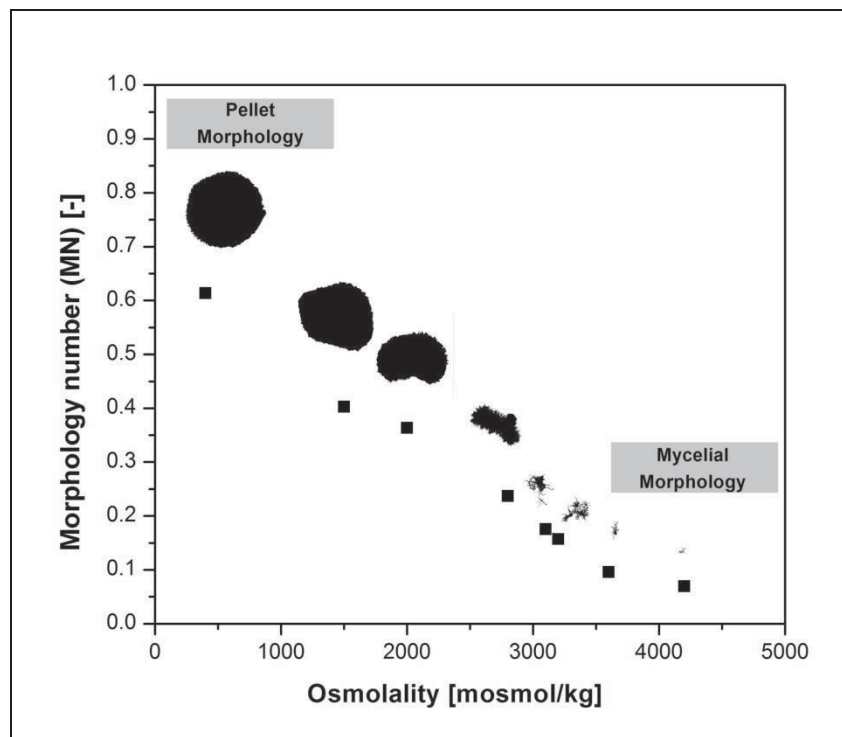


**Figure 4.2:** Combination of image analytical parameters from Figure 4.1 to a dimensionless Morphology number (MN)

When particle shape parameters from Figure 4.1 are combined to the dimensionless Morphology number (MN), a clear, almost linear trend with an increase of osmolality is evident (**Figure 4.2**). Over the whole range of fungal morphology, from large and dense pellets to small and sparse mycelia a general compliance of the MN and the actual change of morphology is apparent. This dimensionless number enables a distinct quantification of fungal morphology, and will help to establish specific morphologic models. However, for thorough comparison of mycelial morphologic growth forms which differ only in the number of tips or branching rates, other means of characterization have to be employed.

Describing mycelia quantitatively essentially involves estimating their space-filling capacity [288]. Like many other natural structures, mycelia are approximately fractal [287]. The concept of fractals was first introduced by Mandelbrot [309] as an extension of the conventional (Euclidean) geometry. Fractal geometry provides the means to describe objects in a non-integer or fractional way. Fractal objects have a quantity known as "self-similarity", as they appear qualitatively the same, irrespective of magnification. Fractal geometry might therefore be a useful measure of complexity [293].

The fractal dimension D can be associated with structural complexity [293, 310]. A fractal dimension between 1 and 2, for example, describes the area filling capacity of an object; a fractal dimension between 2 and 3 is a measure of the volume filling capacity for objects between surface and volume dimension [288]. The fractal nature of mycelia has been studied at two distinct levels using the measures of the surface fractal dimension (box surface dimension $D_{BS}$) and the mass fractal dimension (box mass dimension $D_{BM}$), making it possible to discriminate between systems which are fractal only at their boundaries, like pellets, and true mass fractals like mycelia [290]. To discriminate between pellet and mycelial morphology a fractal quotient, made up of $D_{BM}$ divided by $D_{BS}$ can be used. For ideal mycelia, being true fractals, this fractal quotient should be one, whereas pellets will have values up to two.

To test the suitability of fractal parameters for characterization and quantification of fungal morphology, osmolality was used to specifically create 45 different morphologic forms in shaking flask culture. Fungal particles analyzed for this study were between 0.27 and 2 mm of size. **Figure 4.3** shows the development of fungal morphology with increasing osmolality.
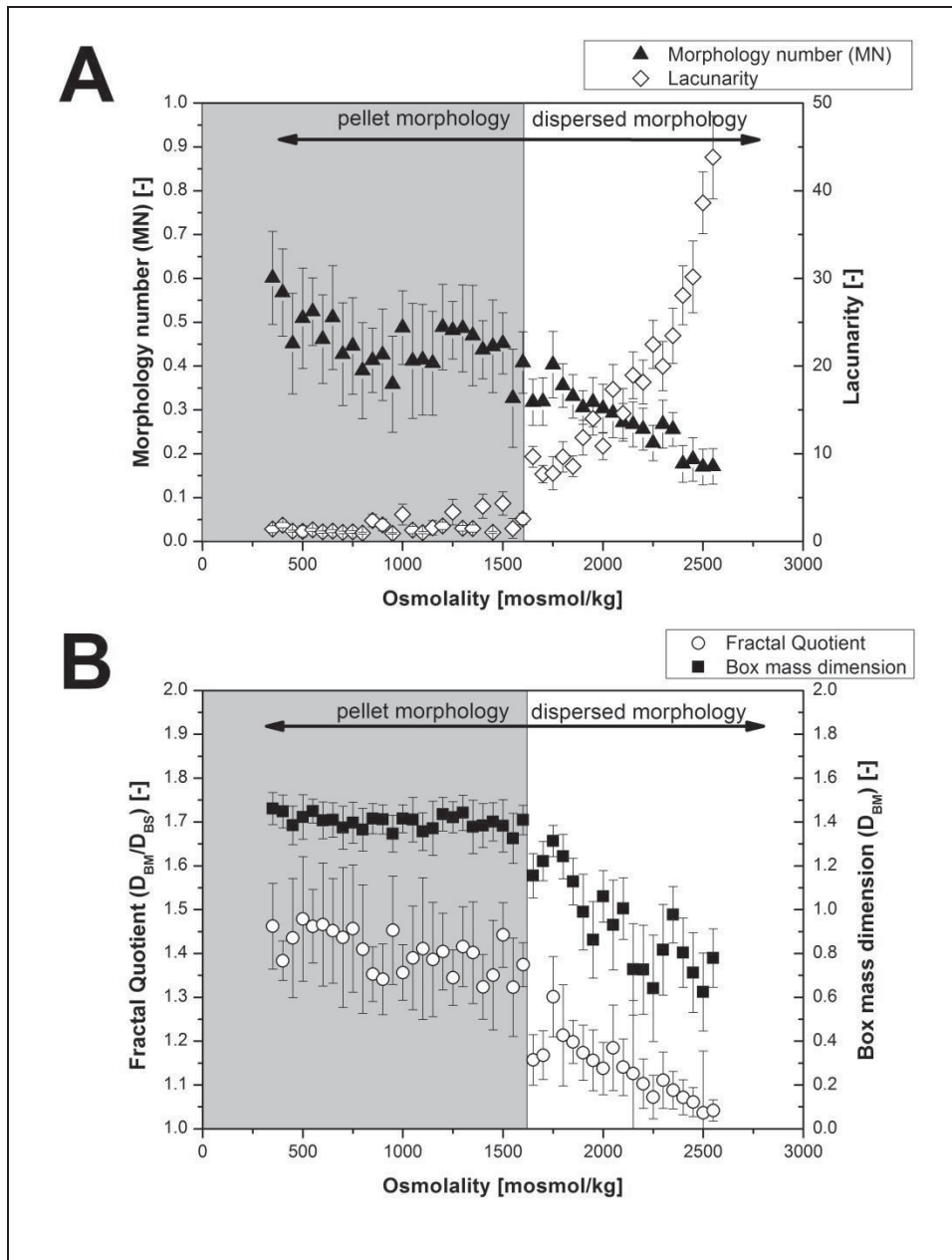


**Figure 4.3:** (A) Development of the Morphology number (MN) and lacunarity ($\Lambda$) as well as (B) the fractal quotient ($D_{BM}/D_{BS}$) and box mass dimension with increasing culture broth osmolality. At around 1600 mosmol $kg^{-1}$ a change from mainly pellet morphology to a mostly disperse morphology can be observed. Error bars are means for three shaking flask cultivations of *A. niger* SKAn 1015.

The Morphology number (Figure 4.3 A) decreases from around 0.5 at an osmolality of 350 mosmol $kg^{-1}$ to 0.2 at an osmolality of 2550 mosmol $kg^{-1}$, illustrating a change from spherical pellet form to an almost perfect mycelial morphology. Basically, pellet morphology can be

observed up to an osmolality of about 1600 mosmol kg$^{-1}$; beyond that *A. niger* morphology is mycelial. While pellet morphology is exhibited, standard deviation is generally higher and a considerable fluctuation is apparent. This is due to a generally high heterogeneity of pellet size, which is one of the most important parameters making up the Morphology number.

In Figure 4.3 B the fractal quotient $D_{BM}/D_{BS}$ and the box mass dimension $D_{BM}$ of fungal particles are depicted as affected by increased osmolality. Both values stay almost constant as long as pellet morphology is exhibited; $D_{BM}$ stays constant at around 1.7, $D_{BM}/D_{BS}$ decreases just barely from 1.45 at standard osmolality of 350 mosmol kg$^{-1}$. Starting with an osmolality of 1550 mosmol kg$^{-1}$ both parameters decrease gradually until at 2550 mosmol kg$^{-1}$ $D_{BM}/D_{BS}$ is 1.0 and almost true fractal mycelial morphology is exhibited. Fractal analysis can obviously be used as a tool to discriminate between pellet and filamentous morphology, and even different mycelial morphologic forms. No significant change of the fractal quotient is obvious while pellet morphology is exhibited, suggesting no morphological change. However, pellets did become smaller from 350 up to 1550 mosmol kg$^{-1}$ while staying approximately spherical. Conventional image analysis parameters, such as the MN in Figure 4.3 A, take into account this change through inclusion of the parameters area and solidity. Obviously, this change in size cannot be detected by analysis of fractal dimensions alone.

The computation of fractal dimensions cannot always provide unique or definite descriptions, the same way, that size or weight are not sufficient for particle description. Due to this shortcoming, a second fractal dimensional parameter, lacunarity $\Lambda$, was considered for further differentiation between sets and textures that share the same fractal dimension values, but which still look different [311], as it is the case with *A. niger* SKAn 1015 pellet morphology. $\Lambda$, as a measure of how data fills space, complements fractal dimension, which basically measures how much space is filled [312]. In Figure 4.3 A it is shown that $\Lambda$ takes an exponential trend with increasing osmolality. This parameter takes into account that fungal pellets at higher osmolality are generally more heterogenic with a higher variance in room filling capacity of the particle, for example through gaps or uneven surface. Between 350 and 1000 mosmol kg$^{-1}$, pellet texture and surface changes only marginally. At higher osmolality, the texture filling capacity of fungal pellets is beginning to change marginally, causing a change in $\Lambda$ from 1 to around 5. $\Lambda$ increases exponentially as soon as the transition from pellet to a dispersed morphological form takes place at 1550 mosmol kg$^{-1}$, meaning a significant change in the morphologic form from compact and rather spherical structures to elongated and porous heterogenic structures. $\Lambda$, as a parameter is exceptionally eligible to describe this transition, but is not suited for comparison of various pellet

morphologies. Similarly, fractal dimension, in the form of the introduced fractal quotient, is not applicable to the whole range of fungal morphology, but only to disperse growth forms of *A. niger* SKAn 1015. Generally, the MN seems to be most useful for overall characterization of *A. niger* morphology, whereas the $D_{BM}/D_{BS}$ and lacunarity $\Lambda$ seem to be more suited to compare different disperse growth forms.

Of all the studies where fractal analysis was applied to characterize fungal morphology only very few authors tried to link fractal dimension with conventional image analysis parameters. Barry and colleagues [290], for example, showed a relationship between fractal dimension and hyphal growth unit of a *Penicillium* and an *Aspergillus* strain. Another attempt to relate fractal dimension with conventional image analysis parameters was made by Finkler and colleagues [313]. They found a very approximate linear correlation ($R^2 = 0.61$) between the convexity of an examined object and its surface fractal dimension. In the present study, a linear correlation between a conventional image analysis parameter and a fractal parameter could be found as well (**Figure 4.4**). The Morphology number MN correlated ($R^2 = 0.85$) with the fractal quotient $D_{BM}/D_{BS}$.


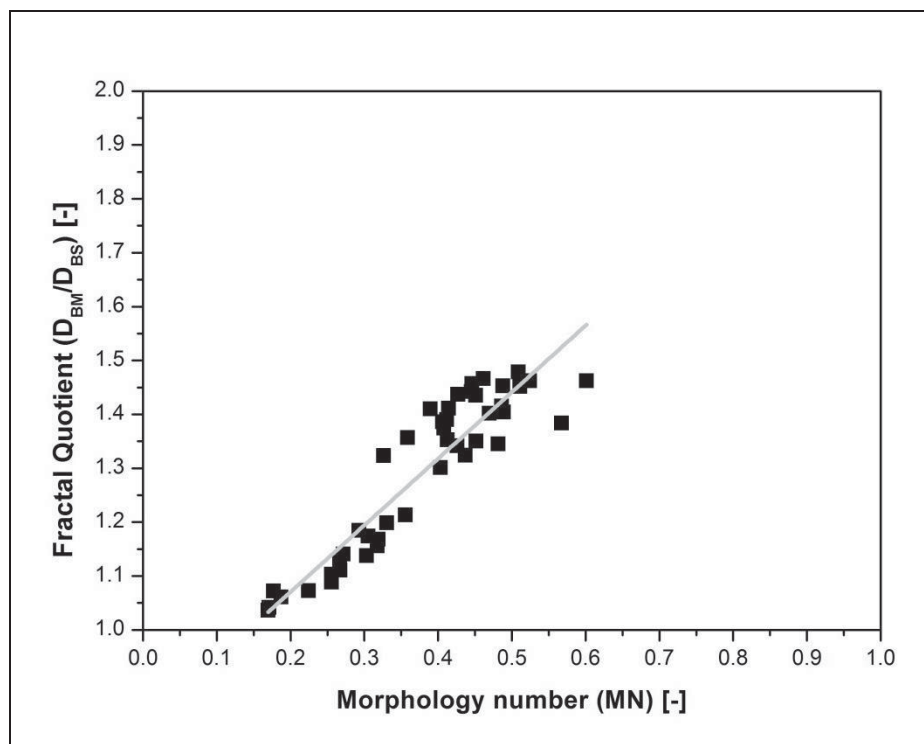
**Figure 4.4:** Correlation of conventional image analysis parameter Morphology number (MN) with the fractal quotient ($D_{BM}/D_{BS}$) ($R^2 = 0.85$). Each dot represents a mean of three 100 mL shaking flask cultivations of *A. niger* SKAn 1015.

### 4.1.2 Osmolality a novel method to improve process performance

The influence of culture broth osmolality on fructofuranosidase production of *A. niger* SKAn 1015 was studied in bioreactor and shaking flask experiments. In about 50 2 L bioreactor cultivations, it was shown that an increase of osmolality in the medium from the standard 400 to 4,900 mosmol kg$^{-1}$ led to a considerable decline in dry cell weight from around 4 to 0.2 g L$^{-1}$, respectively. The growth rate was also reduced (data not shown). Meanwhile, the specific productivity, as defined in chapter 3.7, increased remarkably from 0.5 to 9 U mg$^{-1}$ h$^{-1}$, around eighteen fold (**Figure 4.5** A).



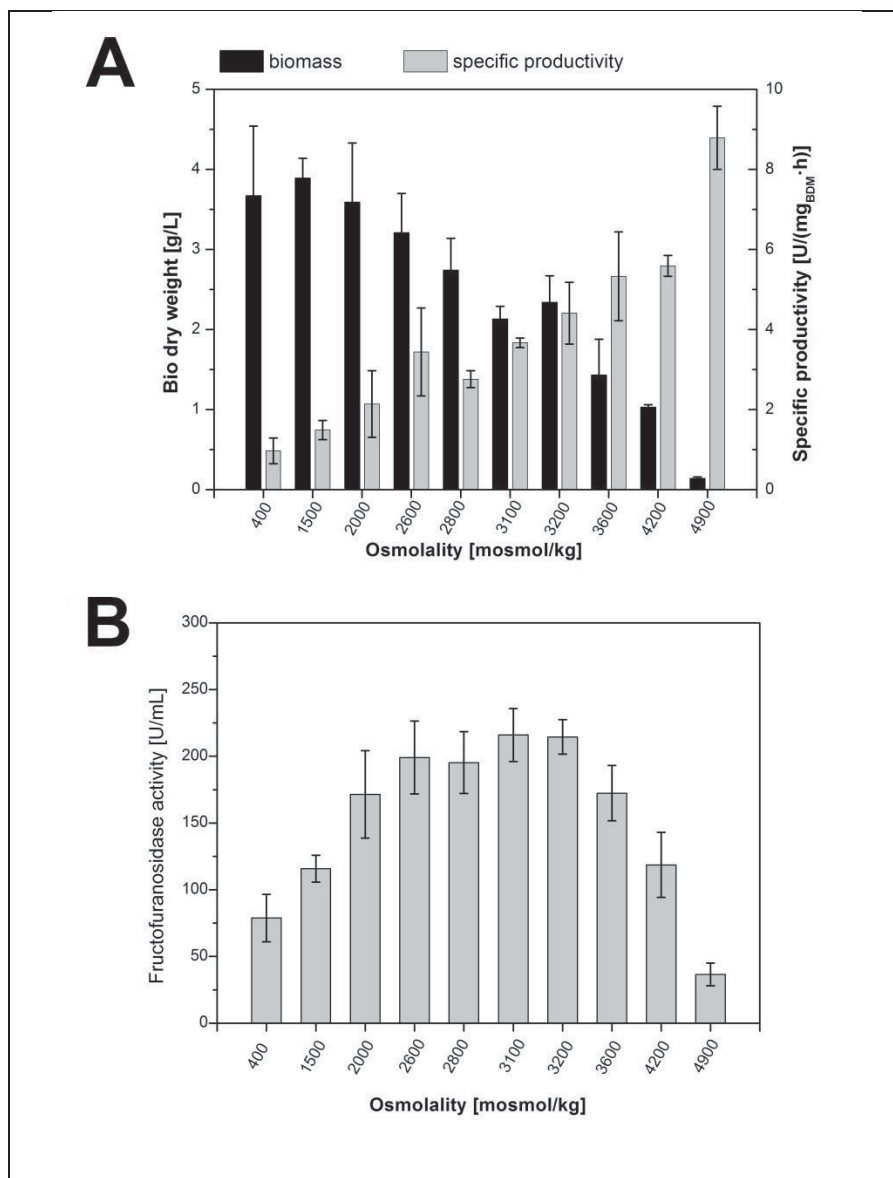**Figure 4.5:** (A) Biomass dry weight (black) and specific productivity (grey) after 72 hours of cultivation of *A. niger* SKAn 1015 at 10 different culture broth osmolalities. The corresponding fructofuranosidase bulk activity [U mL$^{-1}$] is shown in (B). Values are means for at least three 2L cultivations. Culture broth osmolality was increased permanently with sodium chloride prior to inoculation.

This distinct increase is somewhat put into perspective by considering fructofuranosidase bulk activity as depicted in Figure 4.5 B. Up to an osmolality of 2,600 mosmol kg$^{-1}$, the fructofuranosidase bulk activity increased about two and a half times. Optimal fructofuranosidase activity of 220 U mL$^{-1}$ was detected at an osmolality of about 3,000 mosmol kg$^{-1}$. To find the optimal osmolality for the process, a considerable amount of cultivations were conducted at similar osmolality. Thus, osmolality between cultivations (around 3,000 mosmol kg$^{-1}$) was varied only marginally. An osmotic pressure of more than 3,200 mosmol kg$^{-1}$ reduced the volumetric fructofuranosidase activity. Thus, an addition of 1.5 M sodium chloride to the cultivation medium was shown to be beneficial for fructofuranosidase production. For the glucoamylase producing strain *A. niger* AB 1.13, a similar increase of productivity was shown by Wucherpfennig and colleagues [253].

In shaking flasks, considerably more cultivations could be conducted. Here, osmolality was increased by addition of sodium chloride from 350 mosmol kg$^{-1}$ (standard) up to 2,550 mosmol kg$^{-1}$, in steps of 50 osmol kg$^{-1}$. Similar to the cultivations in the bioreactor, biomass decreased from 7 g L$^{-1}$ to around 1 g L$^{-1}$, when culture broth osmolality was increased permanently prior to inoculation (**Figure 4.6**). Biomass in shaking flask culture was generally much higher than in the bioreactor. Specific fructofuranosidase activity increased 12 fold to 84 U mg$^{-1}$ during the investigated range of osmolality. In contrast to the bioreactor cultivations, only the specific activity after 72 hours of cultivation could be considered. Bulk fructofuranosidase was increased 2.4 fold from 50 to 133 U mg$^{-1}$ by an increase in osmolality from 350 to around 1800 mosmol kg$^{-1}$. Interestingly, optimal osmolality for fructofuranosidase production was considerably different than in the bioreactor. Bulk activity of fructofuranosidase was optimal between 1800 and 2200 mosmol kg$^{-1}$, but declined if osmolality was raised beyond that value (Figure 4.6).
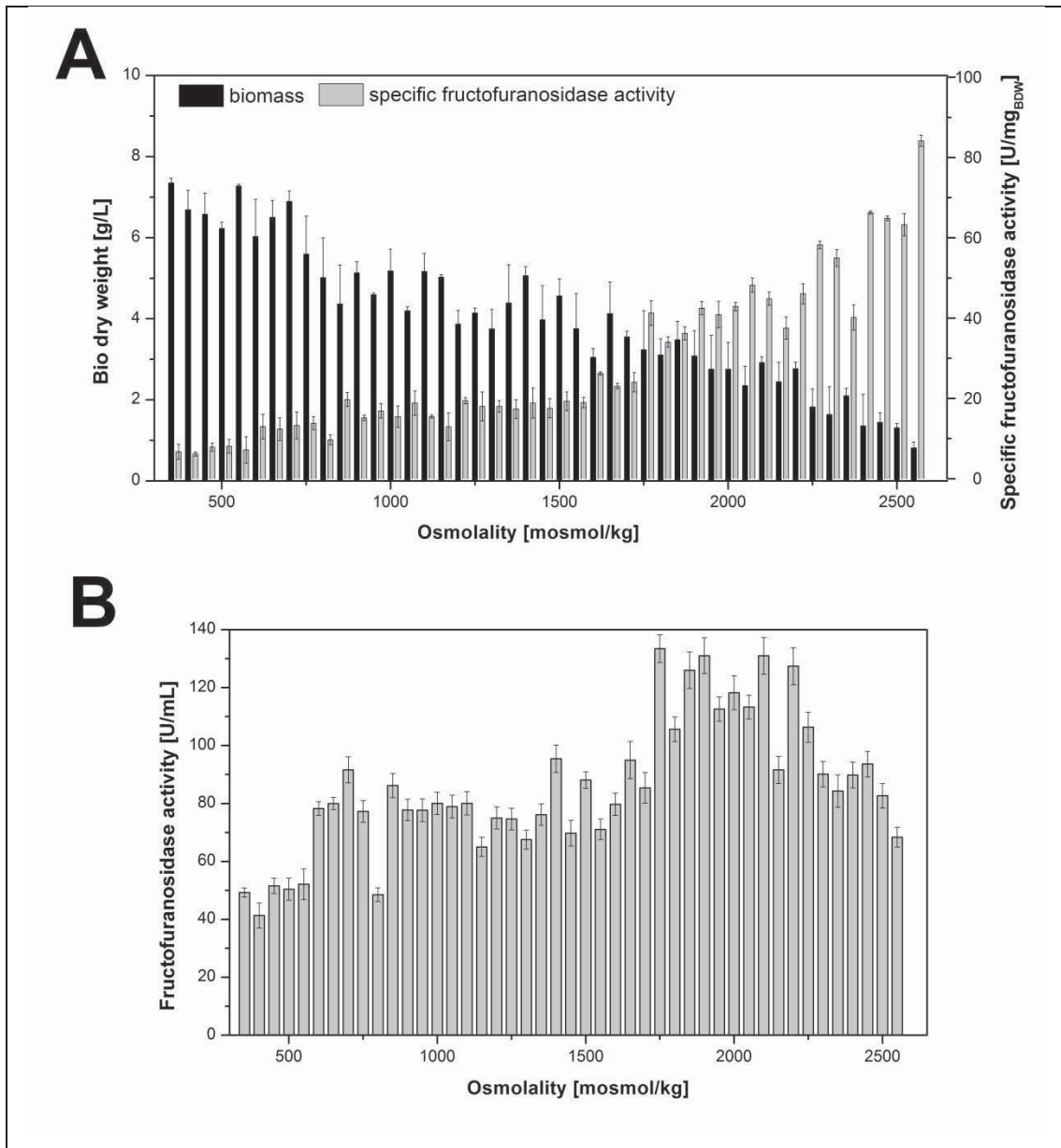
**Figure 4.6:** (A) Biomass dry weight (black) and specific productivity (grey) after 72 hours of cultivation at 45 different culture broth osmolalities. The corresponding fructofuranosidase bulk activity [U mL$^{-1}$] is shown in (B). Values are means for at least three 100 mL shaking flask cultivations of *A. niger* SKAn 1015. Culture broth osmolality was increased permanently with sodium chloride prior to inoculation.

Increased osmolality was, in summary, beneficial to fructofuranosidase production on 2 L bioreactor and 100 mL shaking flask scales. Within the bioreactor considerably more enzyme was produced at a comparatively higher optimal productivity. Since bioreactor cultivations had less biomass than shaking flask cultures, this biomass was therewith much more active. Bulk activity of expressed enzymes only increased up to optimal osmolality, whereas the positive effect of increased productivity outweighed the decrease in biomass. The optimal productivity for production purposes extended over a greater range for bioreactor cultivations, whereas fructofuranosidase activity started to decrease at an osmolality greater than 2,200 mosmol kg$^{-1}$.

To investigate whether increasing osmolality interfered with the fructofuranosidase assay, culture supernatant from a 2 L bioreactor cultivation with 400 mosmol kg$^{-1}$ was sterile filtered. In one half of the sample, the osmolality was increased up to 2,400 mosmol kg$^{-1}$ through addition of sodium chloride; the other half of the sample was left untreated. Subsequently, the fructofuranosidase assay was performed for both samples. The samples with 54.6 ± 0.4 U mL$^{-1}$ were found to have the same fructofuranosidase activity, ruling out the influence of osmolality on the fructofuranosidase assay used in this study. Moreover, no significant impact on dissolved oxygen within the bioreactor could be measured while increasing the osmolality of the cultivation broth, suggesting that osmolality had no effect on the availability of dissolved oxygen for microorganisms.

According to previous studies production of proteins by *A. niger* could be elevated after an administration of an osmotic shock to the culture [146, 147]. In the present study, an osmotic shock significantly increased enzyme activity only when administered to culture broth of standard osmolality (**Figure 4.7**).
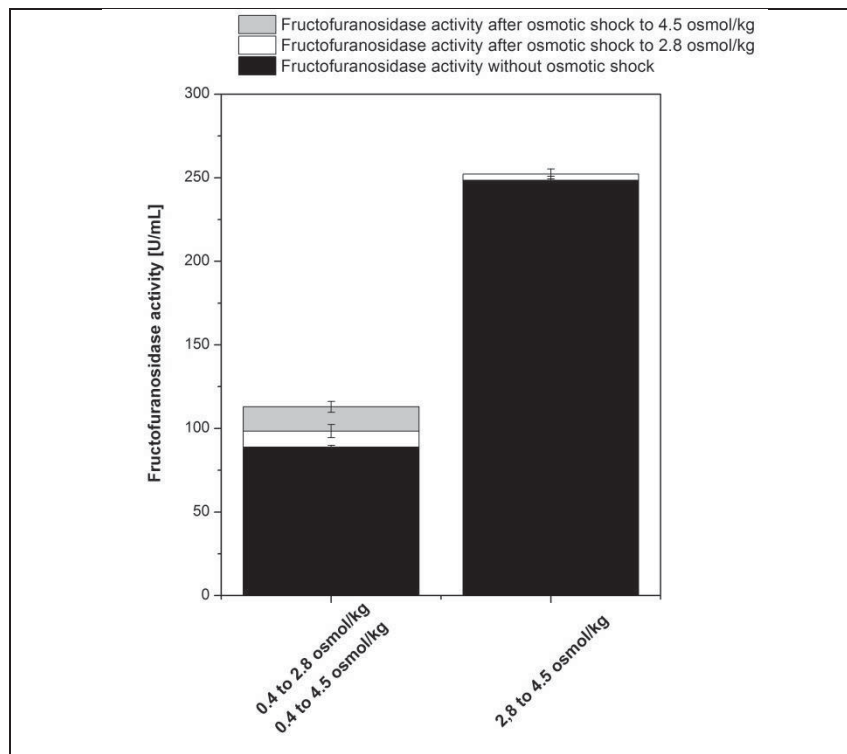


**Figure 4.7:** An osmotic shock was administered to two *A. niger* SKAn 1015 samples, each with different culture broth osmolality. *A. niger* SKAn 1015 was cultivated at 400 and 2,800 mosmol kg$^{-1}$. The 0.4 mosmol kg$^{-1}$ sample was osmotically shocked to 2,800 and additionally to 4,500 mosmol kg$^{-1}$. The osmolality of the other sample was elevated from 2,800 to 4,500 mosmol kg$^{-1}$. All samples were incubated for one hour in shaking flasks at 37°C, 120 min$^{-1}$. Experiments were done in triplicate. Black bars show enzyme activity after one hour incubation without osmotic shock, white and grey bars represent samples after one hour incubation in which osmolality was increased.

In order to investigate the effect of an osmotic shock on fructofuranosidase activity, a 2 L bioreactor cultivation at standard osmolality of 400 mosmol $kg^{-1}$ and a bioreactor cultivation at an elevated osmolality of 2,800 mosmol $kg^{-1}$ were conducted. After 72 hours, biomass was collected from each bioreactor. Half of the sample was subjected to an osmotic shock with sodium chloride, and the other half was left untreated. Both samples were subsequently incubated in shake flasks at 37°C, at 120 $min^{-1}$ for one hour, before measuring the fructofuranosidase activity. For sample cultivated initially at 400 mosmol $kg^{-1}$, fructofuranosidase activity was increased about 10.8 %, from 88,8 to 98,4 U $mL^{-1}$, due to an osmotic shock to 2,800 osmol $kg^{-1}$. When the same sample was administered an osmolality of 4,500 mosmol $kg^{-1}$, fructofuranosidase activity increased even further, to 103.4 U $mL^{-1}$. No significant increase in fructofuranosidase activity could be assessed for *A. niger* SKAn 1015 sample cultivated at 2,800 mosmol $kg^{-1}$ and shocked to 4,500 mosmol $kg^{-1}$. Hence, an osmotic shock was only beneficial for enzyme activity when the fungal biomass was cultivated at standard osmolality and therefore not adapted to a highly osmotic environment.

There are several other terms for osmolality used in the literature, such as osmotic pressure, water potential, water activity or salt stress. The exact term used usually depends on the method of measurement and the area of research. It is arguable whether increased productivity is due to stress physiology. Whether the term "stress" is appropriate at all, depends further on the often unknown adaptation of a fungus to a highly osmotic environment. A non-adapted species will exhibit stress physiologies, but an adapted may not [314]. Many soil fungi can survive extreme external water potentials down to about 20 MPa and some *Aspergilli* are even known to survive down to 40 MPa [315]. *A. nidulans*, for example, was shown by Beever et al. [316] to exhibit optimal growth on 0.5 M NaCl basal medium and a 50 % reduced growth rate on medium amended with 1.6 M NaCl. No growth was found after medium was supplemented with 3.4 M sodium chloride. *Aspergilli* in general were found to be notably resistant to high salt concentrations, as they were shown to grow in the presence of 20 % or more of sodium chloride [317]. The *Aspergillus* strains used in this study might therefore not necessarily exhibit stress physiologies, which are supposedly responsible for a higher rate of protein synthesis. For clarification, some genetic and molecular studies should be conducted.

The maintenance of intracellular pressure, also called turgor, is somewhat critical for fungi, as it is the driving force for apical expansion and therefore fungal growth [318]. Cellular osmotolerance, in general, depends on the maintenance of osmotic gradients across the fungal cell membrane. Cellular water potentials have to be more negative than those in the external environment to maintain inwardly directed water transport [319]. This potential is usually generated through

accumulation or synthesis of osmotically active solutes by the cell [314]. This could be a reason why osmotic shocks in this study were only successful when administered to culture broth at standard osmolality. In this case, the raised extracellular osmolality is likely to have caused an external water efflux, leading to a secretion of produced enzyme. Experiments in this study support this assumption, since an increase of culture broth osmolality from 400 to 4,500 mosmol kg$^{-1}$ led to a considerably higher fructofuranosidase activity than an osmotic shock from 400 to 2,800 mosmol kg$^{-1}$. Fungal biomass cultivated at higher osmolality will have accumulated a sufficient amount of compatible solutes to cope with the osmotic pressure of the medium. When this adapted fungal biomass is additionally exposed to an osmotic shock, no increased enzyme activity can be measured, because the cells are already used to dealing with a highly osmotic environment. However, supplementary research is needed for further clarification in this matter.

According to the literature increase of osmotic pressure has been found to alter transport of substrates [148], causing an elevation in productivity. Furthermore, increased membrane permeability and secretion is believed to be responsible for a rise in productivity through increased osmolality [146, 147]. In the present study, only bulk activity increased with raised osmotic pressure, while biomass associated activity meaning enzyme which was either not secreted or adsorbed to the cell surface [320], increased only slightly (data not shown). Hence, it is likely that more enzyme is secreted, confirming results of earlier studies. Results in this work suggest, additionally, that a permanent increase of culture broth osmolality is more beneficial for enzyme production than osmotic shocks, because biomass cultivated at 2,800 mosmol kg$^{-1}$ generated much more enzyme activity than biomass cultivated in standard medium with a subsequent osmotic shock up to 2,800 osmol kg$^{-1}$.

Furthermore, there was some evidence that the solute used to increase culture broth osmolality had some influence on increased productivity. It was previously shown by Calderntorres and Thomé [321] that different osmotically-active solutes, such as NaCl, KCl and sorbitol, produced different physiological responses in the halophylic yeast *Debaryomyces hansenii*. Media containing high NaCl concentrations were frequently reported to produce unusual and interesting effects, like elongated sporophores and enhanced mycelial growth [317]. Thus, besides sodium chloride, other inert salts were tested for increasing the osmotic pressure of the medium. Inorganic salts like lithium chloride, lithium bromide, caesium chloride, potassium iodide and sodium iodide repressed growth of *A. niger SKAn 1015*. However, only supplementation of potassium chloride yielded comparable results to sodium chloride addition. Interestingly bulk fructofuranosidase was

susceptible to different ratios of sodium and potassium ions (**Figure 4.8**). An excess of either sodium or potassium ions during an increase of osmolality was beneficial to fructofuranosidase activity. However, an excess of sodium ions led to a considerably higher bulk activity of fructofuranosidase than an excess of potassium ions. This positive effect of additional sodium ions increased from 21 U mL$^{-1}$ at 1,500 osmol kg$^{-1}$, to 44 U mL$^{-1}$ at 2,500 mosmol kg$^{-1}$. Therefore the positive effect of elevated osmolality on fructofuranosidase production might be due to a surplus of sodium ions.
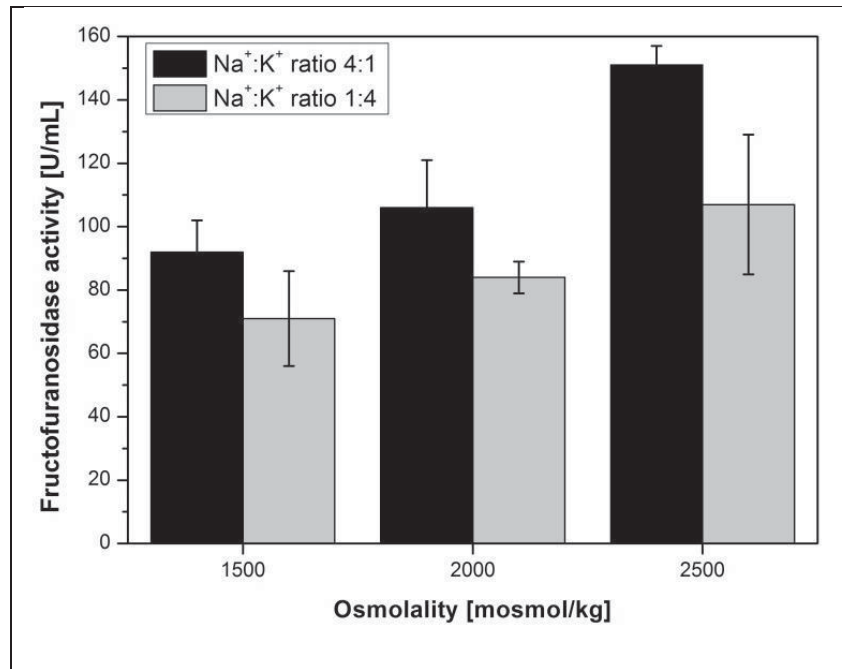


**Figure 4.8:** Mixtures of sodium and potassium chloride with a 1:4 and 4:1 Na$^+$:K$^+$ ratio were used to increase the medium osmolality to 1,500, 2,000 and 2,500 mosmol kg$^{-1}$.

Potassium is the major inorganic cation in the cell cytoplasm, where it is accumulated against a large transmembrane concentration gradient up to $10^3$ to $10^5$-fold in fungi [322]. Generally, fungi have a high tolerance towards potassium ions, as they can colonize media strongly depending on their potassium availability, from the µM range to tens of mM [322]. An increase of osmotic pressure can distinctly alter transport of substrates [148], and thus secretion of fructofuranosidase might also be increased by excess sodium concentrations within the medium. If potassium is lacking but sodium is present, which is a normal situation, this cation, rather than H$^+$ substitutes for the K$^+$ that has not been taken up. Because sodium ions were present in many environments where living cells evolved, the functions or the effects of Na$^+$ on the physiology fungi may be very complex [322].

70

In the literature, various physiological and morphological responses to elevated sodium and potassium ratios were reported; these, however, were mostly organism dependent. Park and colleagues [323, 324] were able to show an influence of salt stress on *A. niger* morphology, as NaCl caused the swelling of the hyphal tip and branch formation within the swollen region. In a study of Kim et al. [325], potassium chloride up to a concentration of 1 M had no effect on morphology of *A. nidulans*. Strains of the halophilic fungal genus *Wallemia* were found to be morphologicaly sensitive to high salinity, as an increased pellet size and wall thickness developed [326]. While in the presence of KCl, growth of the technologically important fungus *Ashbya gossypii* was only slightly inhibited. NaCl, in contrast, had a strong effect, inhibiting growth at 0.2 M, and led to considerably smaller vacuoles [327].

### 4.1.3  Relation of morphology and productivity for cultivations with increased osmolality

One of the industrially most important aspects of fungal morphology is its relation to productivity, because it is desirable to select productive or less productive cultivation batches just from morphologic appearance, or to tell early in a batch process how much product will be formed. A relationship between morphology and productivity was therefore much sought after in many studies. Often optimal product yield corresponded with particular morphologic phenotypes [10-13, 112, 143, 301, 304-306, 328-330]. For best production performance, either a pellet morphology [133, 331] or a mycelial morphology was found to be favorable [10, 12, 143, 304, 306, 330]. However, such a link could not be found in all studies [135, 332]. Macromorphology determines the micro-environment of hyphae through effects on mixing, mass transfer, and culture rheology, which in turn affects protein production [173]. Fungal pellets, for instance, may have dense and inactive cores due to poor diffusion of nutrients, which may lead to cell lysis and thereby loss of the interior pellet structure [100]. Wongwicharn and colleagues [135] were able to show a correlation between the active area of the biomass and protein secretion. Microscopic morphology has other indirect effects on productivity. Hyphal dimensions influence the secretion pathway [46] and protein secretion has been shown to be situated at the tips of fungal hyphae [87]. The branching frequency, especially, is of importance since several studies have showed that metabolite excretion is situated mostly at the hyphal tips [28, 87, 333].

The novel image analytical tools introduced for morphological characterisation of filamentous microorganisms introduced in the present study provide a prospect for establishment of a direct mathematical link between morphology and productivity. The Morphology number MN incorporates all macro morphological traits which were earlier observed to be important for a quantification of fungal morphology.



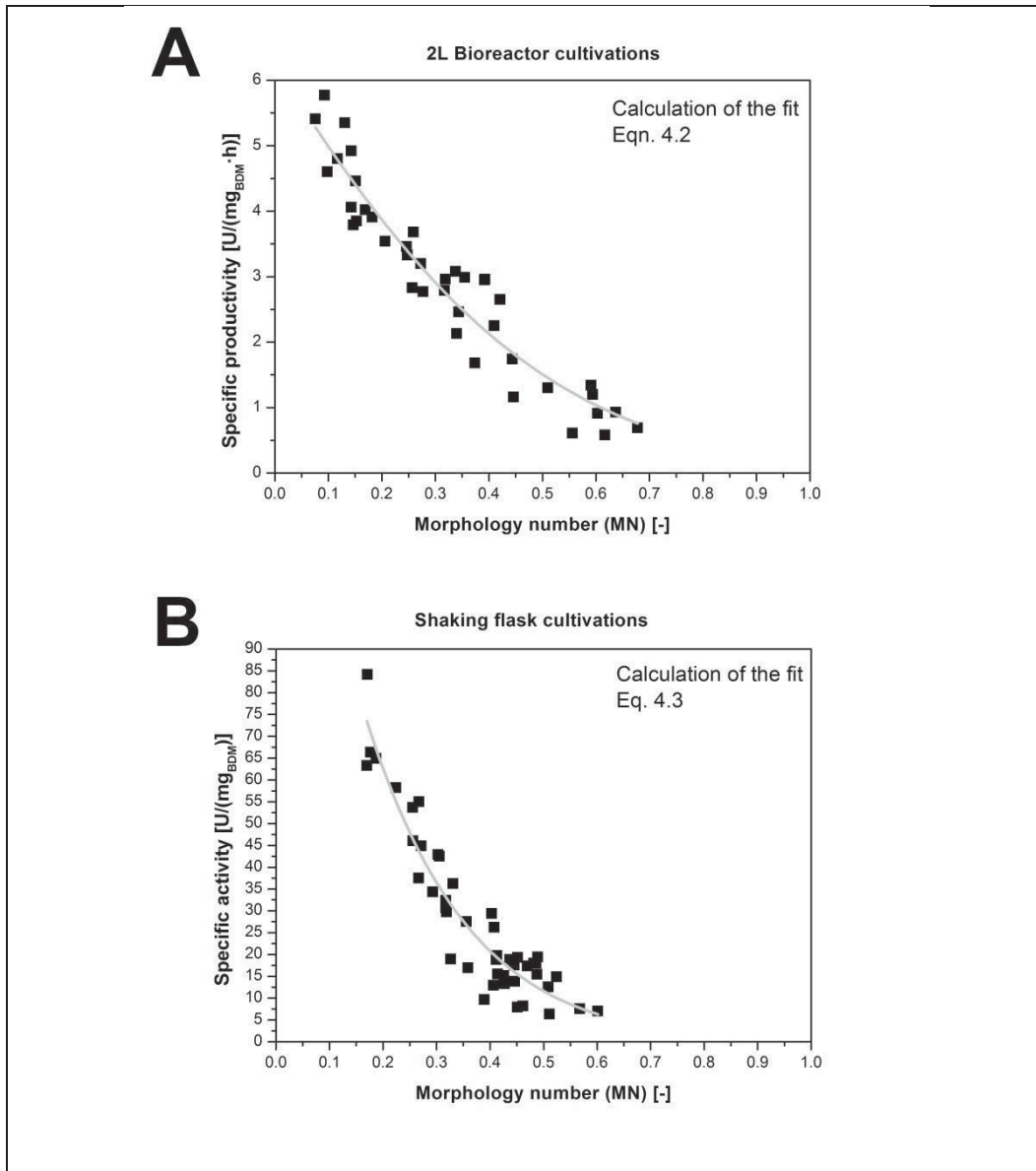**Figure 4.9:** Plot of productivity over morphologic appearance as characterized by the Morphology number (MN). (A) Specific productivity of all conducted *A. niger* SKAn1015 2 L bioreactor cultivations with an exponential fit, $R^2$=0.90. Each dot represents a single 2L cultivation. (B) Specific activity of 45 shaking flask cultivations is shown. $R^2$ of the exponential fit is 0.90. Values are means for 3 shaking flask cultivations.

In **Figure 4.9** A the specific productivity of *A. niger* SKAn1015 2 L bioreactor cultivations is plotted against MN, yielding the following correlation:

$$Specific\ productivity = 6.83 \cdot e^{-2.94 \cdot MN}. \tag{4.2}$$

A very similar correlation was found for *A. niger* SKAn1015 cultivated in 100 mL shaking flasks (Figure 4.9 B). Here MN was linked with specific fructofuranosidase activity producing very similar fit:

$$Specific\ fructofuranosidase\ activity = 188.69 \cdot e^{-5.51 \cdot MN}. \tag{4.3}$$

It is apparent that a small MN, and thus, a filamentous growth form, are clearly beneficial for fructofuranosidase production. Taking into account the constitution of MN, this also means that small, elongated, fungal particles with rough surfaces are the most productive. The validity of obtained correlations can be further confirmed by comparison of measured and predicted values of productivity. In **Figure 4.10**, measured values are depicted on the x-axis. Values gained from correlations (4.2) and (4.3) are illustrated at the y-axis. Thus, a perfect match of predicted and measured values would produce a perfect line. In the graph, data points are scattered evenly on both sides of the perfect fit line, showing the very good quality of the correlation. In graphic B, a cluster of data points can be observed at lower specific activities and at higher values. Predicted values seem to underestimate specific fructofuranosidase activity somewhat. However, both correlations are fairly successful at predicting either specific productivity or specific fructofuranosidase activity from fungal morphology.
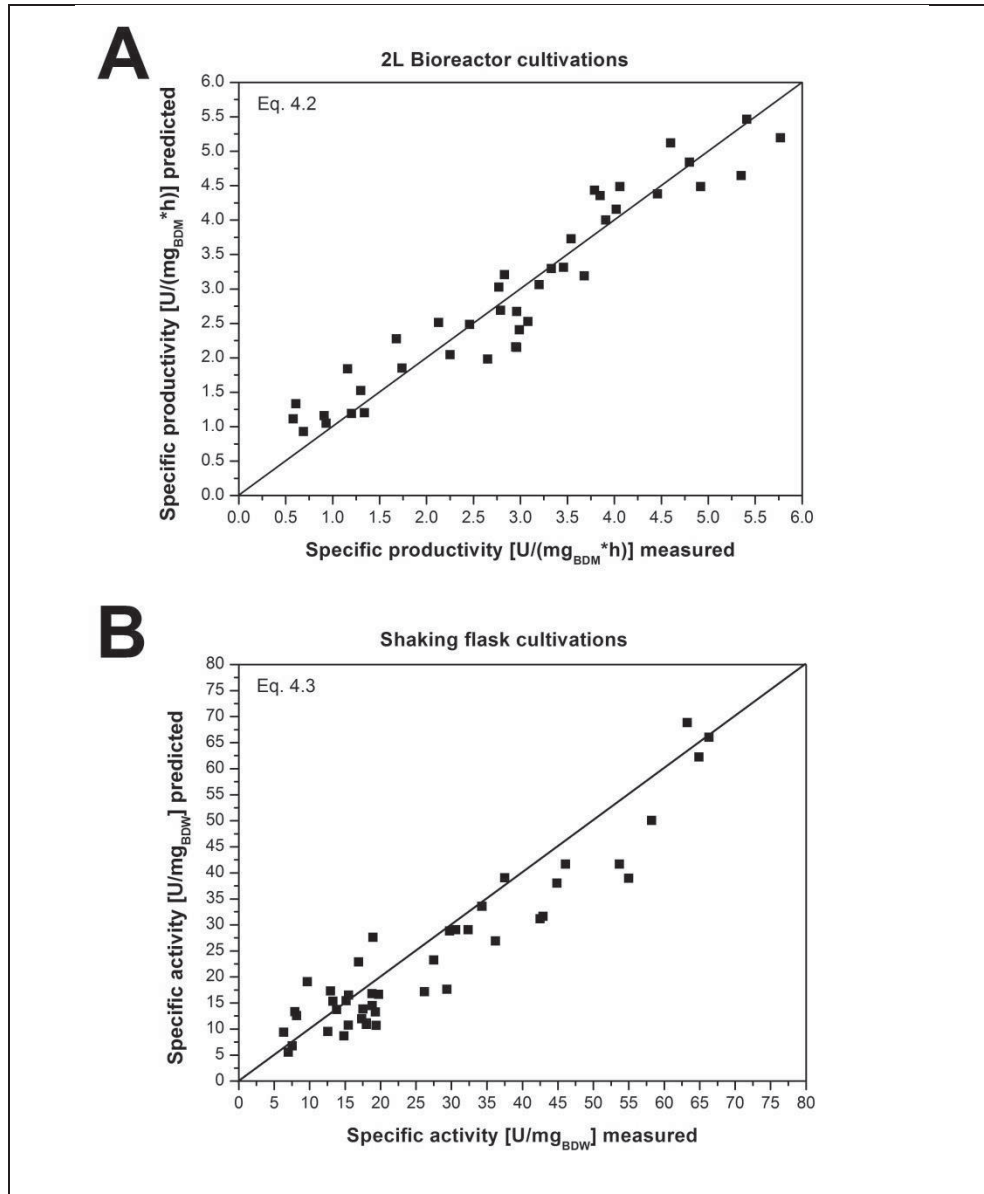
**Figure 4.10:** (A) Actual and predicted values of specific productivity and (B) specific fructofuranosidase activity (B) using the Morphology number (MN) and correlations (4.2, 4.3) gained from bioreactor (A) and shaking flask cultivations (B).

Using MN and the gained correlations, it is possible to predict production performance from quantification of the fungal morphology, proving that there is a clear connection between specific morphological phenotypes and expression of proteins. However, observed changes in productivity might not be due to the change in morphology alone. External osmotic pressure might have affected fungal physiology, and through this, morphology, independently. The observed ruse in productivity, however, was shown to correlate with the active surface area of the fungus, which is a good indication of plausibility. Superior fructofuranosidase production at disperse mycelial morphology was also observed in the studies of Driouch and colleagues [11, 13]; however, morphology in this study was created using micro particles.

Fractal dimension and branching complexity were previously found to be positively correlated with phenol-oxidase expression in *Pycnoporus cinnabarinus*, both parameters influenced by media composition [334]. Macro morphologic traits as included in the Morphology number, are obviously sufficient to describe morphology and its influence on enzyme production, though they do not contain any information about micromorphology. The macromorphology of filamentous fungi was found to have significant impact on the measured mean activities and specific productivities [200]. In addition, macromorphology determines the micro environment of hyphae through effects on mixing, mass transfer, and culture rheology, which in turn affects protein production [173]. Fungal micromorphology has indirect effects on productivity. Hyphal dimensions influence the secretion pathway [46], and protein secretion has been shown to be situated at the tips of fungal hyphae [87]. An abundance of hyphal tips making up a dense mycelium can thus be associated with increased enzyme production [335]. So the increase of productivity at higher osmolality in the present study might be connected with a more mycelial morphology. An advantage of fractal parameters is that they have already been shown to correlate with micro morphologic parameters such as the hyphal growth unit [290]. Therefore, fractal analysis could be used to gain information on micromorphology without getting into tedious, statistically-unsound measurement of single hyphae within a mycelial particle. Accordingly, a link between the fractal dimension and fructofuranosidase activity has to be considered.
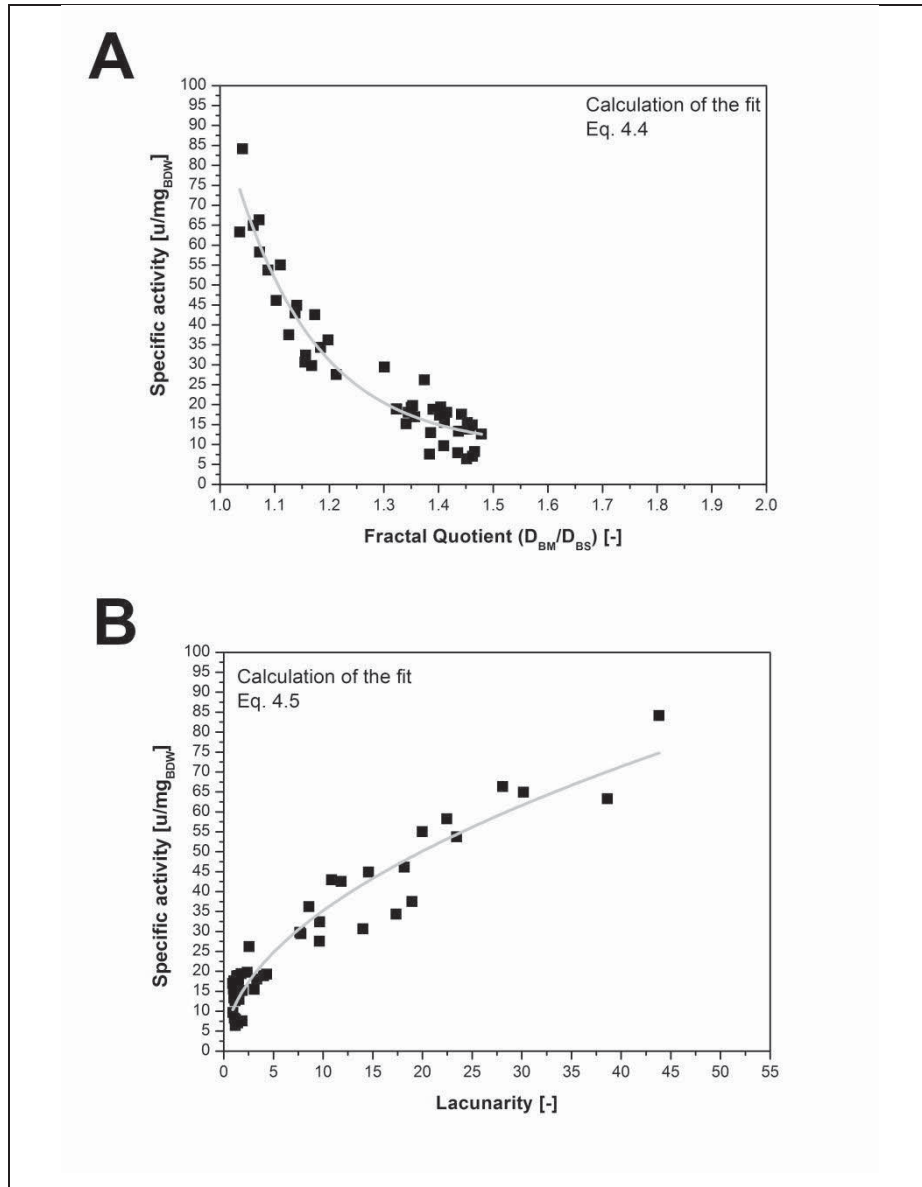
**Figure 4.12:** (A) plot of specific activity over morphologic appearance as characterized by $D_{BM}/D_{BS}$ and (B) lacunarity $\Lambda$. Values are means for 3 shaking flask cultivations of *A. niger* SKAn 1015.

In **Figure 4.12** A specific fructofuranosidase activity over $D_{BM}/D_{BS}$ is depicted. An asymptotic correlation ($R^2 = 0.92$) of the form:

$$Specific\ fructofuranosidase\ activity = 9.06 + 59859.2 \cdot 0.001^{\frac{D_{BM}}{D_{BS}}} \qquad (4.4)$$

exists between both values. Moreover, lacunarity $\Lambda$ was identified as a possible parameter for morphological quantification, and was thus also used for correlation with specific fructofuranosidase activity in Figure 4.12 B. An increased $\Lambda$ indicates a more dispersed heterogenic morphology. The following allometric correlation ($R^2 = 0.92$)

$$Specific\ fructofuranosidase\ activity = 7.64 + 5.15 \cdot \Lambda^{0.096} \qquad (4.5)$$

can be used to conveniently link lacunarity with specific fructofuranosidase activity.
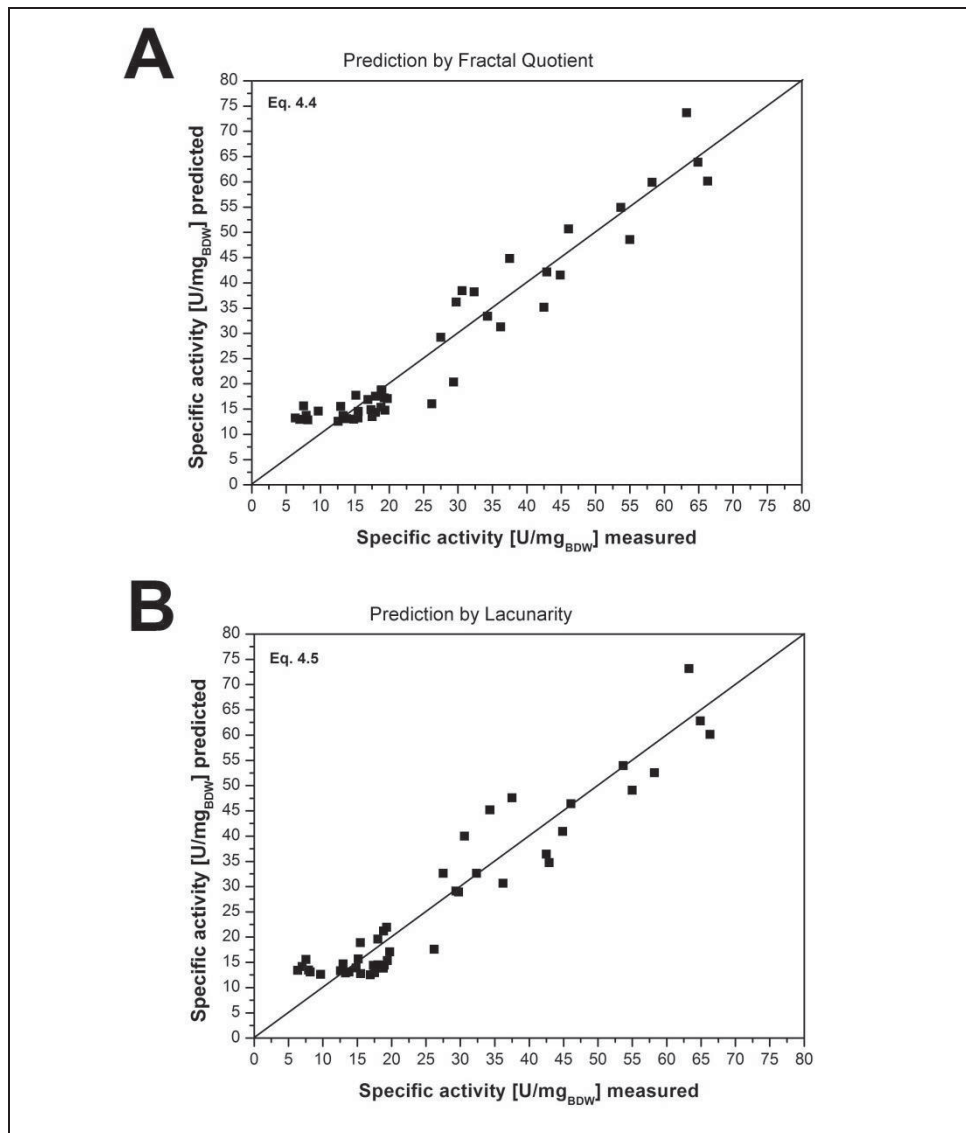


**Figure 4.13:** Actual and predicted values of specific fructofuranosidase activity using (A) fractal quotient, (B) lacunarity and correlations (4.4, 4.5) gained from shaking flask cultivations.

The quality of the correlations between the fractal quotient, lacunarity, and specific fructofuranosidase activity is remarkable (Figures 4.12 and **4.13)**. Despite the fact that both parameters could not be used for differentiation of pellet morphologies, they show a good compliance with productivity. All three parameters were thus suitable to link fungal morphology to enzyme activity. In all cases, a clustering of points can be observed at Morphology numbers between 0.4 and 0.6 (Figure 4.9 B), fractal quotient values between 1.3 and 1.5 (Figure 4.12 A) and a lacunarity between 0 and 5 (Figure 4.12 B). This shows that specific fructofuranosidase activity does not increase significantly as long as strict pellet morphology is exhibited. A mycelial morphology is evidently favorable for production of fructofuranosidase, as found in other studies [10-13, 143, 301, 328].

### 4.1.4 *Influence of osmolality on* A. niger *conidia aggregation*

The early phase of cultivation is of tremendous importance for the morphogenesis of *A. niger*, because conidia aggregation and interaction influence the morphology which is formed later on. Experiments previously done indicated that the decision of whether *A. niger* will grow in pellet or mycelial morphology occurs during the first 8 hours of cultivation, depending on culture conditions. Later on, fungal morphology will remain constant even if culture conditions are changed. *A. niger* SKAN 1015 cultivated as described (chapter 3.2.2) in this study will not develop a mycelial morphology, whereas cells grown at 4.5 osmol/kg will never form pellets. Even elongated fluffy pellets, which are an intermediate morphology, stay constant in their form and shape if any changes in culture conditions take place after this first crucial period. The only exception is external power input and shear stress, which might result in pellet breakage and uncoiling of pellets. Spore aggregation and subsequent germination are the most important parameters which determine fungal morphology, and are therefore included in this study. In a novel approach, spore aggregation was measured using laser diffraction experiments which were carried out without aeration, since bubbles interfered with the scattering pattern of the instrument. It was shown in earlier studies that oxygen requirement is very low in the first hours of germination, and no oxygen limitation was detected by measurement of dissolved oxygen [89].

**Figure 4.14** shows a distinct influence of osmolality on conidia germination, for four representative cultivations from 0.35 to 3.6 osmol kg$^{-1}$. The development of particle size over time during the first 2000 minutes of cultivation is shown by increase of median diameter (top) and the Sauter mean diameter (SMD) (bottom). Each point represents a single measurement. The reason for the sometimes deviating values lies in the measuring method. Fluid dynamic properties within the measuring cell determine which side of the particle is measured; for irregular elongated particles this might lead to considerable differences. Generally, Figure 4.14 reveals that spores germinate later at increased osmolality. Additionally, the time difference between the measured median and Sauter mean diameter SMD (grey) increases.
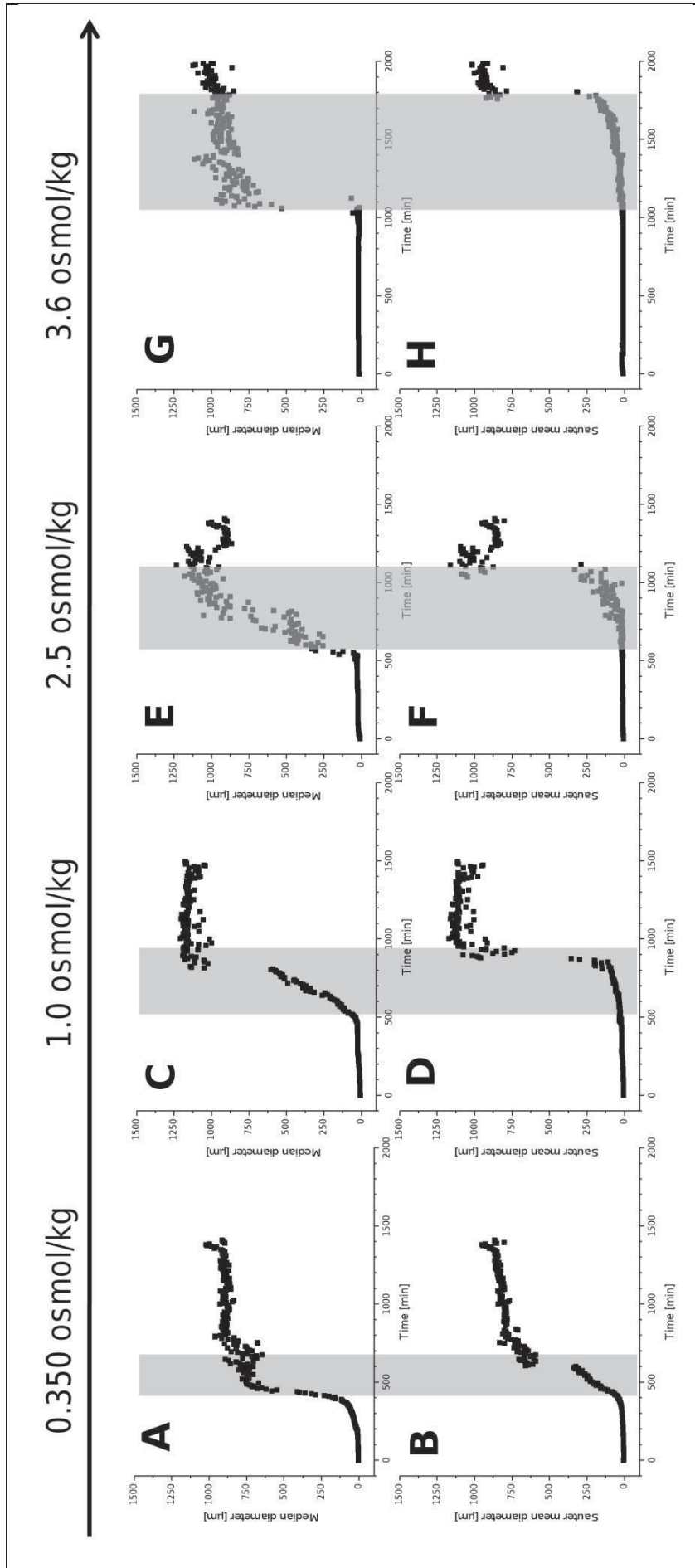
**Figure 4.14:** Depicted are the Median diameter (top) and the Sauter mean diameter (bottom) over time at 0.35 osmol kg$^{-1}$ (A, B), 1.0 osmol kg$^{-1}$ (C, D), 2.5 osmol kg$^{-1}$ (E, F) and 3.6 osmol kg$^{-1}$ (G, H) culture broth osmolality. The grey highlighted area marks the beginning of the sudden increase of the Median diameter, till the Sauter mean diameter has reached a near constant value. The corresponding Δt-value is the germination time. Particle sizes were determined by laser diffraction.

79

The germination process can be split into three steps: germination, isotropic growth (swelling) and polarized growth, due the emergence of the germ tube [336]. Right after inoculation, the culture consist of spores and spore agglomerates, which are all more or less spherical and range from 2 μm for a singular spore up to 20 μm for spores packages in size. During germination, a single small germ tube emerges from the spore, forming small elongated particles [69]. Subsequently, more or less spherical particles of agglomerated mycelia are formed [92]. Trinci et. al [337] first showed a pronounced lag phase prior to the emergence of the germ tube, and an almost linear germination afterwards. The same can be observed in Figure 4.14, graphs A to H, showing a pronounced lag phase of 400 to 1000 minutes prior to the events of germination. The definition of when a spore is germinated is based on a comparison between the length of the germ tube and the diameter of the spore. Germination time is the time until 90 % of conidia have germinated, the exact percentage depending on the study [338].
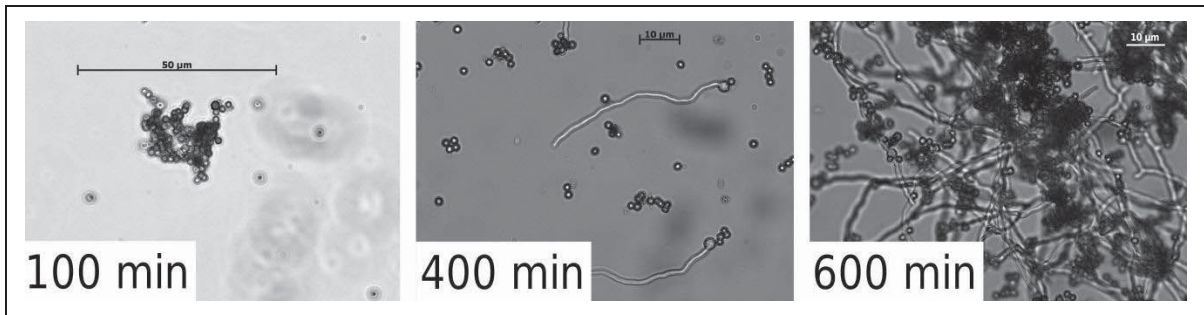


**Figure 4.15:** Pictures with a magnification of 250x of conidia as found in Figure 4.14, cultivation at 350 mosmol kg$^{-1}$ (A,B), 100, 400 and 600 minutes after inoculation.

Laser diffraction was employed in this study to measure the size of sole conidia and conidia-aggregates. This particle size measuring method generates volume equivalent distributions, which can be used to obtain statistical data, like the median or Sauter mean diameter. Due to the measuring principle, the method of laser diffraction cannot differentiate between narrow elongated particles and larger spherical particles. Hence, germinating conidia will be recorded either as rather large particles measuring the elongated side, or spore-like size particles when measuring the considerably smaller width of the germinating conidia. Concurrently with the start of the germination process and the emergence of the germ tube (**Figure 4.15),** the median value of the measured particle size distribution will change abruptly. In a relatively short time frame of approximately 60 minutes, the median can be observed to increase (Figure 4.14) from around 3 μm, the size of *A. niger* conidia, to 1,000 μm, which is the size of germinated spore aggregates and later on the diameter of pellets. In this experimental set up, the median value can therefore be used as an indication of when the conidia start to germinate.

The Sauter mean diameter is defined as the diameter of a particle that has the same volume/surface area ratio as a particle of interest. The SMD increases later and with less velocity than the median value (compare Figure 4.14). The reason for this is that smaller particles are weighted more heavily than in the median value. Thus, the SMD in this experiment can be interpreted as an indication of when the large majority of conidia have germinated. The time difference (grey) between the median diameter and the SDM is the germination time (compare Figure 4.14).
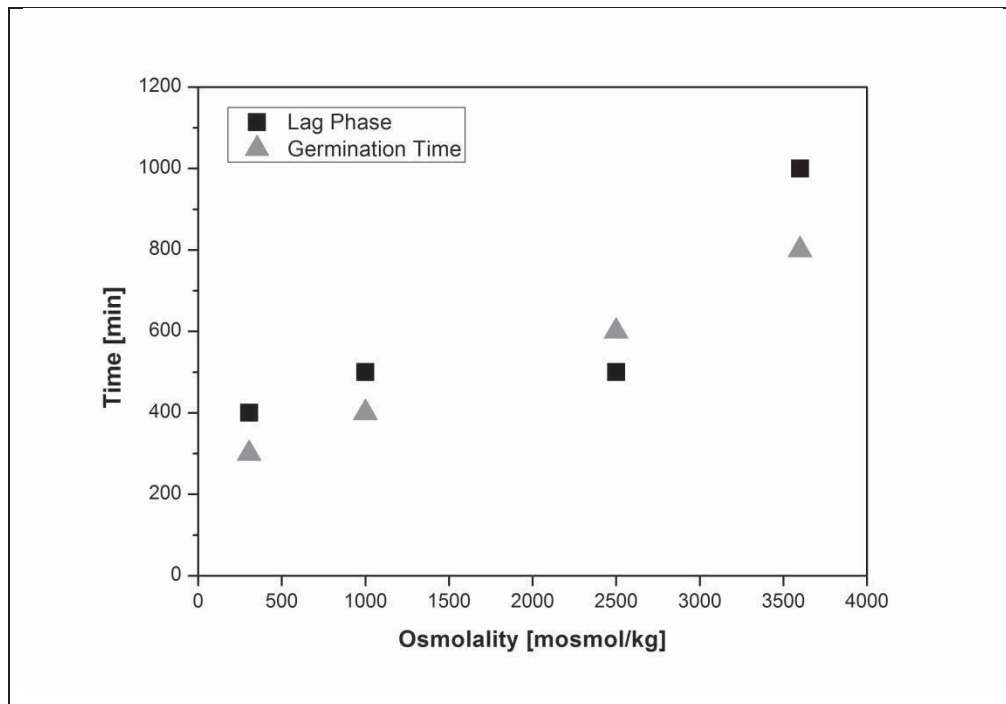


**Figure 4.16:** Germination time (grey triangle) and lag phase (black box) are depicted over osmolality.

In **Figure 4.16** lag phase and germination time as affected by osmolality are displayed. An increase in culture broth osmolality leads to prolongation of the lag phase, an almost linear increase in germination time. Such a dependency was previously shown only for experiments on agar plates by Judet et al. [339], where the authors found that the germination time increased with decreasing water activity within the germination medium. In submerse cultivations, this prolonged germination process is most likely one reason for the considerable impact of osmolality on fungal morphology. Inoculum concentration was previously also shown to effect conidia germination by Grimm et al. and others [92, 340]. Both studies showed a prolonged germination time for increasing spore concentrations. Inoculum concentration was also demonstrated to effect fungal morphology, as a higher number of spores led to more mycelial growth [112]. Thus, increased osmolality and inoculum concentration both result in a prolonged germination time and a more mycelial morphology. It would be interesting to determine whether other parameters associated with mycelia morphology, like low pH [93] or added micro particles [13], also increase

germination time of conidia. Moreover, it should be an emphasis of future research to determine whether, in submerged cultivation, a prolonged germination time and mycelial morphology are directly connected.

### 4.1.5  Morphology engineering in A. niger by variation of spore inoculum

The amount, type, quality and age of the inoculum are the most important factors in determining the morphology of *A. niger*, and the course of fungal cultivations in general [9]. The initial concentration of spores is one of the most established tools for influencing the morphology of *A. niger* [6, 36, 42, 80, 85, 98-105]. Besides osmolality, the spore concentration at the start of cultivation is a good alternative method to test introduced image analysis tools for morphological characterization. In the present study, inoculum concentration of *A. niger* SKAn 1015 was varied between $5 \cdot 10^4$ and $5 \cdot 10^7$ mL$^{-1}$. Because of significant morphological changes in that area, the majority of tested spore concentrations lay between $5 \cdot 10^5$ and $5 \cdot 10^6$ mL$^{-1}$.
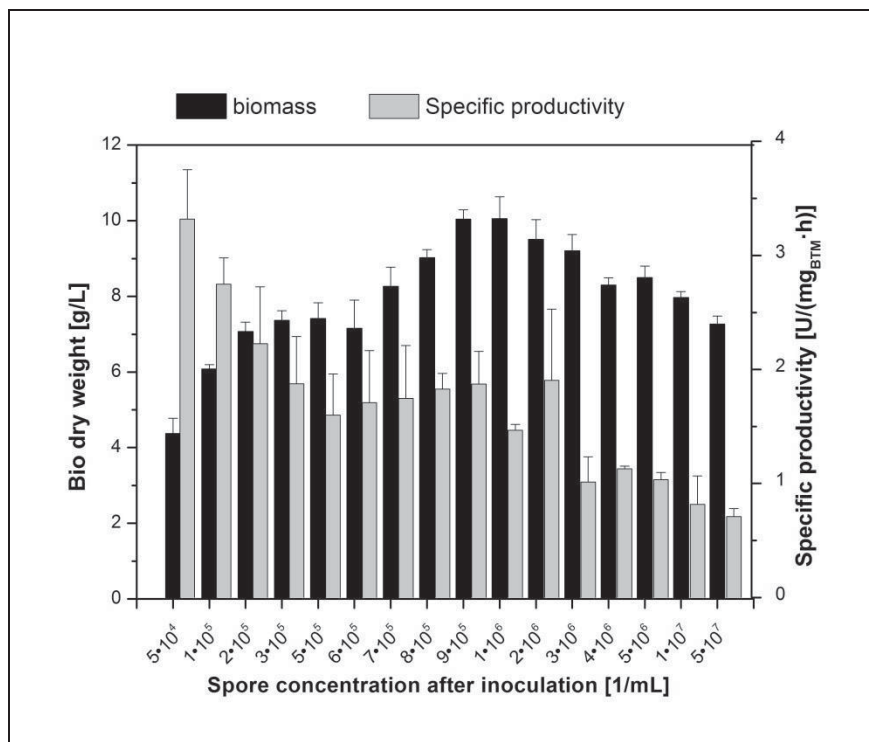


**Figure 4.17:** Biomass dry weight (black) and specific productivity (grey) after 72 hours of cultivation at different spore concentrations. Values are means for at least three 100 mL shaking flask cultivations.

In **Figure 4.17** the dependency of biomass and specific productivity on different spore concentrations is depicted. It is apparent that initially, increasing spore concentrations lead to higher biomasses. While the biomass at $5 \cdot 10^4$ mL$^{-1}$ was only 4 g L$^{-1}$, it could be increased up to 10 g L$^{-1}$ at an initial spore concentration of $1 \cdot 10^6$ mL$^{-1}$. A further increase in spore concentration caused a decline in biomass to 8 g L$^{-1}$ at $5 \cdot 10^7$ mL$^{-1}$, which was the highest concentration of spores used in this study. The initial black staining of the culture broth consisting of un-germinated spores completely vanished for initial spore concentrations below $1 \cdot 10^6$ mL$^{-1}$. For higher concentrations, the stain faded somewhat after cultivation initiation, and stayed constant at $5 \cdot 10^6$ mL$^{-1}$ and beyond. There is obviously an inhibiting effect preventing germination at high spore concentrations. Such a self-inhibiting effect was also reported by Barrios-Gonzalez et al. [341] and by Grimm and colleagues [92] for *A. niger* spore concentrations higher than $10^6$ ml$^{-1}$. A similar inhibiting effect was also described for *Syncephalastrum racemosum* by Hobot und Gull [342], and for *Penicillium paneu* by Chitarra et al. [343]. Quorum sensing is argued to be the reason for the inhibition of the germination process [341, 342], because a washing step after inoculation prevented the inhibitory effect, probably through a removal of the signal molecule [341]. Quorum sensing involves secretion of signal molecules by adjacent cells or, in this case spores. Below or above a certain signal molecule concentration, a physiological response is triggered by cells close by. In the present case the germination of spores was partly inhibited above a concentration of $10^6$ ml$^{-1}$. In this case, the germination inhibition has a protective function, because the germination of a high number of spores would use up nutrients very quickly, preventing long term growth.

When specific productivity is examined (compare Figure 4.17), a different development is apparent, as specific productivity decreases continuously, from 3.25 U mg$_{BTM}$$^{-1}$ h$^{-1}$ at $5 \cdot 10^4$ spores mL$^{-1}$ to 0.75 U mg$_{BTM}$$^{-1}$ h$^{-1}$ at $5 \cdot 10^7$ spores mL$^{-1}$, with increasing spore concentrations. The decline of specific productivity for high spore concentrations, greater than $10^6$ mL$^{-1}$, can be explained by the quorum sensing process, because the inhibition of the germination and resulting growth processes causes a reduced product formation. Moreover, Papagianni and Mattey [112] showed that high spore concentrations lead to low dissolved oxygen rates even right after inoculation, which impairs productivity. This could be another reason for a reduced specific productivity a high spore concentrations. For spore concentrations lower than $10^6$ mL$^{-1}$, however, the decline of the specific productivity with increasing spore concentration is not easily explainable. It is possible that inhibiting effects affect product formation even if growth is undisturbed.

In **Figure 4.18** influence of inoculum spore concentration on fungal morphology (A-C) and correlation of morphology with specific productivity are depicted (D-F). Graphs A to C show a clear effect of the initial spore concentration on fungal morphology, as a more mycelial morphology is induced by increasing spore concentrations, a fact that is already established in the literature [6, 36, 42, 80, 85, 98-105]. All 3 introduced image analytical parameters for morphological characterization of *A. niger* are suitable to describe the morphological transition caused by increasing spore concentration. The parameter lacunarity (C), however, cannot be used to distinguish between different pellet morphologies (as already discussed), which occur until conidia concentrations greater than $3 \cdot 10^6$ mL$^{-1}$ are reached.
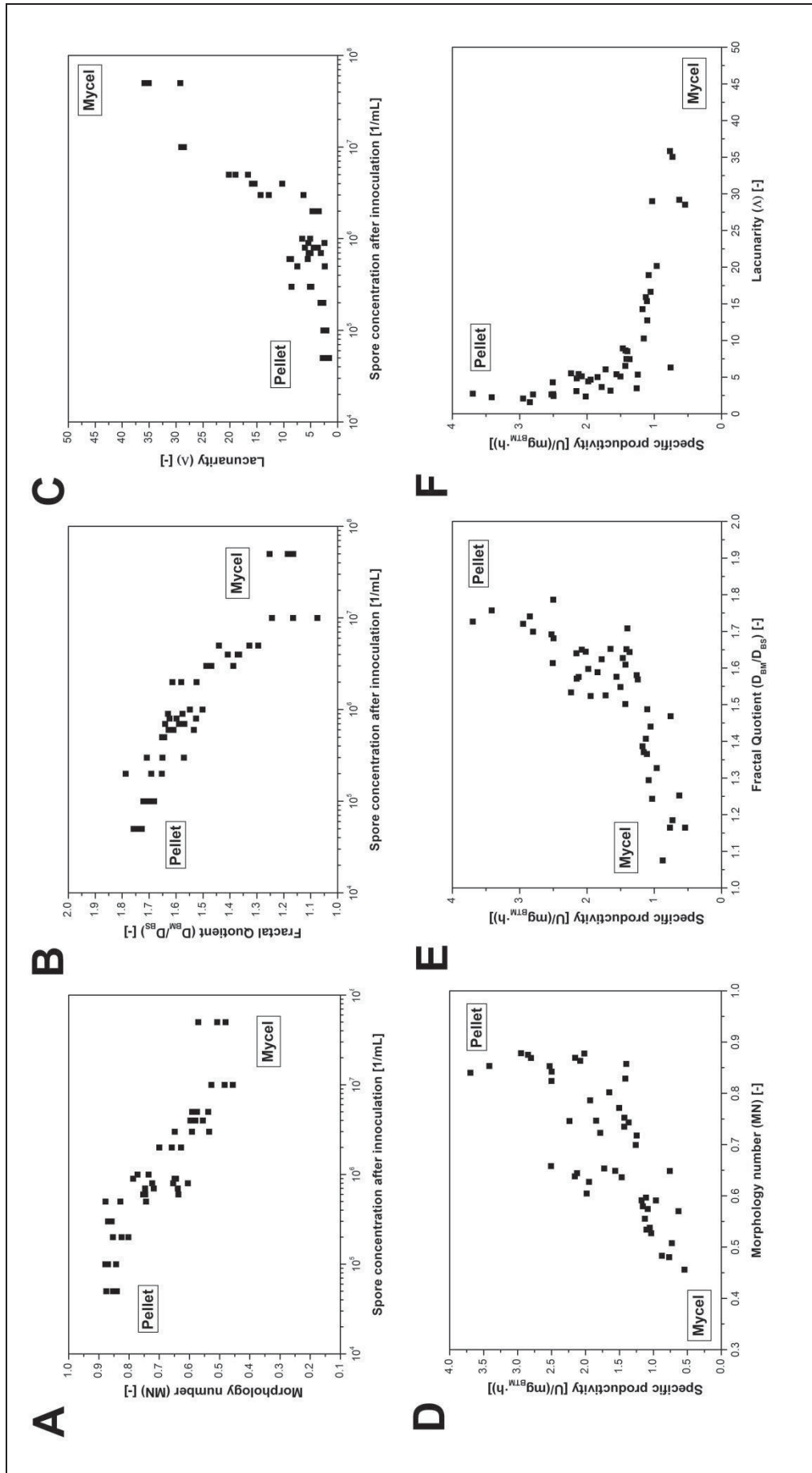
**Figure 4.18:** Effect of initial spore concentration on fungal morphology (A–C) and the relationship between morphology generated by inoculum concentration and specific productivity (D–E). Already introduced morphological parameters Morphology number MN (A, D), fractal quotient $D_{BM}/D_{BS}$ (B, E) and lacunarity $\Lambda$ (C, F) are used for morphological characterization.

Graphs D through F show a declining specific productivity at a more mycelial morphology, which is contradictory to the relationship discovered by changing fungal morphology by osmolality or micro particles. The variation of inoculum spore concentration is obviously not a suitable process parameter to optimize *A. niger* morphology, because increasing spore concentrations lead to inhibiting effects and non-optimal growth conditions. This is also apparent when specific fructofuranosidase activities are compared between osmolality and spore concentration experiments. At standard conditions (inoculum spore concentration of $10^6$ ml$^{-1}$ and 400 mosmol kg$^{-1}$), both experiments show a specific productivity around 1.5 U mg$_{BTM}^{-1}$ h$^{-1}$. The top specific productivity of the inoculums concentration experiment, with 3.25 U mg$_{BTM}^{-1}$ h$^{-1}$ at $5 \cdot 10^4$ mL$^{-1}$, was significantly below 9 U mg$_{BTM}^{-1}$ h$^{-1}$, which was the highest specific productivity of the osmolality experiments. Obviously, there is an ideal inoculum concentration at $10^6$ ml$^{-1}$ causing the highest biomass and bulk enzyme activities. A change of this concentration does influence the morphology, but also impairs productivity.

### 4.1.6  Influence of biomass on culture broth rheology

While specific productivity is the most common parameter selected for improvement during process development, easy purification of the product is equally important. For filamentous microorganisms, an increased culture broth viscosity leads to a more difficult, and therefore economically unfavorable, purification process. A further important aspect directly affecting process economics is the increased energy consumption for agitation of such cultivations. The flow behavior, in turn is heavily dependent on fungal morphology. Numerous studies exist where viscosity is estimated using biomass and some kind of morphological information, mostly based upon image analysis methods [176, 182, 193, 195, 199, 200].

A general problem with most of these studies is the relatively low number of conducted cultivations, as rheological samples are usually extracted from few rather large-scale cultivations. An advantage of these studies is that development of culture broth viscosity over time can be studied very easily. However, since different morphologic forms of *A. niger* SKAn 1015 are created permanently and irreversibly through the process environment, this approach cannot generate sufficient samples for meaningful estimation of rheological parameters from fungal morphology.

A different approach was chosen in the present work to study a large number of morphological growth forms and their relation to culture broth viscosity. 100 mL shaking flasks were used to compare 45 different morphological forms, created through a permanent change of culture broth

osmolality, through addition of sodium chloride prior to inoculation. Through this method, it is possible to study a comparatively large number of samples of the same age and comparable culture conditions with different morphology. Thus, the whole spectrum of *A. niger* morphology is used for holistic estimation of rheology, based on the previously introduced dimensionless Morphology number and other fractal parameters.

Biomass concentration has a significant influence on the viscosity of the culture broth [41, 176, 182, 195]. Ruohang and Web [182] found an exponential dependency of the consistency index (K) on biomass, and a polynomial relationship between the flow behavior index (n) and biomass for cultures of *A. awamori*. This proves that the relationship between biomass and rheology has to be considered before morphologic characteristics can be correlated with rheology. Furthermore, the biomass concentration of *A. niger* SKAn 1015 samples with filamentous morphology was reasonably lower than that of samples with pellet morphology. Process parameters which influence fungal morphology usually do affect biomass concentration as well, so biomass has either to be incorporated in the correlations for prediction of rheology directly, as did Riley and colleagues [176, 195] or considered beforehand. **Figure 4.19** shows the decline of biomass concentration with increasing medium osmolality. Meanwhile, the consistency index K stays approximately constant until 1600 mosmol kg$^{-1}$, and increases at higher osmolalities. This change of the consistency index is concurrent with a change from pellet to a mycelial morphology.
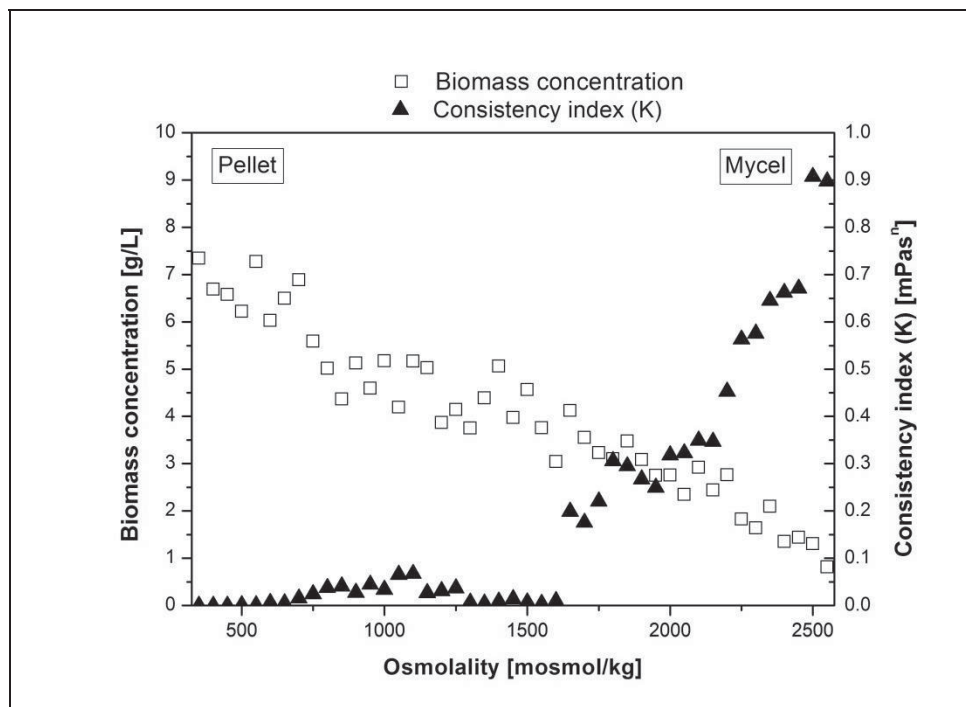


**Figure 4.19:** Development of biomass concentration and consistency index (K) with increased medium osmolality prior to inoculation.

Culture broth viscosity is generally highly biomass dependent. The *A. niger* SKAn 1015 cultivation at 500 mosmol kg$^{-1}$ exhibits a biomass concentration of 6.5 g L$^{-1}$, whereas the cultivation at 2500 mosmol kg$^{-1}$ has a biomass concentration of only 1 g L$^{-1}$. This large difference in biomass has a great effect on the culture broth viscosity. In order to investigate the general effect of fungal morphology on culture broth viscosity without the influence of biomass, there are two approaches. The first would be to compare samples of the same biomass with different morphological growth forms. However, for the strain *A. niger* SKAn 1015 used in this study, a more mycelial morphology goes hand in hand with a change in biomass, irrespective of the method which is used for manipulation of fungal morphology, which could be pH, micro particle supplementation, or, as in the current study, osmolality. Therefore, it is practically impossible to obtain samples with a different morphology but the same biomass. The second approach, chosen in the present study, is to exactly determine the link between biomass and viscosity and incorporate this knowledge in correlations aimed at predicting rheology from morphology. To investigate the influence of biomass concentration on culture broth viscosity, the method introduced by Riley and colleagues [176] was applied. Three separate 2 L stirred tank bioreactor cultivations were conducted, one with pellet morphology, one with mycelial morphology and one with an intermediate clump morphology.
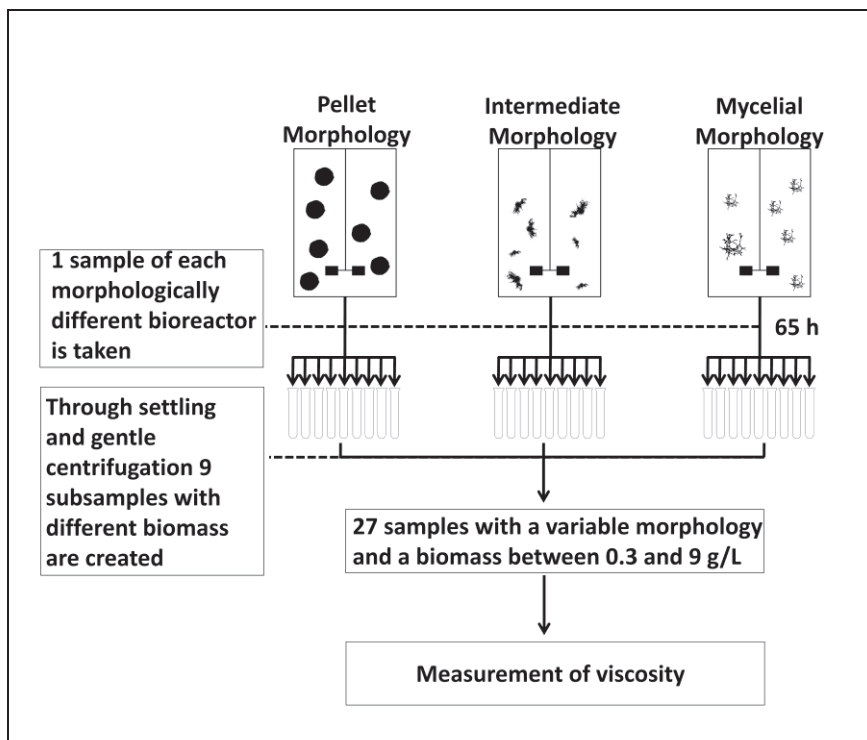


**Figure 4.20:** Creation of subsamples with variable morphology and biomass.

After 65 h of cultivation, samples with differing morphology were collected from the bioreactors (compare **Figure 4.20**). Through settling and gentle centrifugation (Variofuge 3.OR, Heraeus

Centrifuges, UK) 9 subsamples with differing biomass, but identical morphology, were created through centrifugation and re-suspension as shown in other studies [176, 199, 200]. Biomass concentration was adjusted in the usual range of shaking flask and bioreactor cultivations with *A. niger* SKAn 1015 between 0.3 and 9 g $L^{-1}$, which might be considered low compared to industrial cultivations of bulk products, but was a reasonable range for the used strain [10-13, 50, 143, 344]. For each of the obtained 27 samples, viscosity was measured. Consistency index K and flow behavior index n were determined using the Ostwald–de Waele model and correlated with the biomass concentration (**Figure 4.21** A and B).



**Figure 4.21:** (A) Change of the consistency index (K) with increased biomass (Eq. 4.6, $R^2$=0.98), (B) correlation of the flow behavior index (n) with biomass concentration (Eq. 4.7, $R^2$=0.91). Biomass for these correlations was gained from three 2L bioreactor cultivations o *A. niger* SKAn 1015.

For the consistency index K and biomass concentration (Figure 4.21 A) the following correlation was found

$$K(BDW) = 1.3 \cdot 10^{-5} \cdot BDW^{4.8}. \tag{4.6}$$

The correlation of the flow behavior index n with biomass (Figure 4.21 B) led to

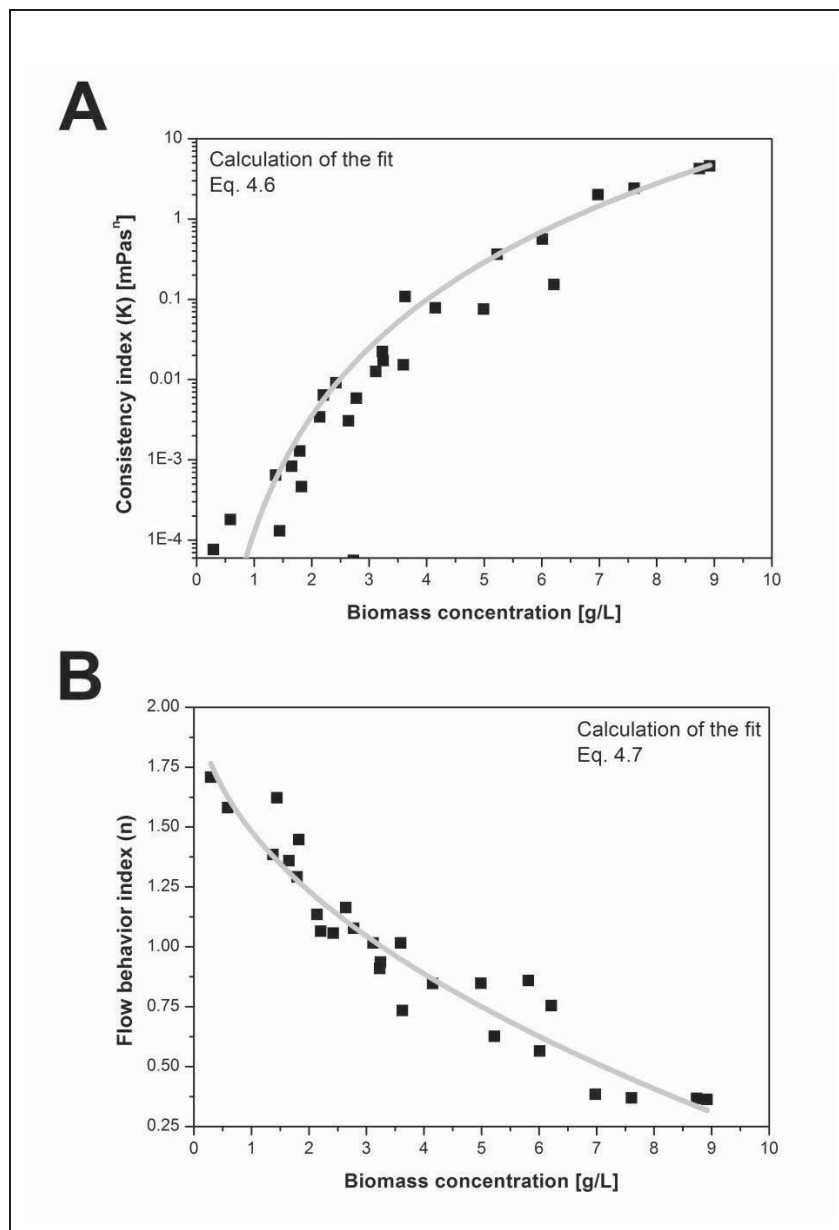$$n(BDW) = 2.1 - 0.6 \cdot BDW^{0.5}. \tag{4.7}$$

Very similar correlations for both rheological parameters were found in the study of Ruohang et al. [182]. In Figure 4.21 A shear thickening is evident for very low biomass concentrations below 2 g L$^{-1}$. This rather rare property was reproduced several times and might be a common trait due to hyphal entanglement and agglomeration. From 2 to 4 g L$^{-1}$, the flow behavior is Newtonian, and at higher biomass concentrations, it becomes pseudoplastic. Correlations (4.6) and (4.7) enable the calculation of a rheological parameter based on biomass exclusively, regardless of morphological growth form.

### 4.1.7  Correlation of fungal morphology with culture broth rheology

The rheological behavior of pellets or mycelia in general was the issue of many studies [41, 43, 182, 193]. The high variability of fungal morphology, however was mostly ignored. It is not sufficient to describe the influence of either pellet or free mycelial morphology; rather, intermediate morphological forms, like small, elongated, and fluffy pellets should be considered as well. The influence of pellet sizes and their surface morphology on rheological behavior of *A. niger* culture for instance, was rarely studied [345]. While still being less viscous than mycelial growth forms, diverse morphological forms of pellets were found to differ significantly in terms of culture broth rheology [345]. The accurate characterization of fungal morphology, therefore, remains a key target for industrial biotechnology, and image analysis methods are central for achieving this goal [21]. Since the introduction of automatic image analysis, lots of quantified information has enabled a detailed characterization of various morphological forms of filamentous fungi [62, 80], and a quantitative characterization of the relationship between fungal morphology and productivity [133]. The combination of relevant image analytical parameters and the already introduced Morphology number (MN) provides a simple way to characterize filamentous morphology. Furthermore, consideration of fractal dimension seems a promising approach to describe, irregular structures of mycelial particles and structures lying between the two extreme forms of pellet and mycelial morphology.

90

To characterize the impact of morphology on rheology regardless of different biomass concentrations, two dimensionless parameters were generated. The quotient of the measured consistency K, divided by K(BDW) with equal biomass obtained by eq. 4.6, results in the dimensionless consistency coefficient

$$K_{BDW} = \frac{K}{K(BDW)} \, . \tag{4.8}$$

The quotient of the flow behavior index n divided by n(BDW) with equal biomass deduced from eq. 4.7 makes up the dimensionless flow coefficient

$$n_{BDW} = \frac{n}{n(BDW)}. \tag{4.9}$$

These calculated parameters $K_{BDW}$ and $n_{BDW}$ are independent of biomass concentration.

Thus, the consistency coefficient $K_{BDW}$ and flow behavior coefficient $n_{BDW}$ are linked with the previously introduced Morphology number (**Figure 4.22**), fractal quotient (**Figure 4.23**) and lacunarity (**Figure 4.24**). $K_{BDW}$ varies from around $10^{-7}$ to 30. $n_{BDW}$ takes values between 0.3 and 3.5. Since the parameters take into account biomass dependency of rheological behavior, both values are not equal to the regular K and n from the Ostwald–de Waele model. These values should not be confused with each other. Textbook correlations of the consistency index K and the flow behavior index n are not necessarily valid for the biomass-independent values of $K_{BDW}$ and $n_{BDW}$. Prior to correlating rheological parameters and fungal morphology, statistical significance of obtained rheological parameters had to be ensured. To this end, a Monte Carlo approach [300] was conducted, and a paired t-test was used to check whether differences in rheological parameters of adjoining shaking flasks were statistically significant. The difference in the predominant majority of the rheological parameters was found to be statistically significant.

In Figure 4.22 A, $K_{BDW}$ is depicted over fungal morphology displayed by MN. An exponential relationship between morphology and the $K_{BDW}$ is obvious ($R^2 = 0.95$)

$$K_{BDW} = 4.12 \cdot 10^5 \cdot (2.5 \cdot 10^{-25})^{MN}. \tag{4.10}$$

In Figure 4.22 B the flow behavior coefficient $n_{BDW}$ can been seen to rise exponentially ($R^2 = 0.78$) with increasing MN

$$n_{BDW} = 0.13 \cdot (2.44 \cdot 10^2)^{MN}. \tag{4.11}$$

**Figure 4.22**: (A) $K_{BDW}$ and (B) $n_{BDW}$ are depicted over Morphology number (MN). Rheological parameters are biomass normalized. Each dot represents morphology and rheology of a single 100 mL shaking flask cultivation of *A. niger* SKAn 1015 after 72 hours of cultivation. Each value is an absolute mean of at least 3 cultivations

A correlation of fractal quotient ($D_{BM}/D_{BS}$) and $K_{BDW}$ is depicted in Figure 4.23 A. The exponential fit again shows a very good correlation ($R^2 = 0.90$) between fungal morphology and the rheological parameter $K_{BDW}$

$$K_{BDW} = 3.10 \cdot 10^{17} \cdot (3.42 \cdot 10^{-16})^{\frac{D_{BM}}{D_{BS}}}. \tag{4.12}$$

$n_{BDW}$ over fractal quotient ($D_{BM}/D_{BS}$) in Figure 4.23 B shows an exponential correlation as well, although with a much poorer fit ($R^2 = 0.64$)

$$n_{BDW} = 3.60 \cdot 10^{-3} \cdot 77.86^{\frac{D_{BM}}{D_{BS}}}.$$    (4.13)
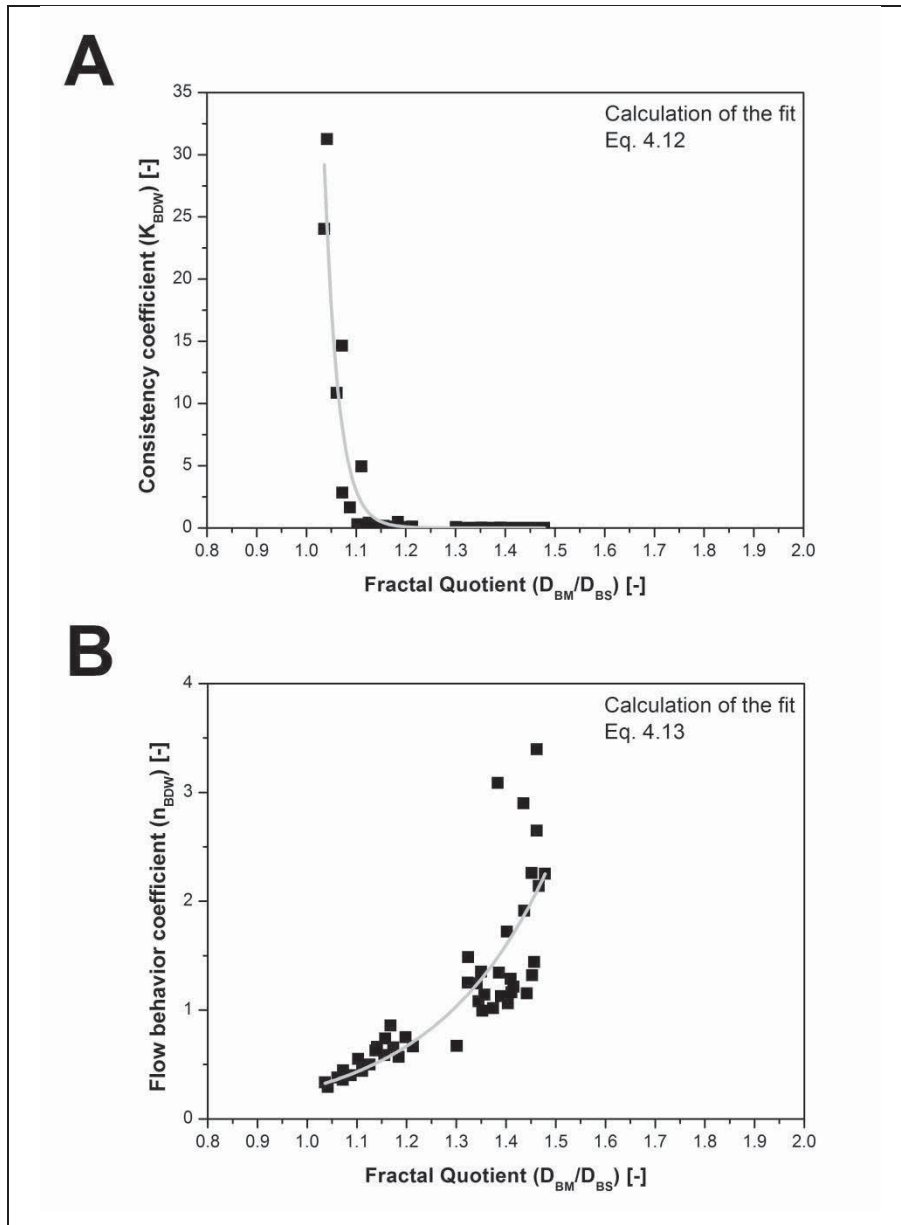


**Figure 4.23**: (A) $K_{BDW}$ and (B) $n_{BDW}$ are depicted over fractal quotient ($D_{BM}/D_{BS}$). Rheological parameters are biomass normalized. Each dot represents morphology and rheology of a single 100 mL shaking flask cultivation of *A. niger* SKAn 1015 after 72 hours of cultivation. Each value is an absolute mean of at least 3 cultivations

93

The morphological parameter Lacunarity $\Lambda$ can also be used to show the interrelation of rheology and morphology. A very good allometric correlation ($R^2 = 0.96$) is reached when $K_{BDW}$ is plotted over $\Lambda$ (Figure 4.24 A)

$$K_{BDW} = 4.11 \cdot 10^{-4} \cdot \Lambda^{2.99}. \tag{4.14}$$

The biomass independent rheological parameter $n_{BDW}$ is also depicted over $\Lambda$ (Figure 4.24 B), although the correlation is fairly poor ($R^2 = 0.52$)

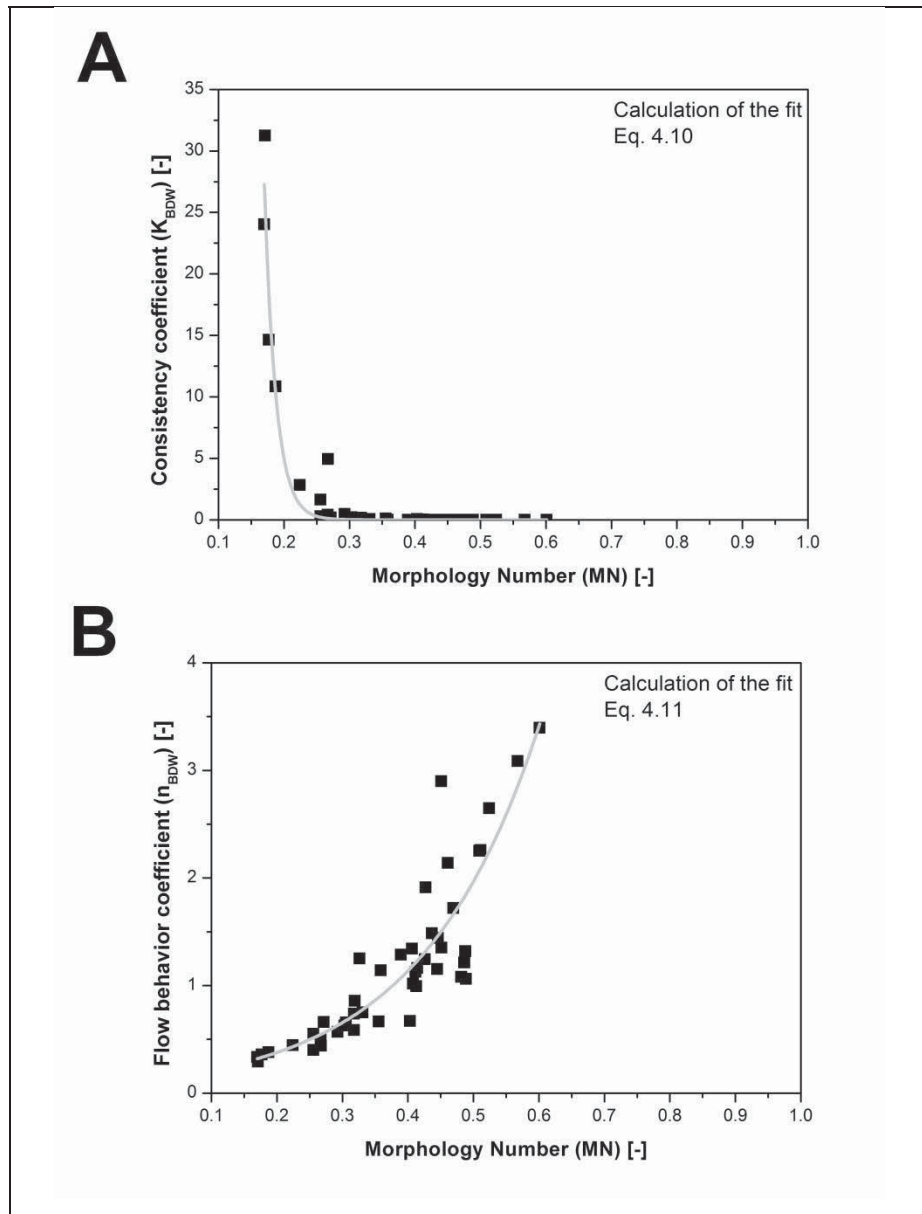$$n_{BDW} = 1.91 \cdot \Lambda^{-0.41}. \tag{4.15}$$
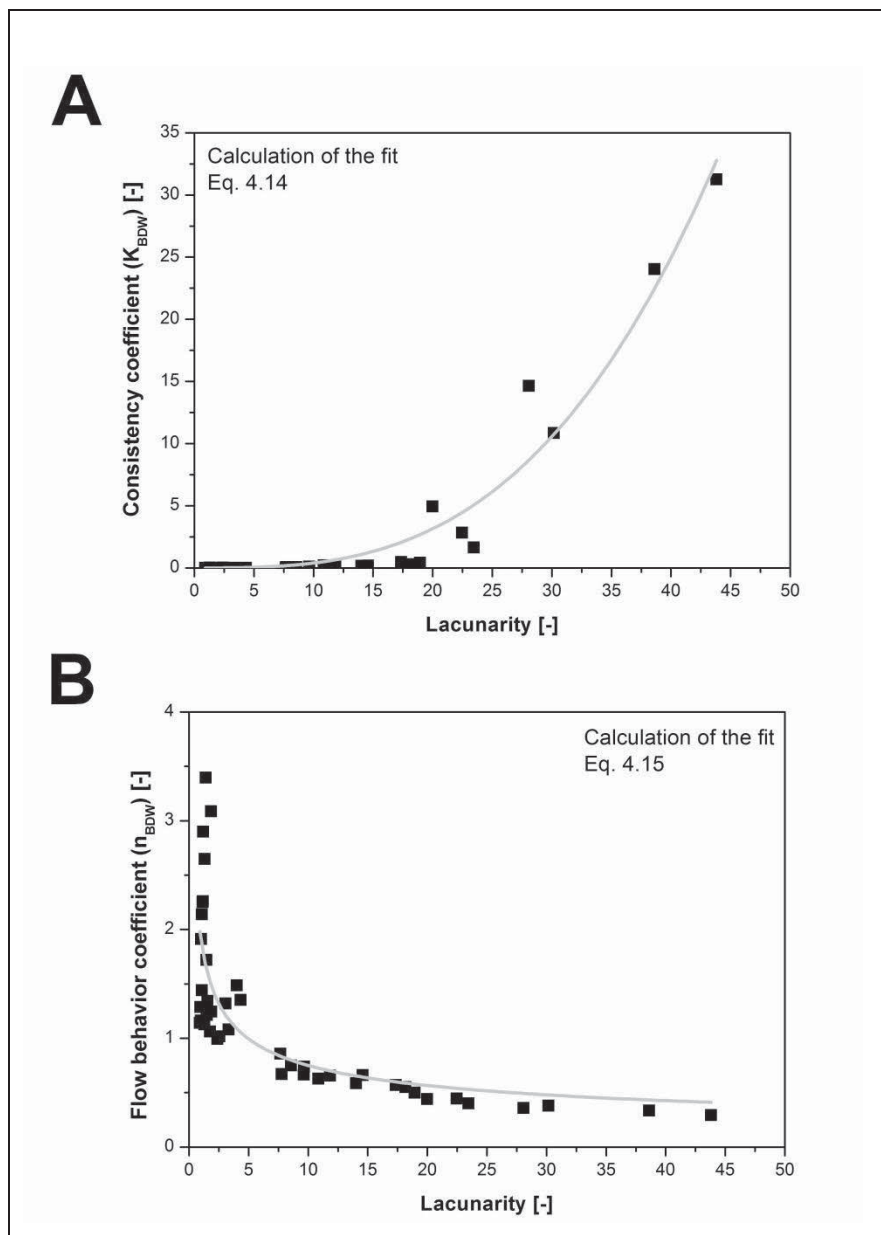


**Figure 4.24**: (A) $K_{BDW}$ and (B) $n_{BDW}$ are depicted over Lacunarity ($\Lambda$). Rheological parameters are biomass normalized. Each dot represents morphology and rheology of a single 100 mL shaking flask cultivation of *A. niger* SKAn 1015 after 72 hours of cultivation. Each value is an absolute mean of at least 3 cultivations

94

All three parameters introduced for characterization of fungal morphology are adequate to study the relationship between fungal morphology and culture broth flow behavior. The biomass rheology correlation was intentionally omitted from these correlations to have a clearer approximation of the impact of fungal morphology, and to increase the applicability for different microorganisms which might show other correlations between biomass and rheological parameters. A strong exponential correlation between fungal morphology and rheology is demonstrated. In general, the classical flow behavior index n remains elusive in most rheologic correlations. Thus, almost all correlations in literature are based on the consistency index K, assuming a constant flow behavior index n. Because n is an exponent, changes in n will have a larger effect on shear stress than a similar change in K, therefore limiting the use of K-values as a single indicator of fluid viscosity to datasets where n is constant [175]. No simple relationship between n and the biomass concentration for *P. chrysogenum* and either *A. oryzae* or *A. niger* was discovered [176, 195]. The inability to find any global value for this parameter was found disturbing by Riley and Thomas [195]. The authors speculated that separate flow behavior and consistency index correlations will be needed for every species, and possibly for different strains. In this study, the flow behavior was shown to correlate nicely with biomass dry weight concentration BDW (compare Figure 4.21), and reasonably well with fungal morphology, depending on the examined fungal parameter (compare Figures 4.22, 4.23 and 4.24).

In **Figure 4.25**, the actual and predicted values of the biomass independent parameters $K_{BDW}$ and $n_{BDW}$ are depicted to describe the quality of the obtained correlations. Predicted values of the consistency coefficient $K_{BDW}$ using correlations eq. 4.10 (Figure 4.25 A), eq. 4.12 (Figure 4.25 B) and eq. 4.14 (Figure 4.25 C) are plotted over measured values, showing the excellence of the correlations. Here the Morphology number (Figure 4.25 A) and the fractal quotient ($D_{BM}/D_{BS}$) (Figure 4.25 B) lead to reasonable results over the whole range of consistency coefficient values. All three models have problems predicting low values of $K_{BDW}$, but correlate well at higher values. This is especially true for $K_{BDW}$ predicted from lacunarity $\Lambda$ (Figures 4.25 C). As stated previously, this morphological parameter is unsuited to describe differences in pellet morphology, which are responsible for the low $K_{BDW}$ values. Moreover, the measuring system has to be taken into account, because the lowest concentrations of biomass had a viscosity which was on the lower limit of the rheological measuring system where the sensitivity of the used rheometer might be insufficient.

Predicted values of $n_{BDW}$ using correlations eq. 4.11 (Figure 4.25 D), eq. 4.13 (Figure 4.25 E) and eq. 4.15 (Figure 4.25 F) and actual values of $n_{BDW}$ are depicted as well. Here, the same tendencies as in graphs A, B and C are apparent. The models fail to predict large values of $n_{BDW}$ representing low viscosity values. Depending on the correlation used, 6 to 7 samples of low viscosity cannot be described by the majority of the correlations. After correction of the biomass influence, samples with lowest viscosities exhibited pellets morphologies. Very large pellets of around 2,000 μm, as common at standard conditions, could especially impair the rheological measurement, as they have a higher tendency to settle and also locally prevent laminar flow through formation of Taylor vortices, even if these could not be observed on a global scale. Correlation (4.11) gained by morphology characterization with the Morphology number (MN) shows the best agreement between predicted and measured values of $n_{BDW}$ (Figure 4.25 D). Evaluation of the data available shows that MN and ($D_{BM}/D_{BS}$) are obviously the best morphological parameter for modeling of the $K_{BDW}$, while the MN is preferable to predict the $n_{BDW}$.
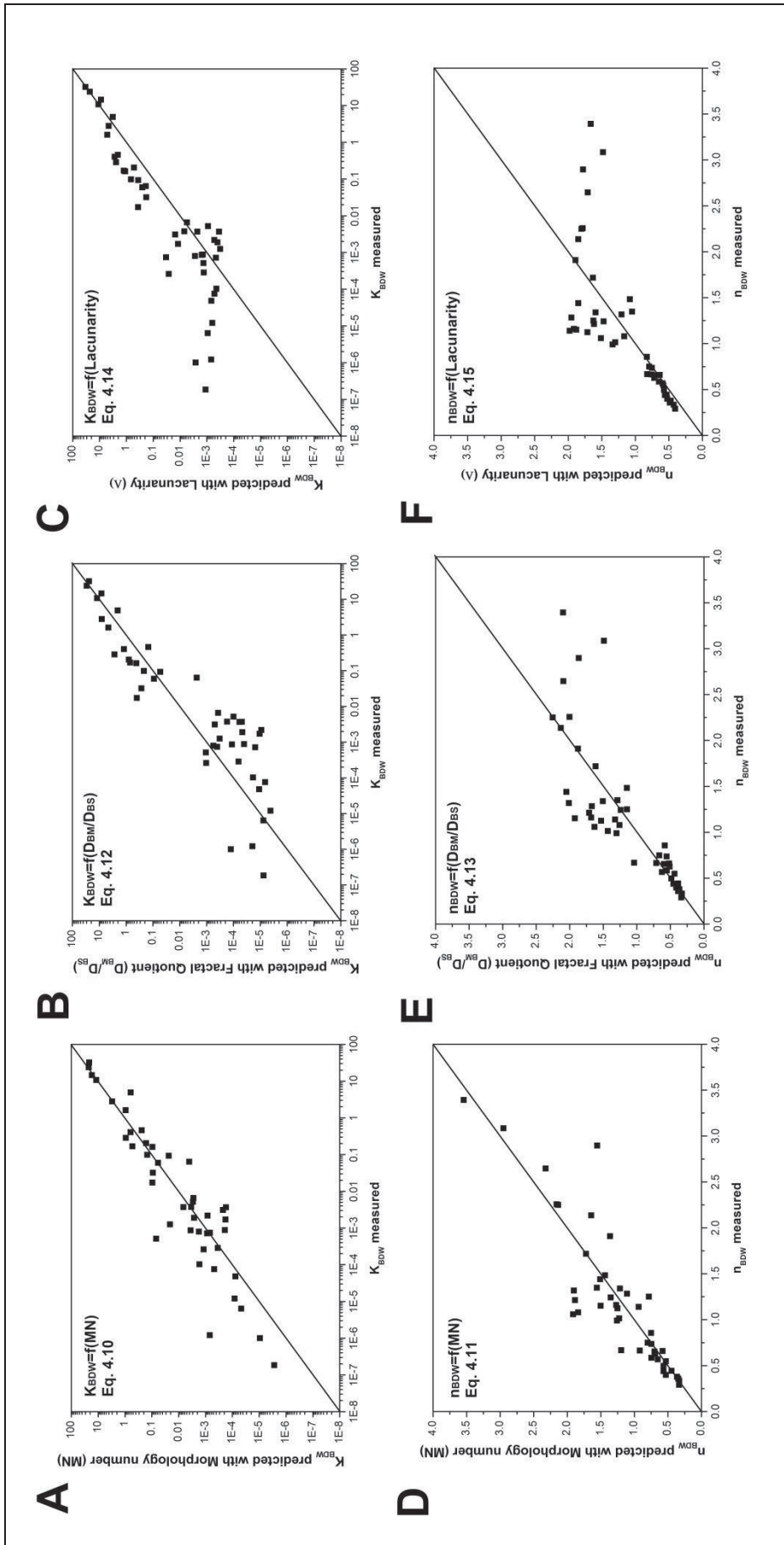
**Figure 4.25**: Actual and predicted values of biomass independent $K_{BDW}$ using correlations 4.10 (A), 4.12 (B) and 4.14 (C). Actual and predicted values of biomass independent $n_{BDW}$ using correlations 4.11 (D), 4.13 (E) and 4.15 (F). Dots are means for at least three 100 mL shaking flask cultivations.

The relationship between particle diameter, pellet concentration, and rheology is obviously increasingly nonlinear and very complex, especially when considering length and branching characteristics of single hyphae [186]. Hyphal entanglement is responsible for significant changes in broth rheology, as found for dispersed growth forms [181]. The degree of hyphal branching, however, seems to decrease culture broth viscosity, because highly branched mutants tended to be less viscous than wild type strains [88]. In most studies, micromorphology was neglected because of the predominance of clumps even for pure mycelial morphology. Furthermore, broth rheology has been often shown to correlate better with clump morphological parameters than with those of free filaments [193, 200]. Clump projected area, for example, was the parameter correlating best with *Penicillium chrysogenum* broth rheology [176]. In this work, Riley and colleagues came up with the following correlation

$$K = BDW^2 \cdot [4 \cdot 10^{-5} \cdot d - 9 \cdot 10^{-4}], \qquad (4.16)$$

where $BDW^2$ is the biomass concentration as dry cell weight, and d is the clump maximum diameter. The flow behavior index n was here either fixed or found from different correlations. The applicability of correlation (4.16) for *A. niger* or *A. oryzae*, however, was limited. A reasonable agreement was found between predicted and measured values for the consistency index for *A. oryzae* cultivations broth but not, however, for broths of *A. niger* [195]. In the present study the Riley-correlation (Eq. 4.16) was tested as well, but did not lead to any satisfactory results for the culture broth of *A. niger* SKAn 1015. This might be due to the rather large difference in diameter of fungal particles between both strains, 100 to 300 μm (*P. chrysogenum*) and 250 to 2,000 μm (*A. niger,* this study), respectively. Furthermore, the biomass concentration was distinctly different, as dry weight between 6 and 30 g L⁻¹ of *P. chrysogenum* was considered in the Riley study [176, 195], whereas the highest biomass concentration reached in cultivations of *A. niger* SKAn 1015 was 9 g L⁻¹. More sensitive measurement techniques, however, allowed a determination of rheology beginning at biomass concentrations of 0.3 g L⁻¹. In contrast to correlations found by Riley et al. [176], the correlations in this study are completely independent of magnification, because analysis was based on pixels which were converted to μm. A resolution of 2048 x 1536 pixels with 3.2 μm per pixel was sufficient to capture all fungal particles and avoid inaccuracies through conversion of units.

### 4.1.8 Estimation of productivity from rheological data

Through comparison of morphological and rheological data, it is evident that a mycelial morphology of *A. niger* is most productive, but also exhibits the highest culture broth viscosity. Since both fructofuranosidase activity and viscosity seem to change in conjunction, even if not directly related, it seems feasible to neglect laborious morphological characterization by image analysis and try to estimate fructofuranosidase activity from rheological data alone.
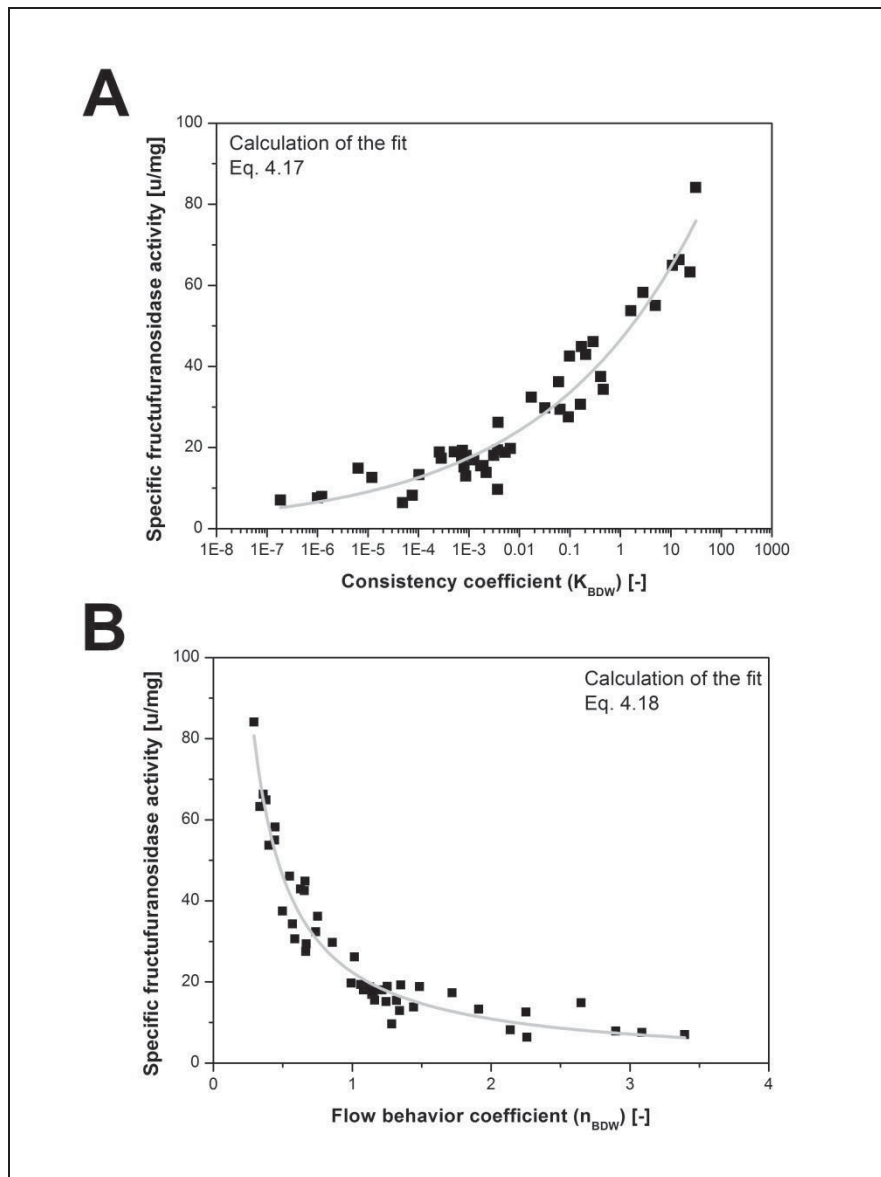


**Figure 4.26:** Specific fructofuranosidase activity correlated with rheological parameters A) $K_{BDW}$ and (B) $n_{BDW}$.

In **Figure 4.26** specific fructofuranosidase activity is thus plotted over $K_{BDW}$ (A) and $n_{BDW}$ (B) reaching the following correlations

$$Specific\ fructofuranosidase\ activity = 46.58 \cdot K_{BDW}{}^{0.14} \qquad (4.17)$$

using $K_{BDW}$ ($R^2 = 0.93$), and

$$Specific\ fructofuranosidase\ activity = 22.40 \cdot n_{BDW}{}^{-1.04}, \qquad (4.18)$$

using $n_{BDW}$ ($R^2 = 0.94$), respectively.

**Figure 4.27** shows the quality of correlations (4.17) and (4.18). Predicted and actual values of fructofuranosidase activity show a very good conformance for both correlations. A direct correlation of productivity and rheological properties is therefore possible, having a high potential for industrial application in enzyme production with *A. niger,* because of the relative simplicity of viscosity measurement once a sufficient protocol is established.
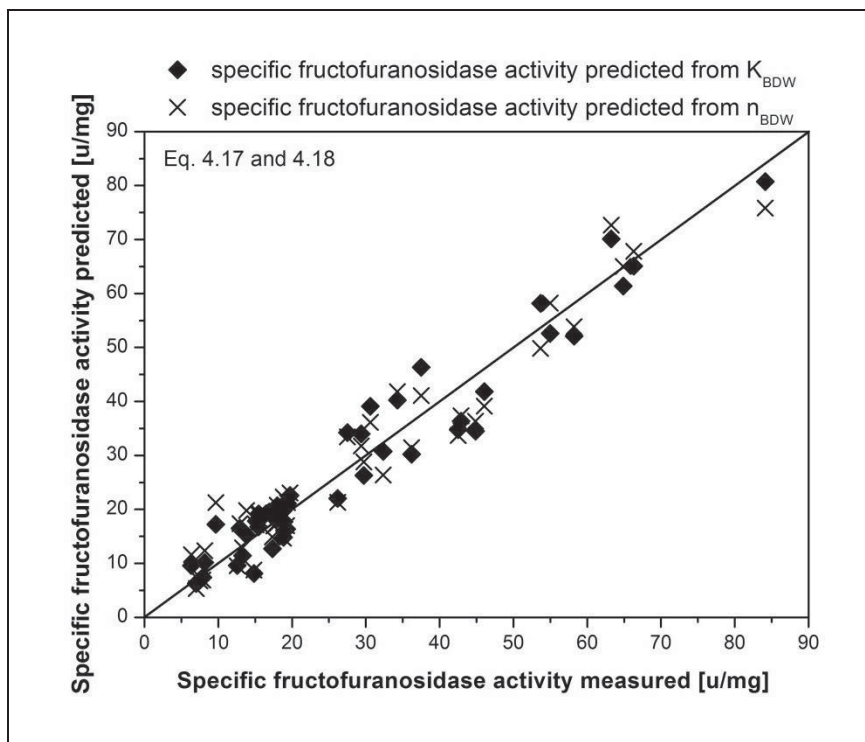


**Figure 4.27:** Actual and predicted values of specific fructofuranosidase activity $K_{BDW}$ (Eq. 4.17) and flow behavior coefficient $n_{BDW}$ (Eq. 4.18). Dots are means for at least three 100 mL cultivations of *A. niger* SKAn 1015.

### 4.1.9  Linking morphology, productivity and rheology to improve process understanding

The exact manipulation and precise characterization of *A. niger* morphology enables the establishment of holistic mathematical models. Schügerl and colleagues [346] pointed out the complex interrelationships between all the factors involved in growth, morphology, physiology and productivity of moulds [59], and reasoned that it would not be possible to make any general conclusions without considering all of the relevant parameters [346]. The following characterization for productivity modeling based on whole broth properties were suggested by Kossen (**Figure 4.28**) [59].
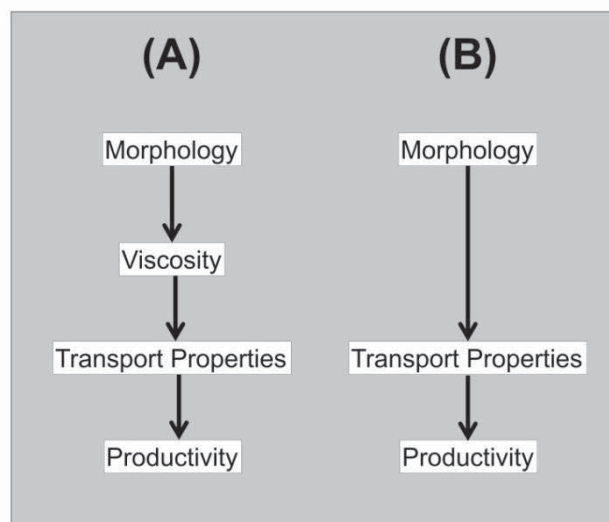


**Figure 4.28:** Proposed routes of productivity modeling based on morphology, described by Kossen [59].

This approach basically comprises a model of the productivity based on morphological and rheological data and transport properties (Figure 4.28 A). Kossen advised to take approach B (Figure 4.28 B), because of general problems in measuring the viscosity of the filamentous cultivation broths [59]. In the present study, these problems were mostly overcome, because with the applied system the whole range of fungal morphology, comprising fairly large pellets and intertwined filaments, could be measured. Nevertheless, a more comprehensive approach was perceived to be more applicable. Fungal morphology, viscosity and productivity are the main process parameters. Transport properties are dependent on morphology and viscosity, and are, in the present approach, omitted.

101
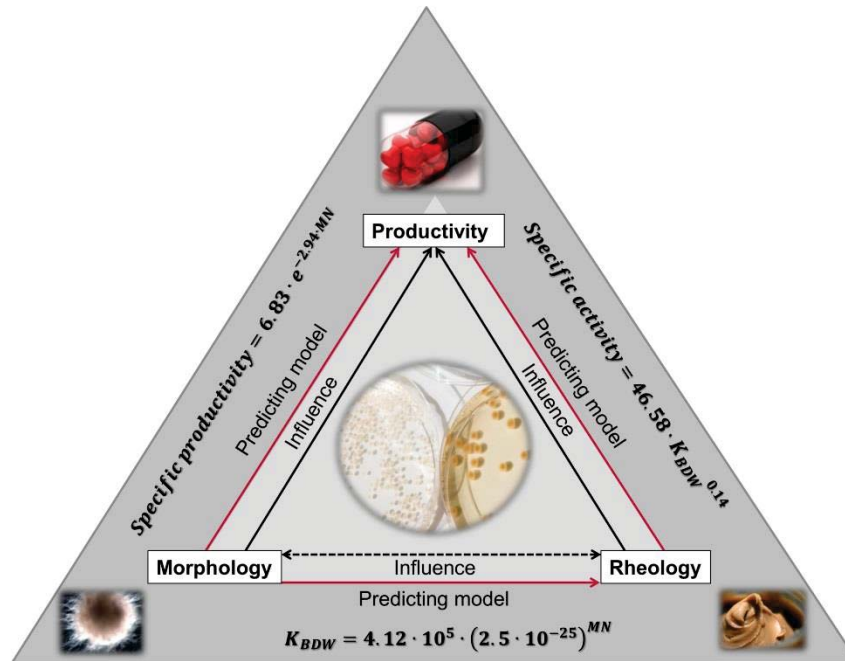
**Figure 4.29:** Established mathematical models between fungal morphology, rheology and productivity.

**Figure 4.29** shows the interrelationship between these three parameters. *A. niger* morphology directly influences productivity and with help of the established model, it is possible to predict specific productivity from the image analytical parameter Morphology number (MN). Culture broth rheology is influenced by fungal morphology as well. Thus, the biomass-independent consistency coefficient $K_{BDW}$ can directly be correlated to MN. Furthermore, in an unconventional approach, a mathematic link was discovered between the specific activity of the produced enzyme fructofuranosidase and rheological properties of the cultivation broth. This was feasible because the intricate relationship between viscosity and transport properties which influence productivity is well known [59]. This model elucidates the connection and interdependence of morphology, rheology and productivity. Either the fractal quotient ($D_{BM}/D_{BS}$) or Lacunarity could also have been used instead of the Morphology number.

## 4.2    Aggregate morphology as a process parameter in submerged cultivation of *Taxus chinensis*

In suspension cultures plant cells generally grow as aggregates ranging from few to thousands of cells with sizes from less than 100 μm to well over 2 mm [347]. Plant cell aggregates have long been recognized as an important feature of plant cell culture systems, as they create microenvironments for individual cells with respect to nutrient limitations, cell-cell signaling, and applied shear in the in vitro environment [347]. The morphology of these aggregates is of some importance, because aggregate size has been proposed to correlate with productivity [7], whereas aggregate coloration was reported to depend on cell age and viability [8]. Both morphologic traits can be analyzed to improve process understanding. Laser diffraction was evaluated as an innovative method for improved size estimation of *Taxus* aggregates, whereas cell viability and coloration were analyzed through a novel image analytic approach and compared with a newly introduced molecular viability assay.

### 4.2.1  Improved measurement of plant cell aggregate size through laser diffraction

*Taxus chinensis* suspension cells were cultivated in shaking flasks for 10 days. Every two days, the biomass was determined and the size distribution of plant cell aggregates was measured by image analysis and laser diffraction. The shaking flasks were inoculated with around 4 g $L^{-1}$ of biomass. After a short lag-phase till day two, a linear increase in bio dry mass was apparent during exponential growth phase from day two up to day eight (**Figure 4.30** A), when biomass increased 3.5 fold from 4 g $L^{-1}$ to roughly 14 g $L^{-1}$. After 10 days, the rate of growth decreased due to depletion of nutrients, and an imminent descent into death phase was indicated.
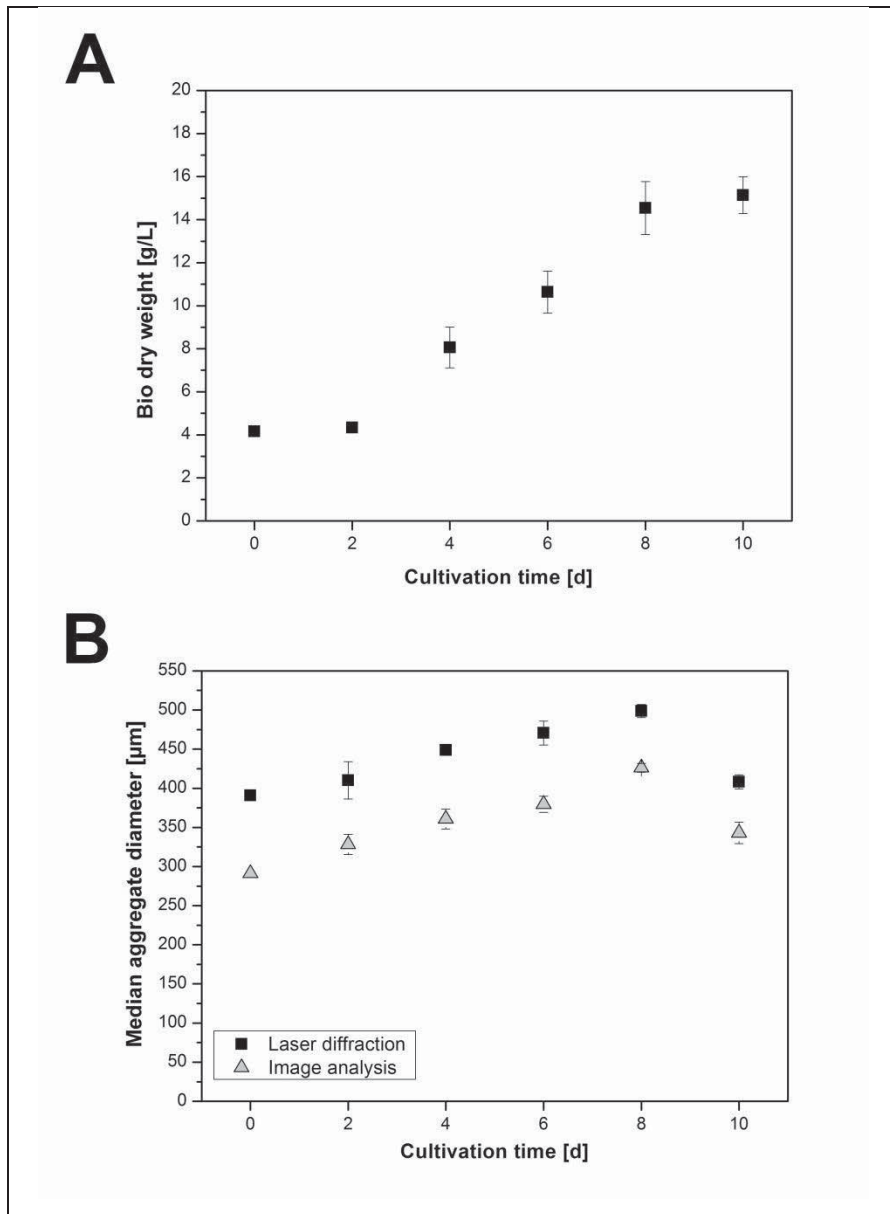
**Figure 4.30:** Median size values of laser diffraction and image analysis and corresponding biomass dry weight (points). Error bars represent standard deviation of three biological replicates.

**Figure 4.31** displays the volume-based size distribution of *Taxus chinensis* aggregates measured by laser diffraction. The reproducibility of the laser diffraction measurements was generally high, which is shown in Figure 4.31 A.
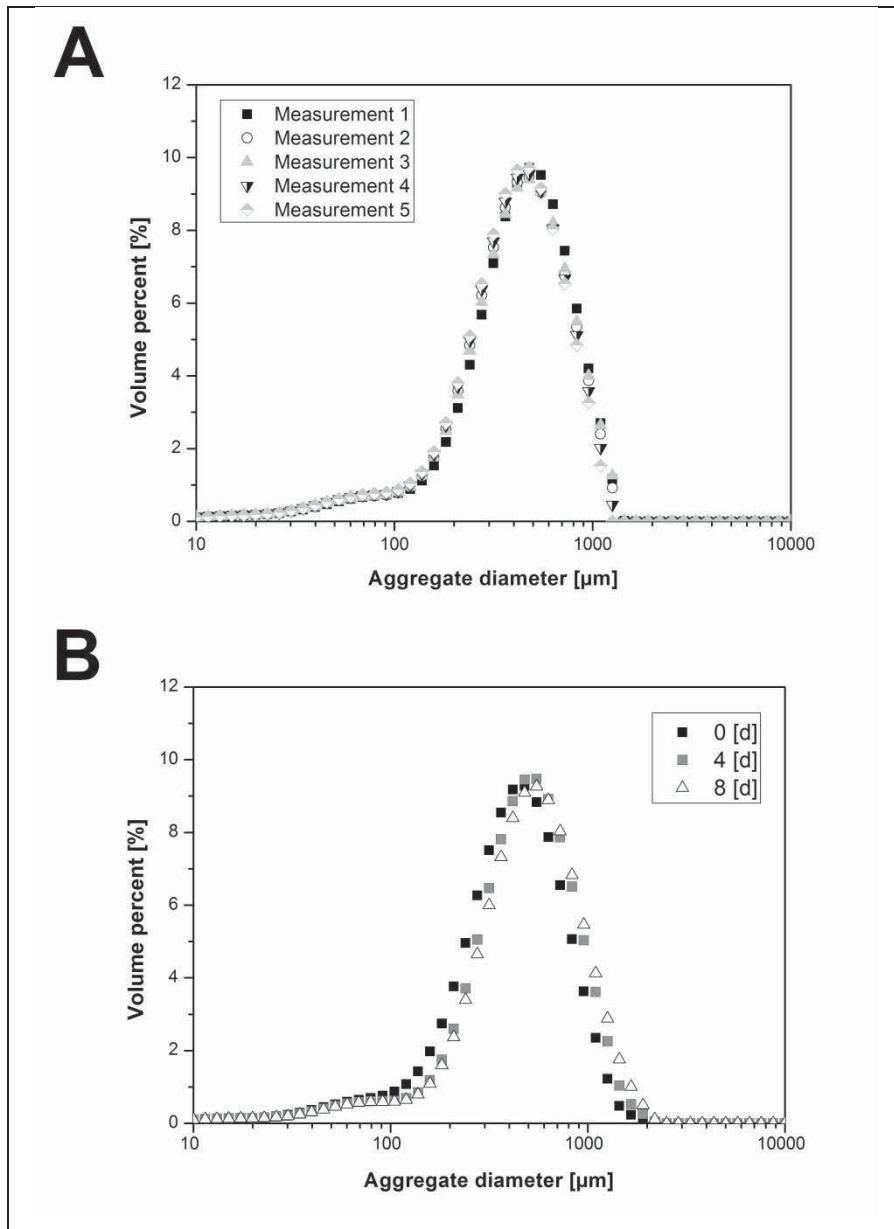
**Figure 4.31:** (A) Volume size distributions generated by five subsequent laser diffraction measurements. (B) Volume size distribution of *Taxus* cell aggregates measured, by laser diffraction right after inoculation, after 4 and 8 days of cultivation.

Here, five subsequent measurements of the same sample produce congruent size distributions. Due to the large number of analyzed samples and the method in general, the distribution was found accurate and smooth. In Figure 4.31 B, growth of *Taxus* aggregates is shown, including size distributions right after inoculation and after 4 and 8 days of cultivation. Plant cell aggregates were normally distributed between 100 and 1100 µm of size, with a slight shoulder made up of smaller

105

aggregates and single cells at 100 μm and below. An increase in size until day 8 was evident. The mode of the distribution was around 500 μm. Aggregate growth was observed by the shift towards larger aggregates after four and eight days of cultivation. The mode of the distribution increased about 50 μm during this time. In Figure 4.30 B, development of the median aggregate diameter with cultivation time is depicted. The median aggregate diameter developed similar to the biomass (compare Figure 4.30 A). Median aggregate size increased 78 % during the exponential growth phase, from around 390 μm prior to inoculation to 500 μm by day eight. In the stationary phase at day ten, the median aggregate size decreased to 400 μm.



**Figure 4.32:** (A) Number-based distributions generated by five subsequent image analysis measurements. (B) Number-based distribution of *Taxus* cell aggregates generated by image analysis of pictures taken by microscope right after inoculation, after 4 and 8 days of cultivation.

The plant cell aggregate distribution as determined by image analysis taken for comparison is depicted in **Figure 4.32**. The obtained number-based distributions were normalized, due to differing particle count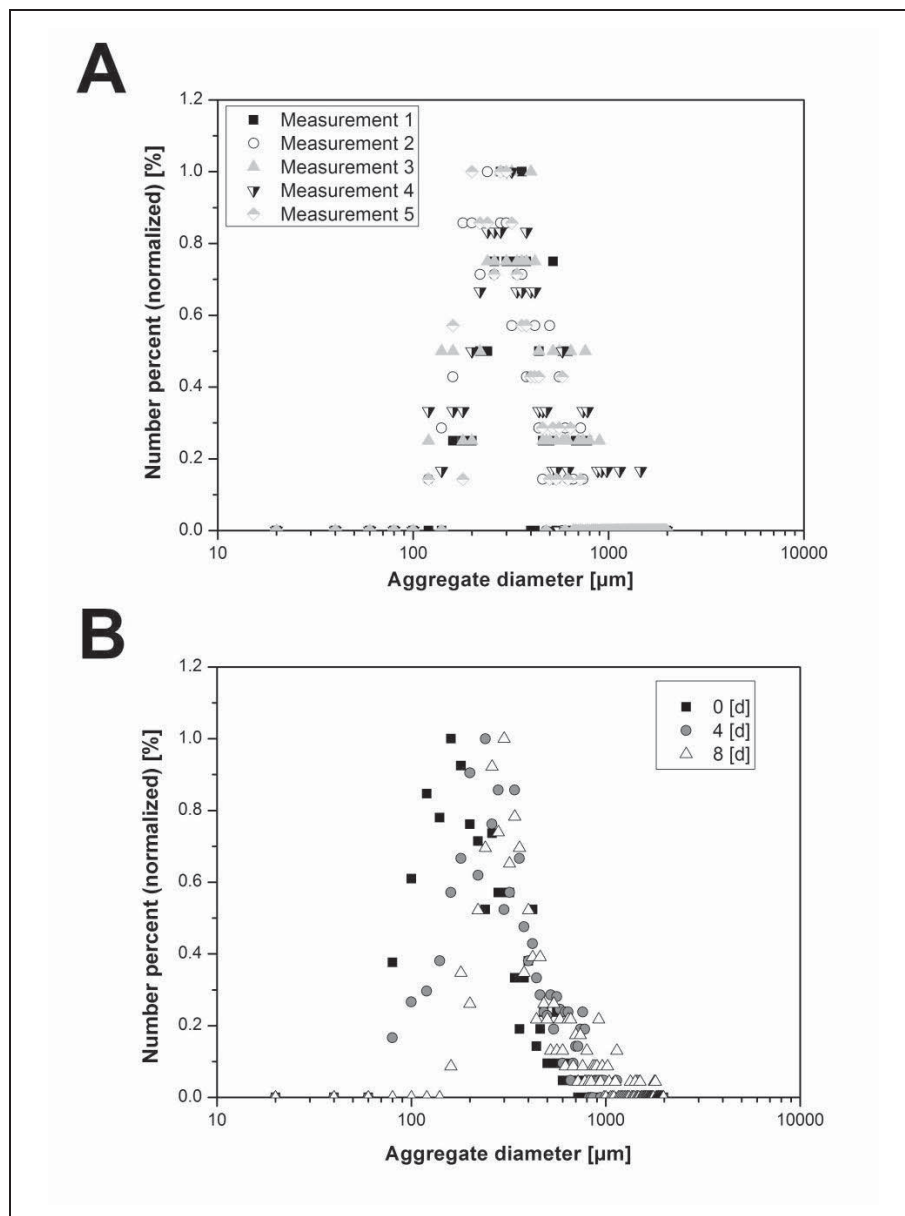s. To illustrate the reproducibility of the image analysis method, a sample was measured 5 times, as shown in Figure 4.32 A. In contrast to the laser diffraction method, a considerable scattering is obvious; even the mode of the distribution fluctuates between 200 and 400 μm. In Figure 4.32 B, aggregate size distributions prior to inoculation, after four and eight days of cultivation are shown. *Taxus* plant cell aggregates measured by image analysis were normally distributed and between 80 and 1100 μm of size. The method of analysis produced lots of scattering and generally coarse distributions. Growth of aggregates was apparent by a distinct shift of the distribution towards larger aggregates after days four and eight. The mode of the distributions obtained by image analysis lies much lower, between 180 and 300 μm, compared to the distribution obtained by laser diffraction.

Figure 4.30 B shows the median diameters of the aggregates measured by both methods. For a better comparison with laser diffraction, the diameter of the major axis is depicted, i.e. for irregular and elongated aggregates the greatest diameter is selected at all times. The maximal median diameter of plant cell aggregates determined by image analysis shows the exact same trend as median diameter measured by laser diffraction, but is located around 100 μm lower, as the aggregate diameter increases from 290 μm to 420 μm.

The size of plant cell aggregates is an important parameter for cultivation of plant cells in suspension [7, 236, 237]. Cells in such aggregates are affected by different microenvironments which depend on the size of the aggregate. Formed gradients and heterogeneities are responsible for changes in the cell metabolism, which influence production of secondary metabolites. Most studies examining cell function are ultimately based on microscopy and image analysis [348], the size of the plant cell aggregates being one of the influencing factors. Information about plant cell aggregate size can also be used to obtain information about total biomass. **Figure 4.33** reveals a linear relationship ($R^2 = 0.99$) between bio dry weight (g L$^{-1}$) and aggregate diameter (μm) during the exponential growth phase. This relationship could be used as an option to determine total biomass in plant cell culture systems, because dry weight measurements are time consuming and require at least a day for drying [234, 349]. Such simple and fast methods are much-needed alternatives for often imprecise bio fresh weight determinations.
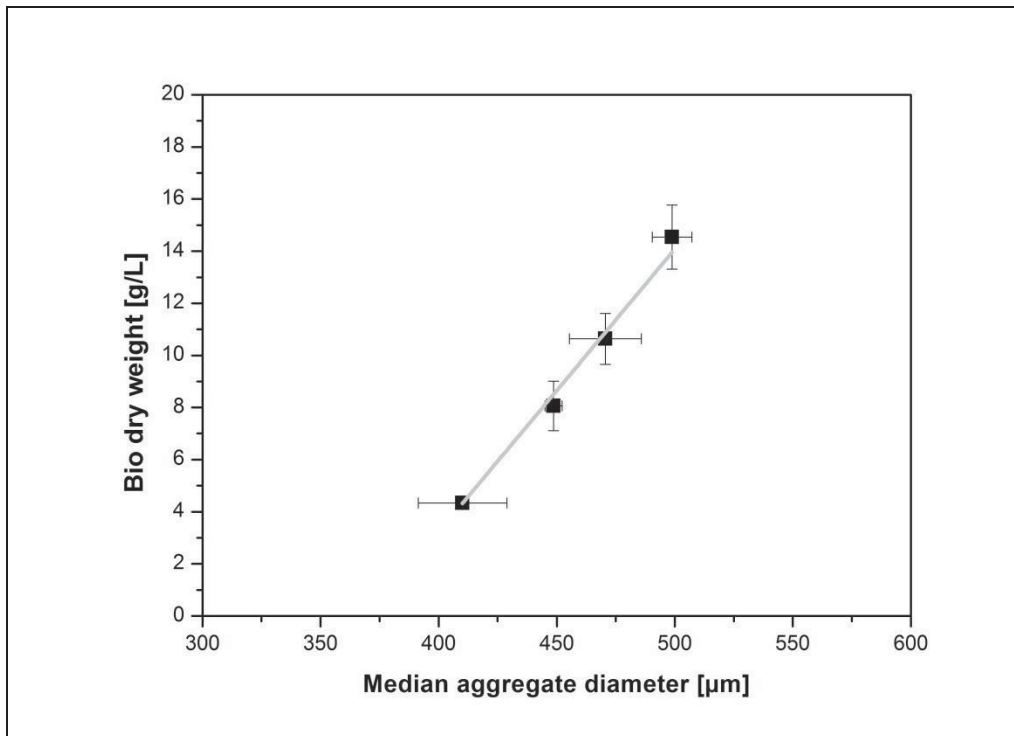
**Figure 4.33:** (A) Linear correlation ($R^2 = 0.99$) of biomass and median aggregate diameter. Error bars are means for three biological samples.

Microscopy is selected as a method for most investigations, because it is readily available in biological labs and it can provide a high resolution for a small sample, which is beneficial for basic research. In the current study, the most common microscopic- image analytic approach to measure particle size was compared to the technically more abstract laser diffraction. Image analysis techniques can be used for identification of aggregate size and have the advantage of enabling the identification of further morphologic parameters, like circularity, roughness or elongation, which were previously found to give an indication of overall culture performance in general and productivity in particular [253].

In the current study, no change of morphological appearance apart from aggregate size was detected, making a more detailed image analysis obsolete. The process of image analysis is mostly divided into sample dilution, image acquisition by microscope and a more or less automated step of image analysis [348]. Every step takes up time and makes the overall process very slow. Preparation and dilution steps also have the potential to impair plant cell aggregate integrity. Through automation of the image acquisition using the flow-through cell, a relatively high number of around 400 particles could be analyzed in the present study. Still, the distribution was coarse, suggesting that even more particles are needed to obtain a more valid and smooth distribution.

Generally, both image analysis and laser diffraction provide the same trend and similar distributions (Figures 4.30 B, 4.31 B and 4.32 B). A linear relationship between the median

108

aggregate diameters measured by both methods is obvious (Figure 4.30 B). The rather large difference in the plant cell aggregate median diameter determined by laser diffraction and image analysis is conspicuous. It might come as a surprise that both methods show such a discrepancy, since the same samples were measured. However, this large difference is typical for comparisons between volume- and number-based distributions, and can be observed in other studies [350]. This is a prime example of how important it is to really be aware of both the method of particle size measurement and the corresponding type of distribution it generates. It is possible to transform a number distribution into a volume distribution and vice versa; however, the mathematical process involves a rather large amount of fitting and generally increases the standard error. Deviation in the mode between distributions by the two methods is even greater (compare Figure 4.31 and 4.32), as the mode gained by laser diffraction is significantly larger than that of the image analysis size distribution.

To understand these differences, it is important to realize that there is a cubic relationship between the size of a particle and its volume, which should be considered when comparing number and volume based distributions. A single 600 µm *Taxus* cell aggregate within a thousand 60 µm single *Taxus* cells would be insignificant in a number-based distribution, but make up half of the actual volume in a volume-based distribution. So, while image analysis favors smaller particles, and produces lower values, laser diffraction is prone to overestimate larger particles leading to greater values for mode and median.

Image analysis generally produces number distributions, and therefore has a high sensitivity towards small particles. While providing a high resolution for single cells, estimation of means for the whole culture remains troublesome, because relatively few particles are examined, and there is a risk of unrepresentative sampling. For example, 1 g biological sample with 100 µm aggregates and a density of 1.0 g mL$^{-1}$ contains $2.55 \cdot 10^6$ particles making it virtually impossible to examine all of them by microscopy [351]. During image analysis, particles at the border of the picture are usually excluded, and smaller particles have a higher chance of being included in the analysis. Missing or ignoring even one 10 µm particle has the same effect as ignoring ten 1 µm particles, or even a thousand when a weight distribution is measured. Image analysis techniques are, therefore, not suitable as a quality or production control technique [351].

The flow orientation of elongated particles within the laser diffraction measuring cell is also an issue, because it might lead to an apparent bimodality of the particle size distribution for some samples [352]. This was not the case for the *Taxus* samples. In the flow-through cell used for microscopic picture acquisition, a flow orientation of *Taxus* aggregates is possible as well, but

since image analysis can detect maximal as well as minimal diameter, the results will not be affected. *Taxus* aggregates have a mostly randomly-oriented, slightly asymmetrical form, and for such particles the size distribution determined by laser diffraction is usually unimodal [352], as seen in Figure 4.31.

A critical radius of plant cell aggregates is often thoufgt to be related to production of secondary metabolites [237], because of oxygen and nutrient penetration and the formation of dead zones in the aggregate core. Measurement of nutrients or oxygen, however, is very difficult, thus most estimations are based on theoretical predictions. For such investigations, plant cell aggregate volume and the number of corresponding cells is estimated from plant cell aggregate diameter. Using different methods for plant cell size assessment, the diameter can deviate as much as 100 µm (compare Figure 4.30). While microcopy and image analysis might indicate that a median *Taxus* aggregate at cultivation day six is made up of 100 cells (**Figure 4.34**), laser diffraction measurements indicate a median cell number of 200 cells per aggregate. The underestimation of cell number based on microscopy and image analysis will lead to an underestimation of critical aggregate radius and optimal aggregate size, emphasising the importance of selecting a suitable method for size determination of plant cell aggregates.
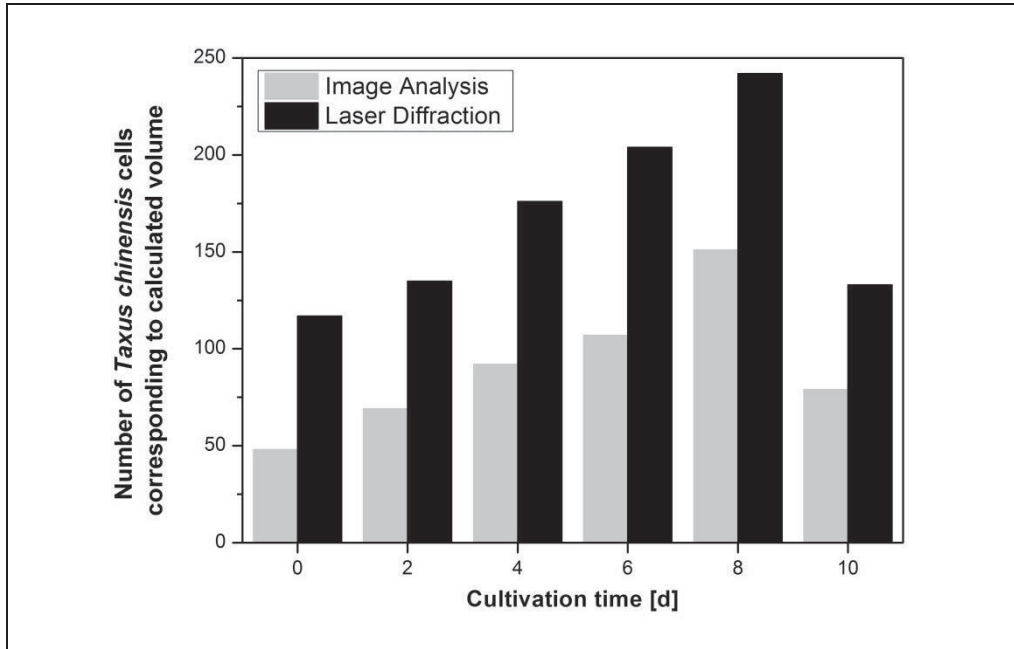


**Figure 4.34:** Number of *Taxus chinensis* cells corresponding to the median aggregate diameter determined by laser diffraction and image analysis, assuming a median cell diameter of 80 µm.

One of the main advantages of laser diffraction, irrespective of the type of size distribution which is generated, is the easy applicability and the speed of measurement. A single aggregate size distribution measurement will take less than 1 minute, in comparison to the hours consumed by

110

image acquisition and analysis. During this short time, a large number of samples can be analyzed increasing the statistical validity of the measurement. The measuring process is completely automated, and no sample preparation is needed. Furthermore, laser diffraction is non-destructive and non-obtrusive, making the reuse of biomass possible. Depending on the biomass concentration, it is even possible to measure under sterile conditions online, using a bypass to and from a bioreactor [253].

Each size characterization technique will measure a different particle property, like maximal and minimal diameter, surface area, projected area or volume, and will correspondingly lead to slightly different values. Therefore, the measuring technique should also be considered when analyzing and comparing information on particle size [351]. In this investigation, laser diffraction was found to produce valid repeatable results which were, in terms of median, close to the more common method of microscopy and image analysis. Image analysis methods should be used for research purposes or when very detailed morphological information is needed. For quality control or production purposes, the newly introduced method of laser diffraction for samples of plant cells is by far the superior method, since it provides a practical, rapid, robust and reproducible way to sample large amounts of material.

### 4.2.2  Novel methods for assessment of plant cell viability

The determination of viability is a standard analytical procedure in industrial cultivation of eukaryotic cells. For processes with *Taxus chinensis* plant cells, no viability estimating techniques besides measurements of cell fresh weights and cell dry weights have so far been established. A reduction of cell growth, however, does not imply a reduction of viability [272]. The ideal test for estimating in vitro cell proliferation is a simple, rapid, efficient, reliable, sensitive, safe and cost-effective measurement of cell viability [353]. Recently, the Alamar Blue (AB) dye has gained popularity as a very simple and versatile way of measuring cell proliferation and cytotoxicity [353]. AB is a nontoxic redox indicator, which can be detected by both fluorescence and by color change. It contains resazurin and resorufin as oxidation-reduction indicators. The oxidized blue, non-fluorescent form of resazurin is converted by reduction into a pink fluorescent dye resorufin [354]. The reduction of AB occurs intracellularly involving reductases and the mitochondrial electron transport chain [355]. AB acts as an electrone acceptor between cytochrome a;a3 and the final reduction step of $O_2$, and does not interfere with the respiratory chain [355, 356]. Other tetrazolium salt based agents like MTT and TTC have a more negative redox potential than the components of the electron transport chain, and thus consume energy in form of ATP during the

reduction. Alamar Blue, on the other hand possesses a more positive redox potential than $FMNH_2$, $FADH_2$, NADH, NADPH and the cytochromes. Thus, a reduction is possible without additional energy [356]. Other advantages of the Alamar Blue assay include the water solubility of the formazan product, economic efficiency, minimal toxicity, and quantification of the reduction product by spectrophotometry and fluorescence [355]. Some studies found some benefit of the fluorometric analysis in terms of a higher sensitivity and consistency compared to photometric measurements [357]. The 'resazurin reduction test' has been used for about 50 years to monitor bacterial and yeast contamination of milk, and also for assessing semen quality [353]. The AB assay has so far been used for the determination of the viability of bacteria, mycobacteria, fungi and several human cell lines [358-362]. It was also used to assess the viability of tomato plant cells [355].

Since the Alamar Blue assay has so far not been used for *Taxus* plant cells, it was necessary to adjust the assay for analysis of *Taxus* cell aggregates. The following factors were identified to significantly influence measurement results and reproducibility of the test: the incubation time, the age of the culture, lighting conditions and type of incubation. These factors were gradually optimized. Byth and colleagues [355] found that common plant cell media and buffers reduce the AB agent. Therefore it was necessary to filter cells and resuspend them in phosphate buffer. 50 mg *Taxus* cells were suspended in 200 µl phosphate buffer. AB was used in a final concentration of 10 % (v/v) within the suspension. To establish the AB assay, a calibration graph with a known composition of viable and dead cells and their corresponding fluorescences had to be established. To this end, *Taxus* cells were eradicated in a controlled manner by incubation for 1 minute in liquid nitrogen. Subsequently, cells were gently defrosted in warm (37 °C) water, and after that, blended with living cells to create the desired quantities of living cells. The proportions of living cells ranged from 0 to 100% in 10% increments.
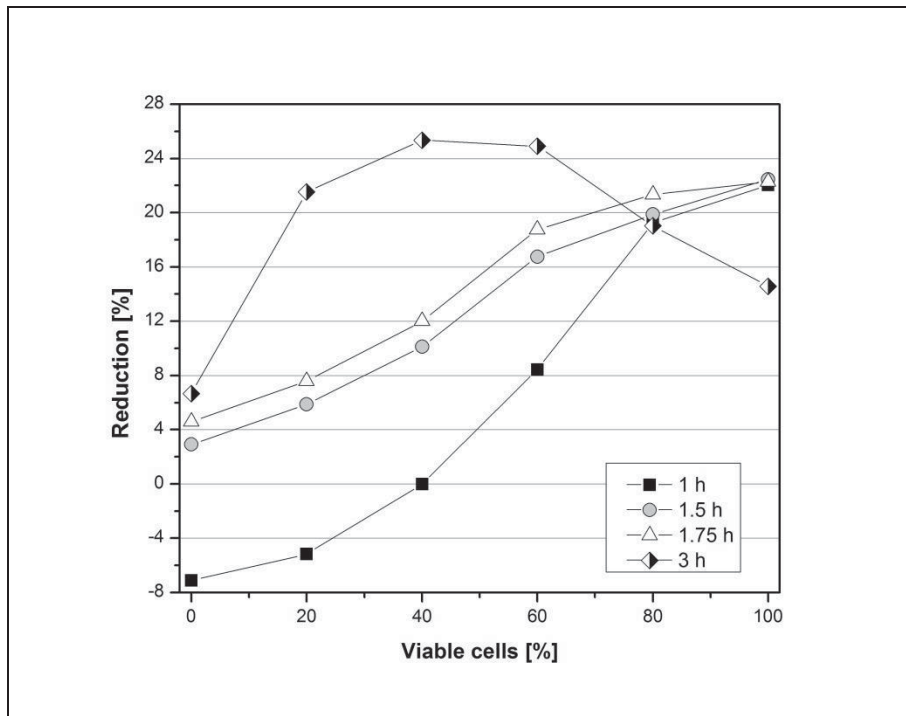
**Figure 4.35:** Evaluation of incubation time for the Alamar Blue assay for the determination of *Taxus chinensis* cells.

The incubation time of the assay was varied from 1 to 3 hours (**Figure 4.35**). Only incubation times of 1,5 and 1.75 hours produced reasonable reduction values and the characteristic sigmoidal trend also described by Byth and colleagues [355]. 1 hour was obviously not long enough for the cellular metabolism to reduce the resazurin to resorufin, whereas some degradation must have taken place after 3 hours of cultivation. Subsequently, an incubation time of 1.5 hours was used.

To create standardized reproducible calibration graphs an optimal viability of the cells used for the calibration had to be ensured. Therefore *Taxus* cells of several culture ages were used to identify an optimal age of the culture. **Figure 4.36** A shows the maximal measured relative fluorescence with respect to culture age. After five days of cultivation the highest relative fluorescence was measured with approximately 700 relative units. Thus, cells cultivated for 5 days have the highest metabolic activity. The resulting calibration curve of the sample cultivated for 5 days is depicted in Figure 4.36 B. The fluorescence values of the various percentages of living cells range from 120 to around 700 fluorescence units. The values rise steadily over the entire range. The relationship between cell viability and relative fluorescence is sigmoidal, which was also reported by Byth and colleagues [355].
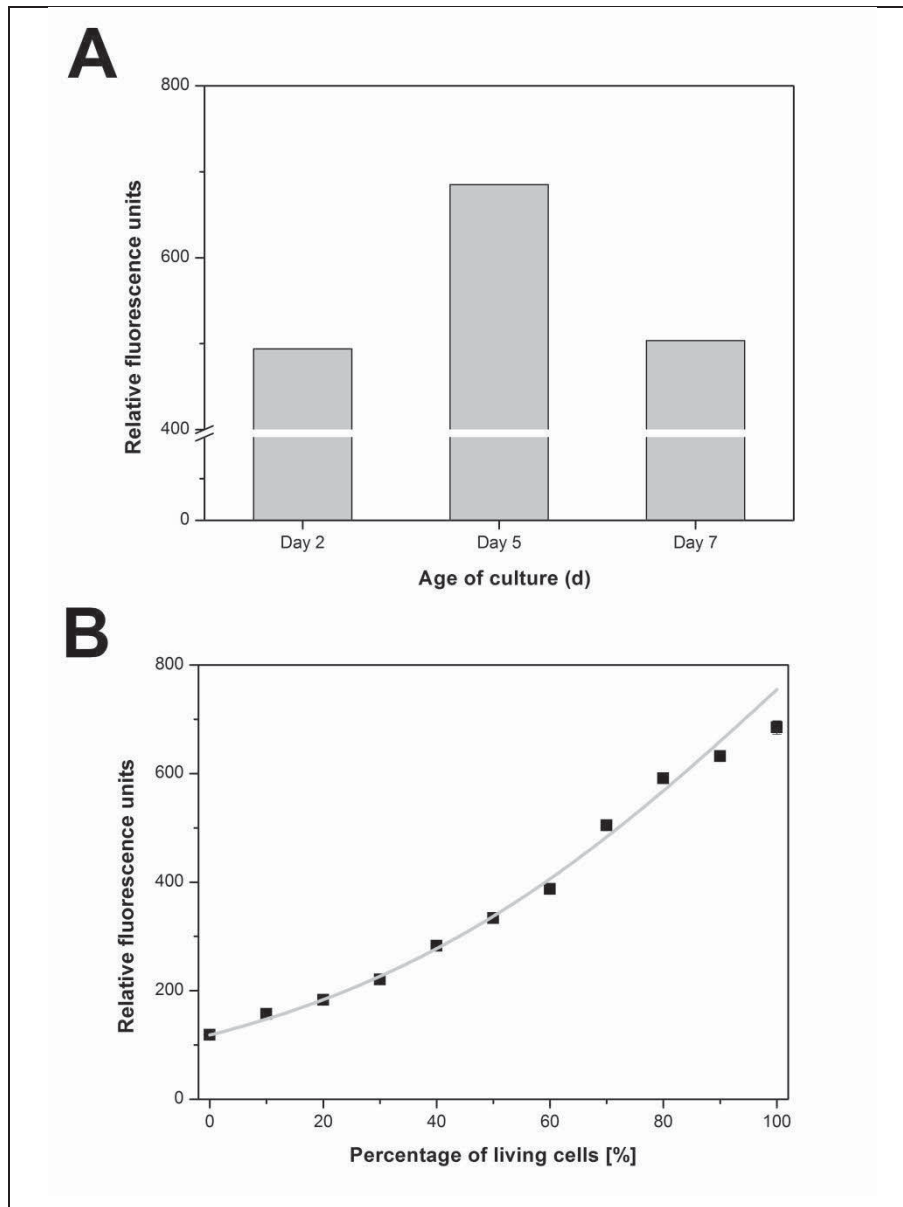
**Figure 4.36:** (A) Maximum measured relative fluorescence is depicted over age of culture in days (B) Regression curve at an culture age of 5 days and an incubation time of 1.5 hours. Values are means for 3 replicates. $R^2$=0.99

The measured fluorescence values of *Taxus chinensis* cells were generally not higher than 700 units, which is significantly lower than the 5500 fluorescence units achieved with tomato cells [355]. This can possibly be explained by varying light conditions, as incubation in bright sunlight produces significantly higher fluorescence values than incubation in the shade. Exposure to light during incubation is essential. To ensure highest possible reproducibility, samples were incubated under artificial light sources and under absence of direct sunlight. Another reason for lower fluorescence values could be the presence of aggregates, which might lead to reduced uptake and release rates and might cause diffusion limitations. For relatively large aggregates, it is likely that only the surface cells will be sufficiently penetrated by the agent. However, there is no way to break up aggregates without impairing general viability. To further improve the reproducibility of

114

the assay, the samples were mixed during the entire incubation period in an overhead rotator (Revolver, Labnet International, Inc. Edison, USA), to make sure that aggregates were suspended at all times. This rotating incubation was responsible for the generally high reproducibility of the assay, with a deviation of less than 1 % between three measurements. In order to further minimize the deviation, it would have to be important to use the exact same number of cells, which would increase both the comparability and reproducibility of the assay. However, since the exact number of cells which form an aggregate cannot be made out, this remains infeasible under industrial conditions.

To determine the validity and suitability of the Alamar Blue viability assay for *Taxus chinensis* suspension cultures, a comparison with the MTT assay, which is already established for plant cells, was conducted. Like the AB assay, this viability test is based on the reducing properties of the mitochondrial electron transport chain. The water-insoluble purple product formazan was extracted with DMSO- and determined by spectrophotometry. Results for the AB and MTT assay for a 7 day old sample are depicted in **Figure 4.37**.
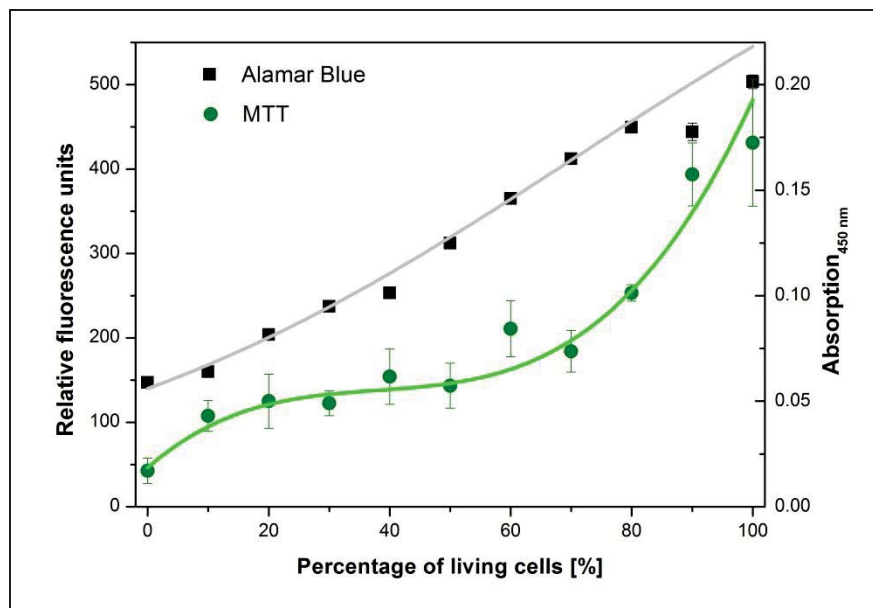


**Figure 4.37:** Regression curve for the Alamar Blue (black) and MTT assay (green). Values are means for four replicates.

Through application of the AB assay, the familiar sigmoidal curve is obtained, whereas the curve of the MTT assay initially stays constant and increases only with a higher percentage of living cells. The values in the range of 40 to 60% viable cells show only minor differences in the absorption. Generally, the errors of the MTT assay are much higher. The MTT assay also yields relatively low absorption values between 0.01 and 0.2. However, these values can be expected, as the MTT assay usually produces absorption values between 0 and 1.5, depending on the cell line

being examined [280, 281]. The AB assay of this 7-day-old sample did not yield the same high fluorescence values as in earlier experiments, implying suboptimal culture conditions. In comparison with the MTT assay the Alamar Blue test provides more reproducible results. Furthermore, the assay is performed in a single step and is non-toxic, compared to the rather time-consuming toxic multi step MTT assay.

Another way of analyzing the cell viability might lie in the analysis of aggregate morphology. Specific aggregate colorations, for example, have been used for characterization of calli, as they are often an indicator of the specific potential of the callus [363]. Callus color may change under varying medium composition [364]. Thus, the color of suspended cells varies, and can be used for evaluation purposes [363]. Especially in suspension cultures for pigment production, the color of cells is directly related to their quality [365]. Taxus suspension cultures have been reported to change appearance in color after exposure to light [8].

Paclitaxel production in calli depends on morphology and age [216]. The callus color was also previously found to correlate with variability in cell growth. Light brown calli showed a higher growth rate than dark and aggregated calli [366]. However, calli were found to produce more paclitaxel at an old age with brown coloration, than at a younger age without the brown stain [367-369]. The intensification of darkening at the stationary growth phase may be related to increased biosynthesis of phenolic compounds [370]. Generally, *Taxus* aggregates can be observed to get larger and increase in brown pigmentation with time (**Figure 4.38**), thus general viability and dark/brown coloration very likely correlate.
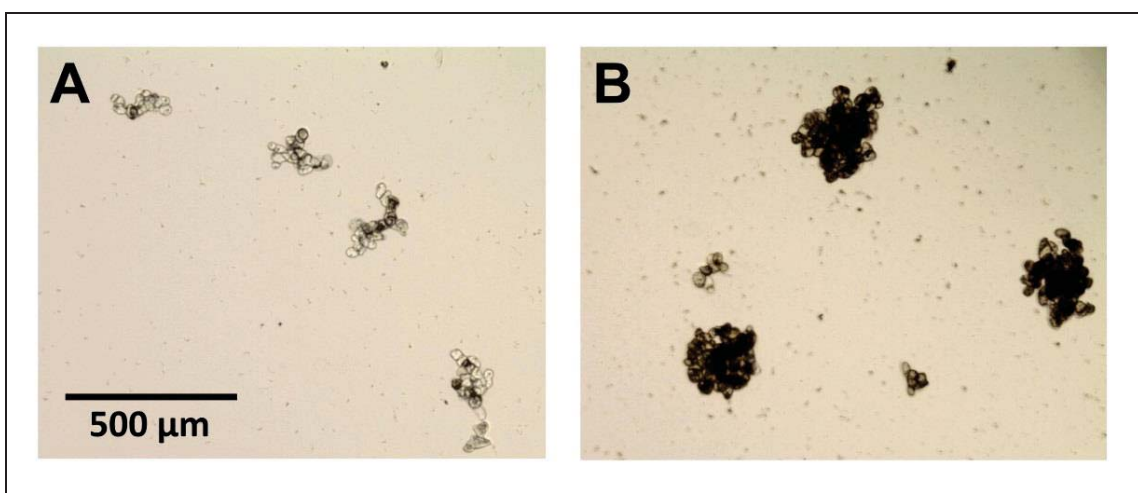


**Figure 4.38:** *Taxus chinesis* aggregates after (A) 1 day of cultivation and (B) after 7 days of cultivation

A large grayish-brown area is distinctive for unhealthy or dead cells, since aggregates with low viability have a large dark area, whereas healthy aggregates show only a small or no dark area.

Through determination of the healthy/dead cell area ratio by image analysis it is possible to determine the percentage of dead cells, and thereby the viability. This can be done as long as the procedure is calibrated with known ratios of live/dead cells. For this purpose, *Taxus* cells were eradicated the in same controlled manner as for the AB assay calibration. The proportions of living cells again ranged from 0 to 100% in 10% increments. In **Figure 4.39,** the relationship between the dark cell area and the percentage of living cells is depicted, and a clear linear relationship is apparent. The significant reproducible behavior between cell coloration and viability makes it possible to estimate cell viability from morphological appearance alone.
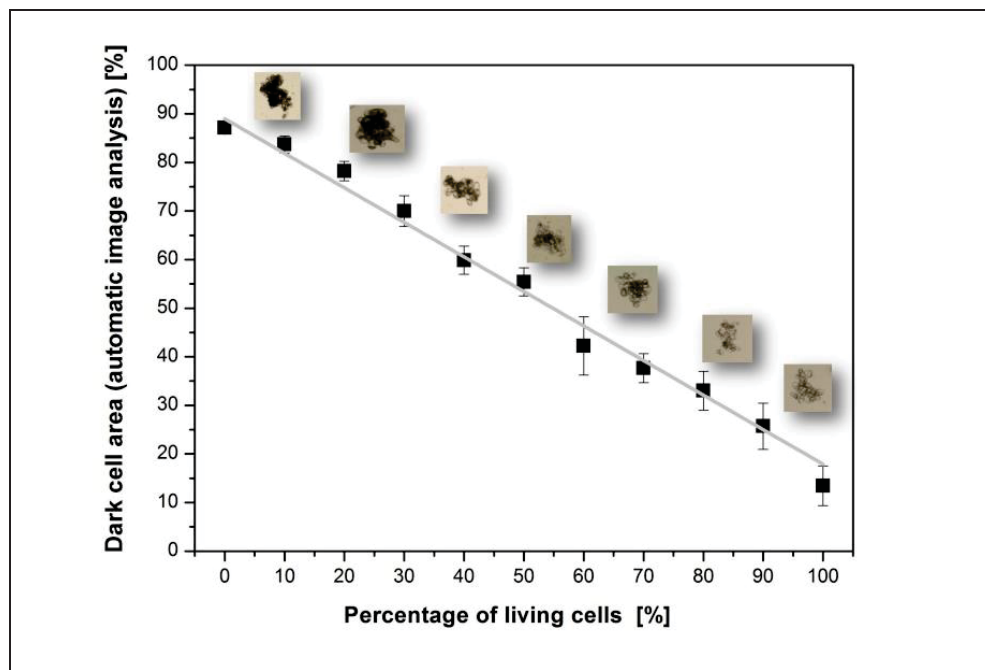


**Figure 4.39:** Relationship between dark cell coloration and viability. Values are means for 3 replicates. $R^2$=0.99

To compare this image-based viability estimation to the AB assay, *Taxus* samples were exposed to various viability-impairing physical and chemical conditions, including UV-light, ethanol, sodium chloride, heat and freezing. Subsequently, both viability estimating methods were conducted, to verify whether both methods produce the same results (**Figure 4.40**).

117
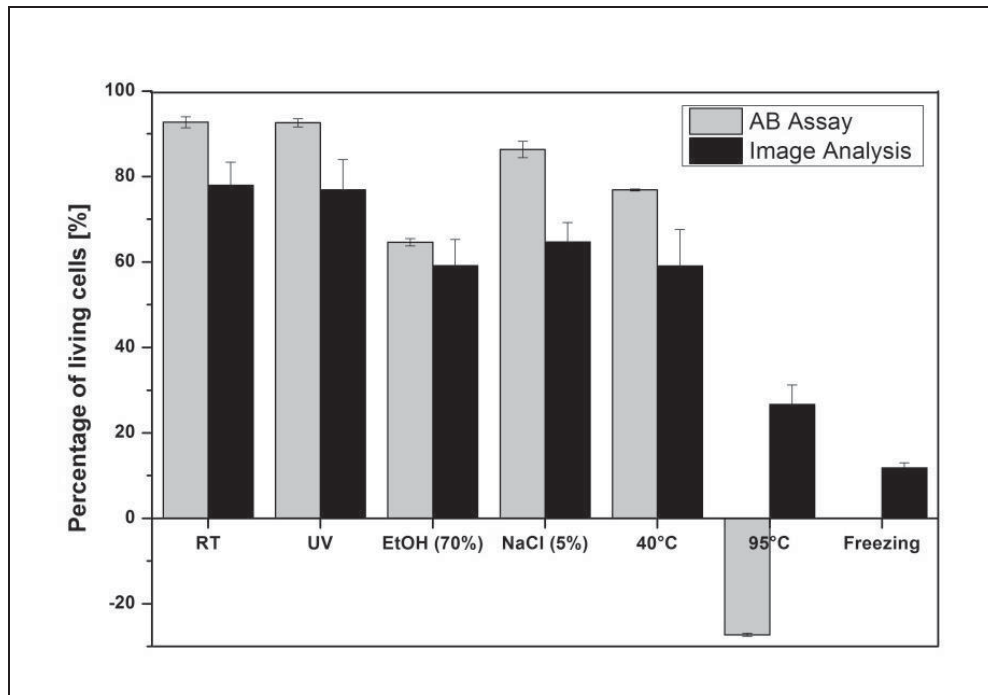
**Figure 4.40:** Proportion of living cells detected by the AB Assay and image analytical measurements after exposure of cells to various physiological properties. RT: standard, UV: exposure to UV-light, EtOH exposure to ethanol (70%), NaCl: addition of sodium chloride (5%), increase of temperature to 40 °C, 95°C and freezing

Generally, both methods show similar results and are comparable, but absolute values vary, because the image analytic technique underestimates viability 10 to 20 % in comparison to the molecular assay. UV-light and sodium chloride do not lead to a significant viability reduction, as the percentage of living cells measured with the AB assay remains at around 90%. Addition of 70 % ethanol in a ratio of 1:1 resulted in a marked reduction in cell viability to about 65%. An increase in temperature to 40 °C led to a decrease in cell viability to about 80 % (AB assay). Heating the sample to 95 °C led to negative results using the AB assay and reduction of living cells to around 28 % by utilization of the image analytic test. The high discrepancy between both viability estimating methods is due to the fairly high temperature where virtually all enzymes and fluorescent proteins are degraded, leading to reduced fluorescence in comparison with the frozen sample. The image analytic method, on the other hand, is based on the brownish color which develops during cell death. At 95 °C, however, cell death is so quick that these phenolic compounds cannot be formed. Freezing led to an eradication of all cells following the AB assay, and produced a rest viability of 10 %, as measured by image analysis.

# 5    Conclusions and future prospects

There has been an impressive amount of research concerning the morphology of filamentous fungi. The implementation of these results in the industry, however, is rather limited [59]. This is partly due to economic pressure and industrial fixation on strain improvement; on the other hand, there is a rather complex interrelationship between all factors involved in fungal growth, such as morphology, physiology, rheology and productivity [346]. Problems concerning fungal morphology are usually solved by empirical methods and experience [59], because most models are too difficult to administer or lack industrial applicability. However, for industrial application it is crucial to distinguish between a well and a poorly producing morphology. Through the introduction of the versatile Morphology number (MN), this thesis provides the means for a desirable characterization of fungal morphology and makes it possible to quantify the interrelation between morphology, productivity and rheology in the form of mathematical models. Thus, morphology, as quantified by the Morphology number, was demonstrated to be an important process parameter for the cultivation of *A. niger* SKAn 1015, because detailed morphologic information allowed the estimation of productivity and rheological properties of the cultivation broth. Moreover, fractal parameters were also found to enable a comprehensive description of fungal morphology. Fractal geometry provides formal mathematical foundations to better understand and characterize a variety of phenomena of complex morphological structures especially related to microscopy [311]. The presented fractal quotient ($D_{BM}/D_{BS}$) and lacunarity ($\Lambda$) were suitable tools for morphological characterization, safe for dense pellet morphologies. Both parameters, however, were not superior to the Morphology number (MN) based on conventional image analytic parameters.

A precise characterization, however, is only the first step towards a desired customization of fungal morphology. Several environomic parameters were already reported in the literature to influence fungal morphology. The influence of mechanical power input by aeration or agitation on fungal morphology, for example, has been studied extensively. However, an increased mechanical power input, which is needed for the creation of mycelial morphology, requires more energy, and therefore makes the process more expensive to operate. The pH value can also significantly affect fungal morphology. Acidic conditions usually lead to a mycelial morphology, and many studies have reported increased productivities at pH 4 and below. For the production of proteins, these acidic conditions are problematic, because not all proteins are stable and active at a low pH. A further established method known to alter fungal morphology is the variation of the inoculum

spore concentration. Yet, as seen and discussed in this study, adjustment of initial spore concentration is not a suitable method for manipulation of fungal morphology, as a high concentration of conidia, known to cause a mycelial morphology, also had inhibiting effects, impairing growth and product formation.

A novel suitable method for customization of fungal morphology is, in contrast, the supplementation of micro particles, which allows a very precise morphology regulation. In the present study, osmolality, a fairly new parameter in process engineering, was introduced, and found to affect fungal morphology and productivity. Osmolality might provide a cheap and reliable approach to increase the productivity in industrial processes. Because of the predictable behavior fungal morphology showed in relation to osmolality, a customization of morphology for process needs seems feasible. Since rheological properties of the culture broth, and thus, downstream processing of the product are heavily dependent on fungal morphology, a tailor-made morphology could prove to be invaluable. In the present work, introduced morphological parameters and osmolality as tool to customize fungal morphology were tested using the fructofuranosidase producing strain *A. niger* SKAn 1015. Both approaches were successfully applied for the glucoamylase producing *A. niger* AB 1.13 as well [253]. A focus of future studies should be to investigate the applicability of introduced methods for further *Aspergillus* strains and also other filamentous organisms like *Streptomyces* or *Penicillium*. It would be also of interest to correlate product purification characteristics directly with fungal morphology, possibly in combination with different micro particle or salt concentrations.

Production of metabolites via plant cell suspension culture is a renewable, environmentally friendly, and economically feasible alternative for extraction from whole plant material [371]. Significant advancements have been made in understanding metabolite production in plant cell cultures, but  so far, controlling variability in product accumulation has often been neglected in favor of improving yield [217]. The size of plant cell aggregates has been often recognized as an intangible parameter, which might be responsible for general variability in plant cell culture processes. The introduced method of laser diffraction for plant cell aggregate size determination is especially suited for industrial application, and will help to establish aggregate size as a process parameter, as proposed earlier [7]. Plant cell suspension cultures in large-scale bioreactors are subject to the hydrodynamic forces resulting from mechanical agitation, and many reactor designs have been suggested over the years to minimize this effect [371]. To this end, an interesting additional application for the introduced adaptable measuring set up for online aggregate measurement has been developed. Instead of the measurement beaker, it is possible to transfer

cells directly from the bioreactor. This system can be used under non-growth conditions (suspension of aggregates in sodium chloride solution) to test various stirrers and reactor geometries for their induced shear stress and effect on plant aggregate integrity. A similar approach was taken by Eslahpazir and colleagues using pellets of *A. niger* [372]. Usually the effect of mechanical stress and power input is measured using a shear sensitive clay polymer floc system [373, 374]. However, the employment of real biological aggregates has obvious advantages, like analogous particle rigidity, size and form. Thus, comminution of native *Taxus* aggregates can provide insight about shear susceptibility of biological samples. It is, moreover, possible to test different reactor geometries and impellers for their effect on aggregate integrity. Excessive shear forces can lead to lysis and reduced viability of plant cells [371].

The introduced Alamar Blue assay was found to be exceptionaly eligible for viability estimation in industrial processes. Moreover, aggregate coloration, as a morphologic attribute, was identified as a good indicator of viability using image analytic methods. A future emphasis of research could be the exploration of CLSM microscopy to identify even individual damaged cells within an aggregate. This technique could prove helpful for further elucidation on the impact of shear stress on plant cell viability. First experiments using CLSM microscopy have already been conducted and shown to be very promising (compare **Figure 5.1**).
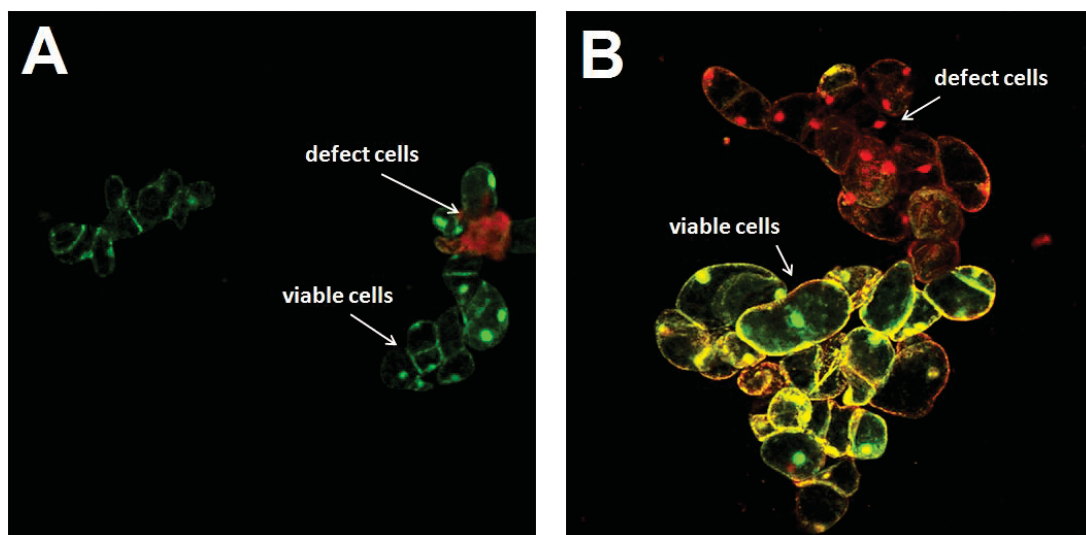


**Figure 5.1:** CLSM picture of *T. chinensis* cells staining with SYTO 9 and PI. (A) shaking flask sample (B) sample after 1.5 hours exposure to UV light. Picture made by Dr. Becky Sommer.

Generally, morphology was identified as an important parameter for both industrially relevant eukaryotic model processes.

# 6 References

1. Von Goethe JW: **The Metamorphose der Pflanzen**. Gotha: Ettingersche Buchhandlung; 1790.
2. Brady RH: **The causal dimension of Goethe's morphology**. *Journal of Social and Biological Structures* 1984, **7**(4):325-344.
3. Blott SJ, Pye K: **Particle shape: a review and new methods of characterization and classification**. *Sedimentology* 2008, **55**(1):31-63.
4. Barrett PJ: **The shape of rock particles, a critical review**. *Sedimentology* 1980, **27**(3):291-303.
5. MacLeod N, Forey PL: **Introduction: Morphology, shape and phylogenetics**. In: *Morphology, Shape and Phylogeny*. Edited by MacLeod N, Forey PL. London: CRC Press; 2002.
6. Lloyd DR, Holmes P, Jackson LP, Emery AN, Al-Rubeai M: **Relationship between cell size, cell cycle and specific recombinant protein productivity**. *Cytotechnology* 2000, **34**(1):59-70.
7. Kolewe ME, Henson MA, Roberts SC: **Analysis of aggregate size as a process variable affecting paclitaxel accumulation in *Taxus* suspension cultures**. *Biotechnol Progr* 2011:1365-1372.
8. Hirasuna TJ, Pestchanker LJ, Srinivasan V, Shuler ML: **Taxol production in suspension cultures of Taxus baccata**. *Plant Cell Tiss Org* 1996, **44**(2):95-102.
9. Papagianni M: **Fungal morphology and metabolite production in submerged mycelial processes**. *Biotechnol Adv* 2004, **22**(3):189-259.
10. Driouch H, Hänsch R, Wucherpfennig T, Krull R, Wittmann C: **Improved enzyme production by bio-pellets of Aspergillus niger: Targeted morphology engineering using titanate microparticles**. *Biotechnol Bioeng* 2012, **109**(2):462-471.
11. Driouch H, Roth A, Dersch P, Wittmann C: **Optimized bioprocess for production of fructofuranosidase by recombinant *Aspergillus niger***. *Appl Microbiol Biotechnol* 2010, **87**(6):2011-2024.
12. Driouch H, Roth A, Dersch P, Wittmann C: **Filamentous fungi in good shape: Microparticles for tailor-made fungal morphology and enhanced enzyme production**. *Bioeng Bugs* 2011, **2**(2):100-104.
13. Driouch H, Sommer B, Wittmann C: **Morphology engineering of *Aspergillus niger* for improved enzyme production**. *Biotechnol Bioeng* 2009, **105**(6):1058-1068.
14. Kaup B-A, Ehrich K, Pescheck M, Schrader J: **Microparticle-enhanced cultivation of filamentous microorganisms: Increased chloroperoxidase formation by *Caldariomyces fumago* as an example**. *Biotechnol Bioeng* 2008, **99**(3):491-498.
15. Archer DB: **Filamentous fungi as microbial cell factories for food use**. *Curr Opin Biotechnol* 2000, **11**(5):478-483.
16. Lubertozzi D, Keasling JD: **Developing *Aspergillus* as a host for heterologous expression**. *Biotechnol Adv* 2009, **27**(1):53-75.
17. Meyer V: **Genetic engineering of filamentous fungi - Progress, obstacles and future trends**. *Biotechnol Adv* 2008, **26**(2):177-185.
18. Gibbs PA, Seviour RJ, Schmid F: **Growth of Filamentous Fungi in Submerged Culture: Problems and Possible Solutions**. *Crit Rev Biotechnol* 2000, **20**(1):17-48.
19. Krull R, Cordes C, Horn H, Kampen I, Kwade A, Neu TR, Nörtemann B: **Morphology of filamentous fungi - Linking cellular biology to process engineering using *Aspergillus niger* Adv Biochem Eng/Biotechnol** 2010, **121**(116):1-21.
20. Zhang Z, Jin B, Kelly J: **Effects of cultivation parameters on the morphology of *Rhizopus arrhizus* and the lactic acid production in a bubble column reactor**. *Eng Life Sci* 2007, **7**:490-496.
21. Barry DJ: **Development of Novel Image Analysis Methods for the Morphological Quantification of Filamentous Fungi**. PhD thesis, Dublin: Dublin Institute of Technology; 2010.
22. Geiser DM, Klich MA, Frisvad JC, Peterson SW, Varga J, Samson RA: **The current status of species recognition and identification in Aspergillus**. *Stud Mycol* 2007, **59**:1-10.
23. Meyer V, Wu B, Ram A: ***Aspergillus* as a multi-purpose cell factory: current status and perspectives**. *Biotechnol Lett* 2011, **33**(3):469-476.
24. Madigan MT: **Brock Biology of Microorganisms**: Pearson/Benjamin Cummings; 2009.
25. Kis-Papo T, Oren A, Wasser SP, Nevo E: **Survival of Filamentous Fungi in Hypersaline Dead Sea Water**. *Microbial Ecol* 2003, **45**(2):183-190.

26.  Magnusun JK, Lasure LL: **Organic acid production by filamentous fungi**. In: *Advances in fungal biotechnology for industry, agriculture, and medicine*. Edited by Tkacz JS, Lange L: Kluver Academic; 2004: 307-340.

27.  Fleißner A, Dersch P: **Expression and export: recombinant protein production systems for *Aspergillus***. *Appl Microbiol Biotechnol* 2010, **87**(4):1255-1270.

28.  Gordon CL, Archer DB, Jeenes DJ, Doonan JH, Wells B, Trinci APJ, Robson GD: **A glucoamylase::GFP gene fusion to study protein secretion by individual hyphae of *Aspergillus niger***. *J Microbiol Meth* 2000, **42**(1):39-48.

29.  Grimm L, Kelly S, Krull R, Hempel D: **Morphology and productivity of filamentous fungi**. *Appl Microbiol Biotechnol* 2005, **69**(4):375-384.

30.  Wang L, Ridgway D, Gu T, Moo-Young M: **Bioprocessing strategies to improve heterologous protein production in filamentous fungal fermentations**. *Biotechnol Adv* 2005, **23**(2):115-129.

31.  Ashokkumar B, Kayalvizhi N, Gunasekaran P: **Optimization of media for ß-fructofuranosidase production by *Aspergillus niger* in submerged and solid state fermentation**. *Process Biochem* 2001, **37**:331-338.

32.  Win TT, Isono N, Kusnadi Y, Watanabe K, Obae K, Ito H, Matsui H: **Enzymatic synthesis of two novel non-reducing oligosaccharides using transfructosylation activity with $\beta$-fructofuranosidase from *Arthrobacter globiformis***. *Biotechnol Lett* 2004, **26**(6):499-503.

33.  Gutiérrez-Alonso P, Fernández-Arrojo L, Plou FJ, Fernández-Lobato M: **Biochemical characterization of a $\beta$-fructofuranosidase from Rhodotorula dairenensis with transfructosylating activity**. *FEMS Yeast Res* 2009, **9**(5):768-773.

34.  Reddy PP, Reddy GSN, Sulochana MB: **Screening of $\beta$-Fructofuranosidase Producers with High Transfructosylation Activity and its 32 Experimental Run Studies on Reaction Rate of Enzyme**. *J Biological Science* 2010, **10**(3):237-241.

35.  Maiorano A, Piccoli R, da Silva E, de Andrade Rodrigues M: **Microbial production of fructosyltransferases for synthesis of pre-biotics**. *Biotechnol Lett* 2008, **30**(11):1867-1877.

36.  Sangeetha PT, Ramesh MN, Prapulla SG: **Fructooligosaccharide production using fructosyl transferase obtained from recycling culture of *Aspergillus oryzae* CFR 202**. *Process Biochem* 2005, **40**(3–4):1085-1088.

37.  Zuccaro A, Götze S, Kneip S, Dersch P, Seibel J: **Tailor-Made Fructooligosaccharides by a Combination of Substrate and Genetic Engineering**. *ChemBioChem* 2008, **9**(1):143-149.

38.  Geier MS, Butler RN, Howarth GS: **Probiotics, prebiotics and synbiotics: A role in chemoprevention for colorectal cancer?** *Cancer Biology & Therapy* 2006, **5**(10):1265-1269.

39.  Rafter J, Bennett M, Caderni G, Clune Y, Hughes R, Karlsson PC, Klinder A, O'Riordan M, O'Sullivan GC, Pool-Zobel B *et al*: **Dietary synbiotics reduce cancer risk factors in polypectomized and colon cancer patients**. *Am J Clin Nut* 2007, **85**(2):488-496.

40.  Fernandez RC, Ottoni CA, da Silva ES, Matsubara RM, Carter JM, Magossi LR, Wada MA, de Andrade Rodrigues MF, Maresma BG, AE M: **Screening of fructofuranosidase-producing microorganisms and effect of pH and temperature on enzymatic rate**. *Appl Microbiol Biotechnol* 2007, **75**:87-93.

41.  Casas López JL, Sánchez Pérez JA, Fernández Sevilla JM, Rodríguez Porcel EM, Chisti Y: **Pellet morphology, culture rheology and lovastatin production in cultures of *Aspergillus terreus***. *J Biotechnol* 2005, **116**(1):61-77.

42.  Gupta K, Mishra P, Srivastava P: **A correlative evaluation of morphology and rheology of *Aspergillus terreus* during lovastatin fermentation**. *Biotechnol Bioprocess Eng* 2007, **12**(2):140-146.

43.  Kim JH, Lebeault JM, Reuss M: **Comparative study on rheological properties of mycelial broth in filamentous and pelleted forms**. *Appl Biochem Biotechnol* 1983, **18**(1):11-16.

44.  Berovič M, Cimerman A, Steiner W, Koloini T: **Submerged citric acid fermentation: rheological properties of *Aspergillus niger* broth in a stirred tank reactor**. *Appl Microbiol Biotechnol* 1991, **34**(5):579-581.

45.  Zhou Y, Du J, Tsao G: **Mycelial pellet formation by *Rhizopus oryzae* ATCC 20344**. *Appl Biochem Biotechnol* 2000, **84-86**(1):779-789.

46.  McIntyre M, Müller C, Dynesen J, Nielsen J: **Metabolic Engineering of the Morphology of *Aspergillus***. *Adv Biochem Eng/Biotechnol* 2001, **73**:103-128.

47. Atkinson B, Daoud I: **Microbial flocs and flocculation in fermentation process engineering**. In: *Adv Biochem Eng/Biotechnol.* vol. 4; 1976: 41-124.

48. Gomez R, Schnabel I, Garrido J: **Pellet growth and citric acid yield of *Aspergillus niger* 110**. *Enzyme Microb Technol* 1988, **10**:188-191.

49. El-Enshasy H, Hellmuth K, Rinas U: **Fungal morphology in submerged cultures and its relation to glucose oxidase excretion by recombinant *Aspergillus niger***. *Appl Biochem Biotechnol* 1999, **81**(1):1-11.

50. Lin P-J, Scholz A, Krull R: **Effect of volumetric power input by aeration and agitation on pellet morphology and product formation of *Aspergillus niger***. *Biochem Eng J* 2010, **49**(2):213-220.

51. Hemmersdorfer H, Leuchtenberger A, Wardsack C, Ruttloff H: **Influence of culture conditions on mycelial structure and polygalactorunidase synthesis of *Aspergillus niger***. *J Basic Microbiol* 1987, **27**:309-315.

52. Reichl U, King R, Gilles ED: **Characterization of pellet morphology during submerged growth of *Streptomyces tendae* by image analysis**. *Biotechnol Bioeng* 1992, **39**(2):164-170.

53. Oncu S, Tari C, Unluturk S: **Effect of Various Process Parameters on Morphology, Rheology, and Polygalacturonase Production by *Aspergillus sojae* in a Batch Bioreactor**. *Biotechnol Progr* 2007, **23**(4):836-845.

54. Hille A, Neu TR, Hempel DC, Horn H: **Oxygen profiles and biomass distribution in biopellets of *Aspergillus niger***. *Biotechnol Bioeng* 2005, **92**(5):614-623.

55. Liu J, Shimizu K, Konishi F, Noda K, Kumamoto S, Kurashiki K, Kondo R: **Antiandrogenic activities of the triterpenoids fraction of *Ganoderma lucidum***. *Food Chem* 2007, **100**:1691-1696.

56. Teng Y, Xu Y, Wang D: **Changes in morphology of *Rhizopus chinensis* in submerged fermentation and their effect on production of mycelium-bound lipase**. *Bioprocess Biosyst Eng* 2009, **32**:397-405.

57. Vecht-Lifshitz S, Magdassi S, Braun S: **Pellet formation and cellular aggregation in *Streptomyces tendae***. *Biotechnol Bioeng* 1990, **35**:890-896.

58. Pazouki M, Panda T: **Understanding the morphology of fungi**. *Bioprocess Biosyst Eng* 2000, **22**(2):127-143.

59. Kossen NW: **The morphology of filamentous fungi**. *Adv Biochem Eng/Biotechnol* 2000, **70**:1-33.

60. Znidarsic P, Pavko A: **The Morphology of Filamentous Fungi in Submerged Cultivations as a Bioprocess Parameter**. *Food Technol Biotechnol* 2001, **39**:237-252.

61. Deckwer WD, Hempel DC, Zeng AP, Jahn D: **Systems Biology Approaches to Bioprocess Development**. *Eng Life Sci* 2006, **6**(5):455 - 469.

62. Paul G, Thomas C: **Characterisation of mycelial morphology using image analysis**. In: *Adv Biochem Eng/Biotechnol*. 1998: 1-59.

63. Metz B, Kossen NWF: **The growth of molds in the form of pellets-a literature review**. *Biotechnol Bioeng* 1977, **19**(6):781-799.

64. Trinci AP: **A study of the kinetics of hyphal extension and branch initiation of fungal mycelia**. *J Gen Microbiol* 1974, **81**(1):225-236.

65. Barry DJ, Williams GA: **Microscopic characterisation of filamentous microbes: towards fully automated morphological quantification through image analysis**. *J of Microsc* 2011, **244**(1):1-20.

66. Nielsen J: **Modeling the morphology of filamentous microorganisms**. *Trends Biotechnol* 1996, **14**:438-443.

67. d'Enfert C: **Fungal Spore Germination: Insights from the molecular Genetics of *Aspergillus nidulans* and *Neurospora crasse***. *Fungal Genet Biol* 1997, **21**:163-172.

68. Harris SD, Hofmann AF, Tedford HW, Lee MP: **Identification and characterization of genes required for hyphal morphogenesis in the filamentous fungus *Aspergillus nidulans***. *Genetics* 1999, **151**(3):1015-1025.

69. Osherov N, May GS: **The molecular mechanisms of conidial germination**. *FEMS Microbiol Lett* 2001, **199**(2):153-160.

70. Maruyama J, Kikuchi S, Kitamoto K: **Differential distribution of the endoplasmic reticulum network as visualized by the BipA-EGFP fusion protein in hyphal compartments across the septum of the filamentous fungus *Aspergillus oryzae***. *Fungal Genet Biol* 2006, **43**(9):642-654.

71.  Maruyama J, Kitamoto K: **Differential distribution of the endoplasmic reticulum network in filamentous fungi**. *FEMS Microbiol Lett* 2007, **272**(1):1-7.

72.  Bartnicki-Garcia S, Bartnicki DD, Gierz G, Lopez-Franco R, Bracker CE: **Evidence that Spitzenkorper behavior determines the shape of a fungal hypha: a test of the hyphoid model**. *Exp Mycol* 1995, **19**(2):153-159.

73.  Reynaga-Pena CG, Bartnicki-Garcia S: **Apical branching in a temperature sensitive mutant of *Aspergillus niger***. *Fungal Genet Biol* 1997, **22**(3):153-167.

74.  Prosser JI, Trinci APJ: **A Model for Hyphal Growth and Branching**. *J Gen Microbiol* 1979, **111**(1):153-164.

75.  Momany M, Hamer JE: **Relationship of actin, microtubules, and crosswall synthesis during septation in *Aspergillus nidulans***. *Cell Motil Cytoskel* 1997, **38**(4):373-384.

76.  Nielsen J: **A Simple morphologically structured model describing the growth of filamentous microorganisms**. *Biotechnol Bioeng* 1993, **41**(7):715-727.

77.  Kaminsky SGW, Hamer JE: *hyp* **Loci Control Cell Pattern Formation in the Vegetative Mycelium of *Aspergillus nidulans***. *Genetics* 1998, **148**:669-680.

78.  Aynsley M, Ward AC, Wright AR: **A mathematical model for the growth of mycelial fungi in submerged culture**. *Biotechnol Bioeng* 1990, **35**(8):820-830.

79.  Nielsen J: **Modelling the growth of filamentous fungi**. In: *Modern Biochemical Engineering*. vol. 46: Springer Berlin / Heidelberg; 1992: 187-223.

80.  Thomas CR: **Image analysis: putting filamentous microorganisms in the picture**. *Trends Biotechnol* 1992, **10**(10):343-348.

81.  White S, McIntyre M, Berry DR, McNeil B: **The autolysis of industrial filamentous fungi**. *Crit Rev Biotechnol* 2002, **22**(1):1-14.

82.  Caldwell IY, Trinci AP: **The growth unit of the mould *Geotrichum candidum***. *Arch Microbiol* 1973, **88**(1):1-10.

83.  Barry DJ, Chan C, Williams GA: **Morphological quantification of filamentous fungal development using membrane immobilization and automatic image analysis**. *J Ind Microbiol Biotechnol* 2009, **36**(6):787-800.

84.  Peberdy JF: **Protein secretion in filamentous fungi – trying to understand a highly productive black box**. *Trends Biotechnol* 1994, **12**:50-57.

85.  Wessels JGH: **Wall growth, protein excretion and morphogenesis in fungi**. *New Phytol* 1992, **123**:397-413.

86.  Wongwicharn A, Harvey LM, McNeil B: **Secretion of heterologous and native proteins, growth and morphology in batch cultures of *Aspergillus niger* B1-D at varying agitation rates**. *J Chem Technol Biotechnol* 1999, **74**:821-828.

87.  Wösten HAB, Moukha SM, Sietsma JH, Wessels JGH: **Localization of growth and secretion of proteins in *Aspergillus niger***. *J Gen Microbiol* 1991, **137**(1):2017-2023.

88.  Bocking SP, Wiebe MG, Robson GD, Hansen K, Christiansen LH, Trinci APJ: **Effect of branch frequency in *Aspergillus oryzae* on protein secretion and culture viscosity**. *Biotechnol Bioeng* 1999, **65**(6):638-648.

89.  Grimm LH, Kelly S, Völkerding II, Krull R, Hempel DC: **Influence of Mechanical Stress and Surface Interaction on the Aggregation of *Aspergillus niger* Conidia**. *Biotechnol Bioeng* 2005, **92**(7):879-888.

90.  Metz B, Kossen NWF: **The Growth of Molds in the Form of Pellets - A Literature Review**. *Biotechnol Bioeng* 1977, **14**:781-799.

91.  Nielsen J, Johansen CL, Jacobsen M, Krabben P, Villadsen J: **Pellet Formation and Fragmentation in Submerged Cultures of *Penicillium chrysogenum* and Its Relation to Penicillin Production**. *Biotechnol Progr* 1995, **11**(1):93-98.

92.  Grimm LH, Kelly S, Hengstler J, Göbel A, Krull R, Hempel DC: **Kinetic studies on the aggregation of *Aspergillus niger* conidia**. *Biotechnol Bioeng* 2004, **87**(2):213-218.

93.  Carlsen M, Spohr AB, Nielsen J, Villadsen J: **Morphology and physiology of an alpha-amylase producing strain of *Aspergillus oryzae* during batch cultivations**. *Biotechnol Bioeng* 1996, **49**(3):266-276.

94.  Amanullah A, Leonildi E, Nienow A, Thomas CR: **Dynamics of mycelial aggregation in cultures of *Aspergillus oryzae***. *Bioprocess Biosyst Eng* 2001, **24**(2):101-107.

95. Lin P-J, Grimm LH, Wulkow M, Hempel DC, Krull R: **Population balance modeling of the conidial aggregation of** *Aspergillus niger*. *Biotechnol Bioeng* 2008, **99**(2):341-350.

96. Emerson S: **The growth phase in** *Neurospora* **corresponding to the logarithmic phase in unicellular organisms**. *J Bacteriol* 1950, **60**(3):221-223.

97. Wittler R, Horst B, Dietrich Werner L, Karl S: **Investigations of oxygen transfer into** *Penicillium chrysogenum* **pellets by microprobe measurements**. *Biotechnol Bioeng* 1986, **28**(7):1024-1036.

98. Bizukojc M, Ledakowicz S: **The morphological and physiological evolution of** *Aspergillus terreus* **mycelium in the submerged culture and its relation to the formation of secondary metabolites**. *World J Microb Biot* 2010, **26**:41-54.

99. El-Enshasy HA, Kleine J, Rinas U: **Agitation effects on morphology and protein productive fractions of filamentous and pelleted growth forms of recombinant** *Aspergillus niger*. *Process Biochem* 2006, **41**:2103-2112.

100. Hille A, Neu TR, Hempel DC, Horn H: **Effective diffusivities and mass fluxes in fungal biopellets**. *Biotechnol Bioeng* 2009, **103**(6):1202-1213.

101. Cui YQ, Lans RGJMvd, Luyben KCAM: **Effects of dissolved oxygen tension and mechanical forces on fungal morphology in submerged fermentation**. *Biotechnol Bioeng* 1998, **57**(4):409-419.

102. Eleazar MES, Gustavo FG, Luc D, Jiménez IH, Ochoa-Tapia JA: **A Method to Evaluate the Isothermal Effectiveness Factor for Dynamic Oxygen into Mycelial Pellets in Submerged Cultures**. *Biotechnol Progr* 2001, **17**(1):95-103.

103. Lejeune R, V. Baron G: **Simulation of growth of a filamentous fungus in 3 dimensions**. *Biotechnol Bioeng* 1997, **53**(2):139-150.

104. Hamanaka T, Higashiyama K, Fujikawa S, Park EY: **Mycelial pellet intrastructure and visualization of mycelia and intracellular lipid in a culture of** *Mortierella alpina*. *Appl Microbiol Biotechnol* 2001, **56**(1):233-238.

105. Hellendoorn L, Mulder H, Heuvel JCvd, Ottengraf SPP: **Intrinsic kinetic parameters of the pellet forming fungus** *Aspergillus awamori*. *Biotechnol Bioeng* 1998, **58**(5):478-485.

106. Cronenberg CCH, Ottengraf SPP, Heuvel JC, Pottel F, Sziele D, Schügerl K, Bellgardt KH: **Influence of age and structure of** *Pencillium chrysogenum* **pellets on the internal concentration profiles**. *Bioprocess Biosyst Eng* 1994, **10**(5):209-216.

107. Huang MY, Bungay HR: **Microprobe measurements of oxygen concentrations in mycelial pellets**. *Biotechnol Bioeng* 1973, **15**(6):1193-1197.

108. Miura Y, Miyamoto K: **Oxygen transfer within fungal pellets**. *Biotechnol Bioeng* 1977, **19**(9):1407-1409.

109. Carmichael RD, Pickard MA: **Continuous and Batch Production of Chloroperoxidase by Mycelial Pellets of** *Caldariomyces fumago* **in an Airlift Fermentor**. *Appl Environ Microbiol* 1989, **55**:17-20.

110. Domingues FC, Queiroz JA, Cabral JM, Fonseca LP: **The influence of culture conditions on mycelial structure and cellulase production by** *Trichoderma reesei* **Rut C-30**. *Enzyme Microb Technol* 2000, **26**(5-6):394-401.

111. Liu Y, Liao W, Chen S: **Study of pellet formation of filamentous fungi** *Rhizopus oryzae* **using a multiple logistic regression model**. *Biotechnol Bioeng* 2008, **99**:117-128.

112. Papagianni M, Mattey M: **Morphological development of** *Aspergillus niger* **in submerged citric acid fermentation as a function of the spore inoculum level. Application of neural network and cluster analysis for characterization of mycelial morphology**. *Microb Cell Fact* 2006, **5**(1):3.

113. Tucker KG, Kelly T, Delgrazia P, Thomas CR: **Fully-automatic measurement of mycelial morphology by image analysis**. *Biotechnol Progr* 1992, **8**(4):353-359.

114. Xu J, Wang L, Ridgway D, Gu T, Moo-Young M: **Increased Heterologous Protein Production in** *Aspergillus niger* **Fermentation through Extracellular Proteases Inhibition by Pelleted Growth**. *Biotechnol Progr* 2000, **16**:222-227.

115. Xu J, Wang L, Ridgway D, Gu T, Moo-Young M: **Increased Heterologous Protein Production in** *Aspergillus niger* **Fermentation through Extracellular Proteases Inhibition by Pelleted Growth**. *Biotechnol Bioeng* 2000, **16**:222-227.

126

116. Johansen CL, Coolen L, Hunik JH: **Influence of Morphology on Product Formation in** *Aspergillus awamori* **during Submerged Fermentations**. *Biotechnol Progr* 1998, **14**(2):233-240.

117. Bizukojc M, Ledakowicz S: **Physiological, morphological and kinetic aspects of lovastatin biosynthesis by** *Aspergillus terreus*. *Biotechnol J* 2009, **4**(5):647-664.

118. Braun S, Vecht-Lifshitz SE: **Mycelial morphology and metabolite production**. *Trends Biotechnol* 1991, **9**:63-68.

119. Carlsen M, Spohr AB, Nielsen J, Villadsen J: **Morphology and Physiology of an alpha Amylase Producing Strain of** *Aspergillus oryzae* **during Batch Cultivations**. *Biotechnol Bioeng* 1996, **49**:266-276.

120. Lejeune R, Nielsen J, Baron GV: **Influence of the pH on the morphology of** *Trichoderma reesei* **QM 9414 in submerged culture**. *Biotechnol Lett* 1995, **17**(3):341-344.

121. Mainwaring DO, Wiebe MG, Robson GD, Goldrick M, J. JD, Archer DB, J. TAP: **Effect of pH on hen egg white lysozyme production and evolution of a recombinant strain of** *Aspergillus niger*. *J Biotechnol* 1999, **75**:1-10.

122. O'Donnell D, Wang L, Xu J, Ridgway D, Gu T, Moo-Young M: **Enhanced heterologous protein production in** *Aspergillus niger* **through pH control of extracellular protease activity**. *Biochem Eng J* 2001, **8**(3):187-193.

123. Pirt SJ, Callow DS: **Continuous-Flow Culture of the Filamentous Mould** *Penicillium Chrysogenum* **and the Control of its Morphology**. *Nature* 1959, **184**(4683):307-310.

124. Vats P, Sahoo DK, Banerjee UC: **Production of phytase (myo-inositolhexakisphosphate phosphohydrolase) by** *Aspergillus niger* **van Teighem in laboratory-scale fermenter**. *Biotechnol Progr* 2004, **20**(3):737-743.

125. Galbraith JC, Smith JE: **Filamentous growth of** *Aspergillus niger* **in submerged shake culture**. *Trans Br mycol Soc* 1969, **52**(2):237-246.

126. Dynesen J, Nielsen J: **Surface Hydrophobicity of** *Aspergillus nidulans* **Conidiospores and Its Role in Pellet Formation**. *Biotechnol Progr* 2003, **19**(3):1049-1052.

127. Priegnitz B-E, Wargenau A, Brandt U, Rohde M, Dietrich S, Kwade A, Krull R, Fleißner A: **The role of initial spore adhesion in pellet and biofilm formation in** *Aspergillus niger*. *Fungal Genet Biol* 2012, **49**(1):30-38.

128. Friedrich J, Cimerman A, Steiner W: **Submerged production of pectolytic enzymes by** *Aspergillus niger* **effect of different aeration/agitation regimes**. *Appl Microbiol Biotechnol* 1989, **31**(5):490-494.

129. Kelly S, Grimm LH, Hengstler J, Schultheis E, Krull R, Hempel DC: **Agitation effects on submerged growth and product formation of** *Aspergillus niger*. *Bioprocess Biosyst Eng* 2004, **26**(5):315-323.

130. Kelly S, Grimm LH, Jonas R, Hempel DC, Krull R: **Investigations of the Morphogenesis of Filamentous Microorganisms**. *Eng Life Sci* 2006, **6**(5):475-480.

131. Lejeune R, Baron GV: **Effect of agitation on growth and enzyme production of** *Trichoderm reesei* **in batch fermentation**. *Appl Microbiol Biotechnol* 1995, **43**(2):249-258.

132. Mitard A, Riba JP: **Morphology and growth of** *Aspergillus niger* **ATCC 26036 cultivated at several shear rates**. *Biotechnol Bioeng* 1988, **32**(6):835-840.

133. Papagianni M, Mattey M, Kristiansen B: **Citric acid production and morphology of** *Aspergillus niger* **as functions of the mixing intensity in a stirred tank and a tubular loop bioreactor**. *Biochem Eng J* 1998, **2**:197-205.

134. Smith JJ, Lilly MD, Fox RI: **The effect of agitation on the morphology and penicillin production of** *Penicillium chrysogenum*. *Biotechnol Bioeng* 1990, **35**(10):1011-1023.

135. Wongwicharn A, McNeil B, Harvey L: **Effect of Oxygen Enrichment on Morphology, Growth, and Heterologous Protein Production in Chemostat Cultures of** *Aspergillus niger* **B1-D**. *Biotechnol Bioeng* 1999, **65**(4):416-424.

136. Cox PW, Paul GC, Thomas CR: **Image analysis of the morphology of filamentous micro-organisms**. *Microbiology* 1998, **144**(4):817-827.

137. Li Q, Harvey LM, McNeil B: **Oxygen enrichment effects on protein oxidation, proteolytic activity and the energy status of submerged batch cultures of** *Aspergillus niger* **B1-D**. *Process Biochem* 2008, **43**(3):238-243.

138. Wongwicharn A, McNeil B, Harvey LM: **Effect of Oxygen Enrichment on Morphology, Growth, and Heterologous Protein Production in Chemostat Cultures of *Aspergillus niger* B1-D**. *Biotechnol Bioeng* 1999, **65**(4):416-424.

139. Nielsen J, Krabben P: **Hyphal growth and fragmentation of *Penicillium chrysogenum* in submerged cultures**. *Biotechnol Bioeng* 1995, **46**(6):588-598.

140. Park JP, Kim YM, Kim SW, Hwang HJ, Cho YJ, Lee YS, Song CH, Yun JW: **Effect of agitation intensity on the exo-biopolymer production and mycelial morphology in *Cordyceps militaris***. *Lett Appl Microbiol* 2002, **34**(6):433-438.

141. Rodríguez Porcel EM, Casas López JL, Sánchez Pérez JA, Fernández Sevilla JM, Chisti Y: **Effects of pellet morphology on broth rheology in fermentations of *Aspergillus terreus***. *Biochem Eng J* 2005, **26**(2-3):139-144.

142. Paul GC, Priede MA, Thomas CR: **Relationship between morphology and citric acid production in submerged *Aspergillus niger* fermentations**. *Biochem Eng J* 1999, **3**:121-129.

143. Wucherpfennig T, Lakowitz, A., Driouch, H., Krull, R., Wittmann, C.: **Customization of *Aspergillus niger* Morphology Through Addition of Talc Micro Particles**. *J Vis Exp* 2012, **61**.

144. Allaway AEaJ, D.H. : **The influence of cations on glucose transport and metabolism by, and the loss of sugars alcohols from, the fungus *Dendryphiella salina***. *New Phytol* 1970, **69**:581-593.

145. Allaway AEaJ, D.H. : **The effect of cations on glucose utilization by, and on the growth of, the fungus *Dendryphiella salina***. *New Phytol* 1971, **70**:511-518.

146. Bobowicz-Lassociska T, Grajek W: **Changes in protein secretion of *Aspergillus niger* caused by the reduction of the water activity by potassium chloride**. *Acta Biotechnol* 1995, **15**(3):277-287.

147. Fiedurek J: **Effect of osmotic stress on glucose oxidase production and secretion by *Aspergillus niger***. *J Basic Microbiol* 1998, **38**(2):107-112.

148. Lee GM, Park SY: **Enhanced specific antibody productivity of hybridomas resulting from hyperosmotic stress is cell line-specific**. *Biotechnol Lett* 1995, **17**(2):145-150.

149. Lee M, Lee G: **Effect of hypoosmotic pressure on cell growth and antibody production in recombinant Chinese hamster ovary cell culture**. *Cytotechnology* 2001, **36**(1):61-69.

150. Oh SKW, Vig P, Chua F, Teo WK, Yap MGS: **Substantial overproduction of antibodies by applying osmotic pressure and sodium butyrate**. *Biotechnol Bioeng* 1993, **42**(5):601-610.

151. Ozturk SS, Palsson BO: **Effect of medium osmolarity on hybridoma growth, metabolism, and antibody production**. *Biotechnol Bioeng* 1991, **37**(10):989-993.

152. Shen D, Kiehl TR, Khattak SF, Li ZJ, He A, Kayne PS, Patel V, Neuhaus IM, Sharfstein ST: **Transcriptomic responses to sodium chloride-induced osmotic stress: A study of industrial fed-batch CHO cell cultures**. *Biotechnol Progr* 2010, **26**(4):1104-1115.

153. Kim S-I, Choi H-K, Kim J-H, Lee H-S, Hong S-S: **Effect of osmotic pressure on paclitaxel production in suspension cell cultures of *Taxus chinensis***. *Enzyme Microb Technol* 2001, **28**(2–3):202-209.

154. Lee J-H, Kim N-S, Kwon T-H, Yang M-S: **Effects of osmotic pressure on production of recombinant human granulocyte-macrophage colony stimulating factor in plant cell suspension culture**. *Enzyme Microb Technol* 2002, **30**(6):768-773.

155. Liu C-Z, Cheng X-Y: **Enhancement of phenylethanoid glycosides biosynthesis in cell cultures of *Cistanche deserticola* by osmotic stress**. *Plant Cell Rep* 2008, **27**(2):357-362.

156. Haack MB, Olsson L, Hansen K, Eliasson LA: **Change in hyphal morphology of *Aspergillus oryzae* during fed-batch cultivation**. *Appl Microbiol Biotechnol* 2006, **70**:482-487.

157. Znidarsic P, Komel R, Pavko A: **Influence of some environmental factors on *Rhizopus nigricans* submerged growth in the form of pellets**. *World J Microb Biot* 2000, **16**(7):589-593.

158. Mussatto S, Rodrigues L, Teixeira J: **$\beta$-Fructofuranosidase production by repeated batch fermentation with immobilized *Aspergillus japonicus***. *J Ind Microbiol Biotechnol* 2009, **36**(7):923-928.

159. Dion W, Carilli A, Sermonti G, Chain E: **The effect of mechanical agitation on the morphology of *Penicillium chrysogenum* Thom in stirred fermentors**. *Rend Ist Super Sanita* 1954, **17**:187-205.

160. Fiddy C, Trinci APJ: **Nuclei, Septation, Branching and Growth of *Geotrichum candidum***. *J Gen Microbiol* 1976, **97**(2):185-192.

161. Metz B, Bruijn EWd, Suijdam JCv: **Methods for quantitative representation of the morphology of molds**. *Biotechnol Bioeng* 1981, **23**(1):149-162.

162. Adams HL, Thomas CR: **The use of image analysis for morphological measurements on filamentous microorganisms**. *Biotechnol Bioeng* 1988, **32**(5):707-712.

163. Packer HL, Thomas CR: **Morphological measurements on filamentous microorganisms by fully automatic image analysis**. *Biotechnol Bioeng* 1990, **35**(9):870-881.

164. Paul GC, Kent CA, Thomas CR: **Quantitative characterization of vacuolization in *Penicillium chrysogenum* using automatic image analysis**. *Transactions of the Institution of Chemical Engineers* 1992, **70**.

165. Paul GC, Kent CA, Thomas CR: **Image analysis for characterizing differentiation of *Penicillium chrysogenum***. *Transactions of the Institution of Chemical Engineers* 1994, **72**(2):95-105.

166. Paul GC, Thomas CR: **A structured model for hyphal differentiation and penicillin production using *Penicillium chrysogenum***. *Biotechnol Bioeng* 1996, **51**(5):558-572.

167. Cox PW, Thomas CR: **Classification and measurement of fungal pellets by automated image analysis**. *Biotechnol Bioeng* 1992, **39**(9):945-952.

168. Müller C, Hansen K, Szabo P, Nielsen J: **Effect of Deletion of Chitin Synthase Genes on Mycelial Morphology and Culture Viscosity in *Aspergillus oryzae***. *Biotechnol Bioeng* 2003, **81**(5):525-534.

169. Park EY, Koizumi K, Higashiyama K: **Analysis of Morphological Relationship Between Micro- and Macromorphology of *Mortierella* Species Using a Flow-Through Chamber Coupled with Image Analysis**. *J Eukaryot Microbiol* 2006, **53**(3):199-203.

170. Rühl M, Kües U: **Automated image analysis to observe pellet morphology in liquid cultures of filamentous fungi such as the basidiomycete *Coprinopsis cinerea***. *Curr Trends Biotechnol Pharm* 2009, **3**(3):241-253.

171. Treskatis SK, Orgeldinger V, Wolf H, Gilles ED: **Morphological characterization of filamentous microorganisms in submerged cultures by on-line digital image analysis and pattern recognition**. *Biotechnol Bioeng* 1997, **53**(2):191-201.

172. Galindo E, Larralde-Corona CP, Brito T, Córdova-Aguilar MS, Taboada B, Vega-Alvarado L, Corkidi G: **Development of advanced image analysis techniques for the in situ characterization of multiphase dispersions occurring in bioreactors**. *J Biotechnol* 2005, **116**(3):261-270.

173. Wucherpfennig T, Kiep KA, Driouch H, Wittmann C, Krull R: **Morphology and Rheology in Filamentous Cultivations**. In: *Adv Appl Microbiol.* Edited by Allen I. Laskin SS, Geoffrey MG, vol. Volume 72: Academic Press; 2010: 89-136.

174. Charles M: **Technical aspects of the rheological properties of microbial cultures**. In: *Adv Biochem Eng/Biotechnol.* vol. 8; 1978: 1-62.

175. Olsvik E, Kristiansen B: **Rheology of filamentous fermentations**. *Biotechnol Adv* 1994, **12**(1):1-39.

176. Riley GL, Tucker KG, Paul GC, Thomas CR: **Effect of biomass concentration and mycelial morphology on fermentation broth rheology**. *Biotechnol Bioeng* 2000, **68**(2):160-172.

177. Roels JA, Berg JVD, Voncken RM: **The rheology of mycelial broths**. *Biotechnol Bioeng* 1974, **16**(2):181-208.

178. Gavrilescu M, Tudose RZ: **Hydrodynamics of non-Newtonian liquids in external-loop airlift bioreactors**. *Bioprocess Biosyst Eng* 1997, **18**(1):17-26.

179. Moo-Young M, Benoit H, Allen DG, Robert B, Yoshinori K: **Oxygen transfer to mycelial fermentation broths in an airlift fermentor**. *Biotechnol Bioeng* 1987, **30**(6):746-753.

180. Sinha J, Tae Bae J, Pil Park J, Hyun Song C, Won Yun J: **Effect of substrate concentration on broth rheology and fungal morphology during exo-biopolymer production by *Paecilomyces japonica* in a batch bioreactor**. *Enzyme Microb Technol* 2001, **29**(6-7):392-399.

181. Metz B, Kossen NWF, Suijdam JCv: **The rheology of mould suspensions**. *Adv Biochem Eng/Biotechnol* 1979, **11**:104-156.

182. Ruohang W, Webb C: **Effect of Cell Concentration on the Rheology of Glucoamylase Fermentation Broth**. *Biotechnol Tech* 1995, **9**(1):55-58.

183. Gbewonyo K, Wang DIC: **Enhancing gas-liquid mass transfer rates in non-newtonian fermentations by confining mycelial growth to microbeads in a bubble column**. *Biotechnol Bioeng* 1983, **25**(12):2873-2887.

184. Kilonzo PM, Margaritis A: **The effects of non-Newtonian fermentation broth viscosity and small bubble segregation on oxygen mass transfer in gas-lift bioreactors: a critical review**. *Biochem Eng J* 2004, **17**(1):27-40.

185. Deindoerfer FH, John MW: **Rheological examination of some fermentation broths**. *J Biochem Microb Technol Eng* 1960, **2**(2):165-175.

186. Petersen N, Stocks S, Gernaey K, V. : **Multivariate models for prediction of rheological characteristics of filamentous fermentation broth from the size distribution**. *Biotechnol Bioeng* 2008, **100**(1):61-71.

187. Oolman T, Blanch HW, Erickson LE: **Non-Newtonian Fermentation Systems**. *Crit Rev Biotechnol* 1986, **4**(2):133 - 184.

188. Bongenaar JJTM, Kossen NWF, Metz B, Meijboom FW: **A method for characterizing the rheological properties of viscous fermentation broths**. *Biotechnol Bioeng* 1973, **15**(1):201-206.

189. Cheng DCH: **Yield stress: A time-dependent property and how to measure it**. *Rheol Acta* 1986, **25**(5):542-554.

190. Allen DG, Campbell WR: **The prediction of transport parameters in filamentous fermentation broths based on results obtained in pseudoplastic polymer solutions**. *Can J Chem Eng* 1991, **69**(2):498-505.

191. Reuss M, Debus D, Zoll G: **Rheological aspects of fermentation fluids**. *Chem Eng* 1982, **381**:233-236.

192. Kim JC, Lim JS, Kim JM, Kim C, Kim SW: **Relationship between morphology and viscosity of the main culture broth of *Cephalosporium acremonium* M25**. *Korea-Aust Rheol J* 2005, **17**(1):15-20.

193. Olsvik E, Tucker K, Thomas C, Kristiansen B: **Correlation of *Aspergillus niger* broth rheological properties with biomass concentration and the shape of mycelial aggregates**. *Biotechnol Bioeng* 1993, **42**:1046-1052.

194. Olsvik ES, Kristiansen B: **Influence of oxygen tension, biomass concentration, and specific growth rate on the rheological properties of a filamentous fermentation broth**. *Biotechnol Bioeng* 1992, **40**(11):1293-1299.

195. Riley G, Thomas C: **Applicability of *Penicillium chrysogenum* rheological correlations to broths of other fungal strains**. *Biotechnol Lett* 2010, **32**(11):1623-1629.

196. Karsheva M, Hristov J, Penchev I, Lossev V: **Rheological behavior of fermentation broths in antibiotic industry**. *Appl Biochem Biotechnol* 1997, **68**(3):187-206.

197. Olsvik ES, Kristiansen B: **On-line rheological measurements and control in fungal fermentations**. *Biotechnol Bioeng* 1992, **40**(3):375-387.

198. Warren SJ, Keshavarz-Moore E, Shamlou PA, Lilly MD, Thomas CR, Dixon K: **Rheologies and morphologies of three actinomycetes in submerged culture**. *Biotechnol Bioeng* 1995, **45**(1):80-85.

199. Tucker K: **Relationship between mycelial morphology biomass concentration and broth rheology in submerged fermentations**. PhD thesis, Birmingham, UK: University of Birmingham; 1994.

200. Tucker K, Thomas C: **Effect of biomass concentration and morphology on the rheological parameters of *Penicillum chrysogenum* fermentation broths**. *Trans Inst Chem Eng* 1993, **71**:111-117.

201. Mohseni M, Allen DG: **The effect of particle morphology and concentration on the directly measured yield stress in filamentous suspensions**. *Biotechnol Bioeng* 1995, **48**(3):257-265.

202. Hageneder F: **Yew: A History**: Sutton; 2007.

203. Eichenberger C, Heiselmayer P: **Die Eibe (*Taxus Baccata*) in Salzburg Versuch einer Monographie**, vol. 7. Salzburg: WUV-Universitätsverlag Wien - Salzburg; 1995.

204. Caesar GJ: **The Gallic Wars** 53 BC.

205. Tekol Y: **The medieval physician Avicenna used an herbal calcium channel blocker, *Taxus baccata* L**. *Phytother Res* 2007, **21**(7):701-702.

130

206. Alam G: **Database on Medical Plants (Asia)**. Calcutta: CUTS Centre for International Trade, Economics & Environment; 2004.

207. Küpeli E, Erdemoğlu N, Yeşilada E, Şener B: **Anti-inflammatory and antinociceptive activity of taxoids and lignans from the heartwood of *Taxus baccata* L**. *J Ethnopharmacol* 2003, **89**(2–3):265-270.

208. Renneberg R: **Biotech History: Yew trees, paclitaxel synthesis and fungi**. *Biotechnol J* 2007, **2**(10):1207-1209.

209. Itokawa H: **Introduction**. In: *Taxus - The genus Taxus.* Edited by Lee HIaK-H. London: Taylor & Francis Group; 2003.

210. Wani MC, Taylor HL, Wall ME, Coggon P, McPhail AT: **Plant antitumor agents. VI. Isolation and structure of taxol, a novel antileukemic and antitumor agent from *Taxus brevifolia***. *J Am Chem Soc* 1971, **93**(9):2325-2327.

211. Manfredi JJ, Parness J, Horwitz SB: **Taxol binds to cellular microtubules**. *J Cell Biol* 1982, **94**(3):688-696.

212. Kingston DGI: **Recent Advances in the Chemistry of Taxol 1,2**. *J Nat Prod* 2000, **63**(5):726-734.

213. Wilson SA, Roberts SC: **Recent advances towards development and commercialization of plant cell culture processes for the synthesis of biomolecules**. *Plant Biotechnology Journal* 2011:no-no.

214. Cragg GM, Boyd MR, Cardellina II JH, Grever MR, Schepartz S, Snader KM, Suffness M: **The Search for New Pharmaceutical Crops: Drug Discovery and Development at the National Cancer Institute**. New York: Wiley; 1993.

215. Nims E, Dubois CP, Roberts SC, Walker EL: **Expression profiling of genes involved in paclitaxel biosynthesis for targeted metabolic engineering**. *Met Eng* 2006, **8**(5):385-394.

216. Malik S, Cusidó RM, Mirjalili MH, Moyano E, Palazón J, Bonfill M: **Production of the anticancer drug taxol in *Taxus baccata* suspension cultures: A review**. *Process Biochem* 2011, **46**(1):23-34.

217. Roberts SC: **Production and engineering of terpenoids in plant cell culture**. *Nat Chem Biol* 2007, **3**(7):387-395.

218. Smith R, Cameron S: **Domesticating ground hemlock (*Taxus canadensis*) for producing taxanes: a case study**. In: *Proceedings of 29th annual meeting of the plant growth regulation society of America: 2002*; 2002: 40-45.

219. Holton RA, Somoza C, Kim HB, Liang F, Biediger RJ, Boatman PD, Shindo M, Smith CC, Kim S: **First total synthesis of taxol. 1. Functionalization of the B ring**. *J Am Chem Soc* 1994, **116**(4):1597-1598.

220. Wuts PGM: **Semisynthesis of taxol**. *Curr Opin Drug Discov Dev* 1998, **1**(3):329-337.

221. Vongpaseuth K, Roberts SC: **Advancements in the understanding of paclitaxel metabolism in tissue culture**. *Curr Pharm Biotechnol* 2007, **8**:219-236.

222. Mountford PG: **The Taxol® Story – Development of a Green Synthesis via Plant Cell Fermentation**. In: *Green Chemistry in the Pharmaceutical Industry.* Wiley-VCH Verlag GmbH & Co. KGaA; 2010: 145-160.

223. Sabater-Jara A, Tudela L, López-Pérez A: **In vitro culture of *Taxus* sp.: strategies to increase cell growth and taxoid production**. *Phytochemistry Reviews* 2010, **9**(2):343-356.

224. Raskin I, Ribnicky DM, Komarnytsky S, Ilic N, Poulev A, Borisjuk N, Brinker A, Moreno DA, Ripoll C, Yakoby N *et al*: **Plants and human health in the twenty-first century**. *Trends in Biotechnology* 2002, **20**(12):522-531.

225. Newman DJ, Cragg GM, Snader KM: **Natural Products as Sources of New Drugs over the Period 1981−2002**. *J Nat Prod* 2003, **66**(7):1022-1037.

226. Georgiev M, Pavlov A, Bley T: **Hairy root type plant in vitro systems as sources of bioactive substances**. *Appl Microbiol Biotechnol* 2007, **74**(6):1175-1185.

227. Pant S, Samant S: **Population ecology of the endangered Himalayan Yew in Khokhan Wildlife Sanctuary of North Western Himalaya for conservation management**. *Journal of Mountain Science* 2008, **5**(3):257-264.

228. McDonald K, Jackman A, Hurst S: **Characterization of plant suspension cultures using the focused beam reflectance technique**. *Biotechnology Letters* 2001, **23**(4):317-324.

229. Georgiev M, Weber J, Maciuk A: **Bioprocessing of plant cell cultures for mass production of targeted compounds**. *Appl Microbiol Biotechnol* 2009, **83**(5):809-823.

230. Haberlandt G: **Experiments on the culture of isolated plant cells**. *Bot Rev* 1969, **35**(1):68-88.

231. Hall R: **Plant cell culture initiation**. *Mol Biotechnol* 2000, **16**(2):161-173.

232. Verpoorte R, Contin A, Memelink J: **Biotechnology for the production of plant secondary metabolites**. *Phytochemistry Reviews* 2002, **1**(1):13-25.

233. Srivastava S, Srivastava AK: **Hairy Root Culture for Mass-Production of High-Value Secondary Metabolites**. *Crit Rev Biotechnol* 2007, **27**(1):29-43.

234. Kolewe ME, Henson MA, Roberts SC: **Characterization of aggregate size in *Taxus* suspension cell culture**. *Plant Cell Rep* 2010, **29**(5):485-494.

235. Hulst AC, Meyer MMT, Breteler H, Tramper J: **Effect of aggregate size in cell cultures of Tagetes patula on thiophene production and cell growth**. *Applied Microbiology and Biotechnology* 1989, **30**(1):18-25.

236. Edahiro Ji, Seki M: **Phenylpropanoid metabolite supports cell aggregate formation in strawberry cell suspension culture**. *J Biosci Bioeng* 2006, **102**(1):8-13.

237. Hulst AC, Meyer MMT, Breteler H, Tramper J: **Effect of aggregate size in cell cultures of *Tagetes patula* on thiophene production and cell growth**. *Appl Microbiol Biotechnol* 1989, **30**(1):18-25.

238. Jianfeng X, Zhiguo S, Pusun F: **Suspension culture of compact callus aggregate of *Rhodiola sachalinensis* for improved salidroside production**. *Enzyme Microb Technol* 1998, **23**(1-2):20-27.

239. Madhusudhan R, Ramachandra Rao S, Ravishankar GA: **Osmolarity as a measure of growth of plant cells in suspension cultures**. *Enzyme and Microbial Technology* 1995, **17**(11):989-991.

240. Zhao D, Huang Y, Jin Z, Qu W, Lu D: **Effect of aggregate size in cell cultures of Saussurea medusa on cell growth and jaceosidin production**. *Plant Cell Reports* 2003, **21**(11):1129-1133.

241. Bolta Ž, Baričevič D, Raspor P: **Biomass segregation in sage cell suspension culture**. *Biotechnology Letters* 2003, **25**(1):61-65.

242. Pépin M, Smith M, Reid J: **Application of imaging tools to plant cell culture: Relationship between plant cell aggregation and flavonoid production**. *In Vitro Cellular &amp; Developmental Biology - Plant* 1999, **35**(4):290-295.

243. Fu C, Zhao D, Huang Y, Ma F: **Cellular aggregate size as the critical factor for flavonoid production by suspension cultures of *Saussurea medusa***. *Biotechnol Lett* 2005, **27**(2):91-95.

244. Kieran PM, MacLoughlin PF, Malone DM: **Plant cell suspension cultures: some engineering considerations**. *Journal of Biotechnology* 1997, **59**(1-2):39-52.

245. Trejo-Tapia G, Hernández-Trujillo R, Trejo-Espino JL, Jiménez-Aparicio A, Rodríguez-Monroy M: **Analysis of morphological characteristics of *Solanum chrysotrichum* cell suspension cultures**. *World J Microb Biot* 2003, **19**(9):929-932.

246. Pearson AP, Glennon B, Kieran PM: **Comparison of Morphological Characteristics of *Streptomyces natalensis* by Image Analysis and Focused Beam Reflectance Measurement**. *Biotechnol Progr* 2003, **19**(4):1342-1347.

247. Jeffers P, Raposo S, Lima-Costa M-E, Connolly P, Glennon B, Kieran PM: **Focussed beam reflectance measurement (FBRM) monitoring of particle size and morphology in suspension cultures of *Morinda citrifolia* and *Centaurea calcitrapa***. *Biotechnology Letters* 2003, **25**(23):2023-2028.

248. Rudolph G, Lindner P, Bluma A, Joeris K, Martinez G, Hitzmann B, Scheper T: **Optical Inline Measurement Procedures for Counting and Sizing Cells in Bioprocess Technology**. In: *Optical Sensor Systems in Biotechnology*. Edited by Rao G, vol. 116: Springer Berlin / Heidelberg; 2010: 125-142.

249. Ley I: **Assessing resolution and sensitivity in a laser diffraction particle size analyser**. *Am Lab* 2000, **32**(16):33-38.

250. Lehmann M, Berthold C, Pabst W, Gregorova E, Nickel KG: **Particle Size and Shape Characterization of Kaolins-Comparison of Settling Methods and Laser Diffraction**. *Key Engineering Methods* 2004, **264-268**:1387-1390.

132

251. Lin P-J, Scholz A, Krull R: **Effect of volumetric power input by aeration and agitation on pellet morphology and product formation of Aspergillus niger**. *Biochemical Engineering Journal* 2010, **49**(2):213-220.

252. Rønnest N, Stocks S, Lantz A, Gernaey K: **Comparison of laser diffraction and image analysis for measurement of *Streptomyces coelicolor* cell clumps and pellets**. *Biotechnol Lett* 2012, **34**(8):1465-1473.

253. Wucherpfennig T, Hestler T, Krull R: **Morphology engineering - Osmolality and its effect on *Aspergillus niger* morphology and productivity**. *Microb Cell Fact* 2011, **10**(58).

254. Kongsawadworakul P, Chrestin H: **Laser Diffraction: A New Tool for Identification and Studies of Physiological Effectors Involved in Aggregation-Coagulation of the Rubber Particles from *Hevea Latex***. *Plant and Cell Physiol* 2003, **44**(7):707-717.

255. Meijer JJ, ten Hoopen HJG, Luyben KCAM, Libbenga KR: **Effects of hydrodynamic stress on cultured plant cells: A literature survey**. *Enzyme Microb Technol* 1993, **15**(3):234-238.

256. Midler M, Finn RK: **A model system for evaluating shear in the design of stirred fermentors**. *Biotechnol Bioeng* 1966, **8**(1):71-84.

257. Mandels M: **The culture of plant cells**. In: *Advances in Biochemical Engineering, Volume 2*. vol. 2: Springer Berlin Heidelberg; 1972: 201-215.

258. Dunlop EH, Namdev PK, Rosenberg MZ: **Effect of fluid shear forces on plant cell suspensions**. *Chem Eng Sci* 1994, **49**(14):2263-2276.

259. Joshi JB, Elias CB, Patole MS: **Role of hydrodynamic shear in the cultivation of animal, plant and microbial cells**. *Chem Eng J and the Biochem Eng J* 1996, **62**(2):121-141.

260. Papoutsakis ET: **Fluid-mechanical damage of animal cells in bioreactors**. *Trends Biotechnol* 1991, **9**(1):427-437.

261. Kieran PM, MacLoughlin PF, Malone DM: **Plant cell suspension cultures: some engineering considerations**. *J Biotechnol* 1997, **59**(1-2):39-52.

262. Scragg AH, Allan EJ, Leckie F: **Effect of shear on the viability of plant cell suspensions**. *Enzyme Microb Technol* 1988, **10**(6):361-367.

263. Takeda T, Tamura M, Ohtaki M, Matsuoka H: **Gene expression in cultured strawberry cells subjected to hydrodynamic stress**. *Biochem Eng J* 2003, **15**(3):211-215.

264. Tanaka H: **Technological problems in cultivation of plant cells at high density**. *Biotechnol Bioeng* 1981, **23**(6):1203-1218.

265. Tanaka H, Semba H, Jitsufuchi T, Harada H: **The effect of physical stress on plant cells in suspension cultures**. *Biotechnol Lett* 1988, **10**(7):485-490.

266. Hooker BS, Lee JM, An G: **Response of plant tissue culture to a high shear environment**. *Enzyme Microb Technol* 1989, **11**(8):484-490.

267. Leckie F, Scraggs AH, Cliffe KR: **Effect of impeller design and speed on the large-scale cultivation of suspension cultures of *Catharanthus roseus***. *Enzyme Microb Technol* 1991, **13**(10):801-810.

268. Zhao D, Xing J, Li M, Lu D, Zhao Q: **Optimization of growth and jaceosidin production in callus and cell suspension cultures of *Saussurea medusa***. *Plant Cell Tiss Org* 2001, **67**(3):227-234.

269. Märkl H, Bronnenmeier R, Wittek B: **Hydrodynamische Belastbarkeit von Mikroorganismen**. *Chem-Ing-Tech* 1987, **59**(12):907-917.

270. Zhong C, Yuan Y-J: **Responses of *Taxus cuspidata* to hydrodynamics in bubble column bioreactors with different sparging nozzle sizes**. *Biochem Eng J* 2009, **45**(2):100-106.

271. Patterson Jr MK: **Measurement of growth and viability of cells in culture**. In: *Method Enzymol*. Edited by William B. Jakoby IHP, vol. Volume 58: Academic Press; 1979: 141-152.

272. Zilkah S, Gressel J: **The estimation of cell death in suspension cultures evoked by phytotoxic compounds: Differences among techniques**. *Plant Sci Lett* 1978, **12**(3–4):305-315.

273. Gilissen LJW, Hänisch ten Cate CH, Keen B: **A rapid method of determining growth characteristics of plant cell populations in batch suspension culture**. *Plant Cell Rep* 1983, **2**(5):232-235.

274. Patterson B, Murata T, Graham D: **Electrolyte Leakage Induced by Chilling in *Passiflora* Species Tolerant to Different Climates**. *Funct Plant Biol* 1976, **3**(4):435-442.

275. Widholm JM: **The Use of Fluorescein Diacetate and Phenosafranine for Determining Viability of Cultured Plant Cells**. *Biotech Histochem* 1972, **47**(4):189-194.
276. Towill LE, Mazur P: **Studies on the reduction of 2,3,5-triphenyltetrazolium chloride as a viability assay for plant tissue cultures**. *Can J Bot* 1975, **53**(11):1097-1102.
277. Cook JA, Mitchell JB: **Viability measurements in mammalian cell systems**. *Anal Biochem* 1989, **179**(1):1-7.
278. Jacyn Baker C, Mock NM: **An improved method for monitoring cell death in cell suspension and leaf disc assays using evans blue**. *Plant Cell Tiss Org* 1994, **39**(1):7-12.
279. Putnam KP, Bombick DW, Doolittle DJ: **Evaluation of eight in vitro assays for assessing the cytotoxicity of cigarette smoke condensate**. *Toxicol in Vitro* 2002, **16**(5):599-607.
280. Berridge MV, Tan AS: **Characterization of the cellular reduction of 3-(4,5-dimethylthiazol-2-yl)-2,5-diphenyltetrazolium bromide (MTT): subcellular localization, substrate dependence, and involvement of mitochondrial electron transport in MTT reduction**. *Arch Biochem Biophys* 1993, **303**(2):474-482.
281. Mosmann T: **Rapid colorimetric assay for cellular growth and survival: Application to proliferation and cytotoxicity assays**. *J Immunol Methods* 1983, **65**(1–2):55-63.
282. Stubberfield LCF, Shaw PJA: **A comparison of tetrazolium reduction and FDA hydrolysis with other measures of microbial activity**. *J Microbiol Meth* 1990, **12**(3–4):151-162.
283. Malinin TI, Perry VP: **A review of tissue and organ viability assay**. *Cryobiology* 1967, **4**(3):104-115.
284. Gamborg O, Miller R, Ojima K: **Nutrient Requirements of suspension cultures of soybean root cells**. *Exp Cell Res* 1986, **50**:151-158.
285. Huggett A, Nixon D: **Use of glucose oxidase, peroxidase, and O-dianisidine in determination of blood and urinary glucose**. *Lancet* 1957, **273**(6991):368-370.
286. Collins TJ: **ImageJ for microscopy**. *BioTechniques* 2007, **43**(1 Suppl):25-30.
287. Obert M, Pfeifer P, Sernetz M: **Microbial growth patterns described by fractal geometry**. *J Bacteriol* 1990, **172**(3):1180-1185.
288. Papagianni M: **Quantification of the fractal nature of mycelial aggregation in *Aspergillus niger* submerged cultures**. *Microb Cell Fact* 2006, **5**(5).
289. Ryoo D: **Fungal fractal morphology of pellet formation in *Aspergillus niger***. *Biotechnol Tech* 1999, **13**(1):33-36.
290. Barry DJ: **Relating Fractal Dimension to Branching Behaviour in Filamentous Microorganisms**. *ISAST Transactions on Electronics and Signal Processing* 2009, **4**(1):71 - 76.
291. Borys P, Krasowska M, Grzywna ZJ, Djamgoz MBA, Mycielska ME: **Lacunarity as a novel measure of cancer cells behavior**. *Biosystems* 2008, **94**(3):276-281.
292. Gould DJ, Vadakkan TJ, PochÉ RA, Dickinson ME: **Multifractal and Lacunarity Analysis of Microvascular Morphology and Remodeling**. *Microcirculation* 2011, **18**(2):136-151.
293. Smith Jr TG, Lange GD, Marks WB: **Fractal methods and results in cellular morphology — dimensions, lacunarity and multifractals**. *J Neurosci Meth* 1996, **69**(2):123-136.
294. **Fractal Dimension and Lacunarity** [http://rsbweb.nih.gov/ij/plugins/fraclac/fraclac.html]
295. Chow C, Kaneko T: **Automatic boundary detection of the left ventricle from cineangiograms**. *Comput Biomed Res* 1972, **5**(4):388-410.
296. **ISO 13320:2009 Particle Size Analysis - Laser Diffraction Methods. Part 1:General Principles**. *ISO Standards Authority* 2009.
297. Saveyn H, Mermuys D, Thas O, van der Meeren P: **Determination of the Refractive Index of Water-dispersible Granules for Use in Laser Diffraction Experiments**. *Part Part Syst Char* 2002, **19**(6):426-432.
298. Barnes HA: **Measuring the viscosity of large-particle (and flocculated) suspensions - a note on the necessary gap size of rotational viscometers**. *J Non-Newtonian Fluid Mech* 2000, **94**(2-3):213-217
299. Goudar CT, Strevett KA, Shah SN: **Influence of microbial concentration on the rheology of non-Newtonian fermentation broths**. *Appl Microbiol Biotechnol* 1999, **51**(3):310-315.
300. Caflisch RE: **Monte Carlo and quasi-Monte Carlo methods**. *Acta Numerica* 1998, **7**:1-49.
301. Ahamed A, Vermette P: **Effect of culture medium composition on *Trichoderma reesei's* morphology and cellulase production**. *Bioresour Technol* 2009, **100**(23):5979-5987.

134

302. Callow NV, Ju L-K: **Promoting pellet growth of *Trichoderma reesei* Rut C30 by surfactants for easy separation and enhanced cellulase production**. *Enzyme Microb Technol* 2012, **50**(6–7):311-317.

303. Ghojavand H, Bonakdarpour B, Heydarian SM, Hamedi J: **The inter-relationship between inoculum concentration, morphology, rheology and erythromycin productivity in submerged cultivation of *Saccharopolyspora erythraea***. *Braz J Chem Eng* 2011, **28**:565-574.

304. Singh K, Wangikar P, Jadhav S: **Correlation between pellet morphology and glycopeptide antibiotic balhimycin production by *Amycolatopsis balhimycina* DSM 5908**. *J Ind Microbiol Biotechnol* 2012, **39**(1):27-35.

305. Babič J, Pavko A: **Enhanced enzyme production with the pelleted form of *D. squalens* in laboratory bioreactors using added natural lignin inducer**. *J Ind Microbiol Biotechnol* 2012, **39**(3):449-457.

306. Liu Y-S, Wu J-Y: **Effects of Tween 80 and pH on mycelial pellets and exopolysaccharide production in liquid culture of a medicinal fungus**. *J Ind Microbiol Biotechnol* 2012, **39**(4):623-628.

307. Ding Z WQ, Peng L, Zhang L, Gu Z, Shi G, Zhang K: **Relationship between mycelium morphology and extracellular polysaccharide production of medicinal mushroom *Ganoderma lucidum* in submerged culture**. *J Med Plants Res* 2012, **6**:2868-2874.

308. Eck B: **Technische Strömungslehre**, 3 edn: Springer; 1949.

309. Mandelbrot BB: **The Fractal Geometry of Nature**. New York: W. H. Freeman and Co.; 1982.

310. Cutting J, Garvin J: **Fractal curves and complexity**. *Atten Percept Psycho* 1987, **42**(4):365-370.

311. Landini G: **Fractals in microscopy**. *J of Microsc* 2011, **241**(1):1-8.

312. Tolle CR, McJunkin TR, Rohrbaugh DT, LaViolette RA: **Lacunarity definition for ramified data sets based on optimal cover**. *Physica D* 2003, **179**(3-4):129-152.

313. Finkler L, Ginoris Y, Luna C, Alves T, Pinto J, Coelho M: **Morphological characterization of *Cupriavidus necator* DSM 545 flocs through image analysis**. *World J Microb Biot* 2007, **23**(6):801-808.

314. Hooley P, Fincham DA, Whitehead MP, Clipson NJW: **Fungal Osmotolerance**. In: *Adv Appl Microbiol*. Edited by Allen I. Laskin JWB, Geoffrey MG, vol. Volume 53: Academic Press; 2003: 177-211.

315. Griffin DH: **Fungal Physiology**, 2 edn. New York.: Wiley-Liss; 1994.

316. Beever RE, Laracy EP: **Osmotic adjustment in the filamentous fungus *Aspergillus nidulans***. *J Bacteriol* 1986, **168**(3):1358-1365.

317. Tresner HD, Hayes JA: **Sodium chloride tolerance of terrestrial fungi**. *Appl Microbiol* 1971, **22**(2):210-213.

318. Money NP: **Wishful Thinking of Turgor Revisited: The Mechanics of Fungal Growth**. *Fungal Genet Biol* 1997, **21**(2):173-187.

319. Clipson NJW, Jennings DH: ***Dendryphiella salina* and *Debaryomyces hansenii*: models for ecophysiological adaptation to salinity by fungi which grow in the sea**. *Can J Bot* 1992(70):2097 - 2105.

320. Emmler M, Jungebloud A, Göcke Y, Cordes C, Horn H, Hempel DC: **Apparent Delay of Product Secretion by Product Adsorption in *Aspergillus niger***. *Eng Life Sci* 2006, **6**(5):488-491.

321. Calderntorres M, Thomé PE: **Subcellular level variation in protein accumulation of the halophylic yeast *Debaryomyces hansenii* grown under conditions of high osmolarity**. *J of Basic Microb* 2001, **41**(5):231-240.

322. Rodríguez-Navarro A: **Potassium transport in fungi and plants**. *Biochimica et Biophysica Acta (BBA) - Reviews on Biomembranes* 2000, **1469**(1):1-30.

323. Park J-C, Matsuoka H, Takatori K, Kurata H: **Adaptation of *Aspergillus niger* to acidic conditions and its relationship to salt stress and miconazole**. *Mycol Res* 1996, **100**(7):869-874.

324. Park J-C, Nemoto Y, Homma T, Jing W, Chen Y, Matsuoka H, Ohno H, Takatori K, Kurata H: **Adaptation of *Aspergillus niger* to short-term salt strees**. *Appl Microbiol Biotechnol* 1993, **40**(2):394-398.

325. Kim Y, Nandakumar MP, Marten MR: **Proteome map of *Aspergillus nidulans* during osmoadaptation**. *Fungal Genet Biol* 2007, **44**(9):886-895.

326. Kralj Kuncic M, Kogej T, Drobne D, Gunde-Cimerman N: **Morphological Response of the Halophilic Fungal Genus *Wallemia* to High Salinity**. *Appl Environ Microbiol* 2010, **76**(1):329-337.

327. Förster C, Marienfeld S, Wendisch F, Krämer R: **Adaptation of the filamentous fungus *Ashbya gossypii* to hyperosmotic stress: different osmoresponse to NaCl and mannitol stress**. *Appl Microbiol Biotechnol* 1998, **50**(2):219-226.

328. Choy V, Patel N, Thibault J: **Application of image analysis in the fungal fermentation of *Trichoderma reesei* RUT-C30**. *Biotechnol Progr* 2011, **27**(6):1544-1553.

329. Sitanggang AB, Wu H-S, Wang SS, Ho Y-C: **Effect of pellet size and stimulating factor on the glucosamine production using *Aspergillus* sp. BCRC 31742**. *Bioresour Technol* 2010, **101**(10):3595-3601.

330. Tepwong P, Giri A, Ohshima T: **Effect of mycelial morphology on ergothioneine production during liquid fermentation of *Lentinula edodes***. *Mycoscience* 2012, **53**(2):102-112.

331. Dobson L, O'Cleirigh C, O'Shea D: **The influence of morphology on geldanamycin production in submerged fermentations of *Streptomyces hygroscopicus* & *var.geldanus***. *Appl Microbiol Biotechnol* 2008, **79**(5):859-866.

332. Amanullah A, Blair R, Nienow AW, Thomas CR: **Effects of Agitation Intensity on Mycelial Morphology and Protein Production in Chemostat Cultures of Recombinant *Aspergillus oryzae***. *Biotechnol Bioeng* 1999, **62**(4):434-446.

333. Müller C, McIntyre M, Hansen K, Nielsen J: **Metabolic Engineering of the Morphology of *Aspergillus oryzae* by Altering Chitin Synthesis**. *Appl Environ Microbiol* 2002, **68**(4):1827-1836.

334. Jones CL, Lonergan GT: **Prediction of phenol-oxidase expression in a fungus using the Fractal Dimension**. *Biotechnol Lett* 1997, **19**(1):65-69.

335. Spohr A, Carlsen M, Nielsen J, Villadsen J: **Morphological characterization of recombinant strains of *Aspergillus oryzae* producing alpha-amylase during batch cultivations**. *Biotechnol Lett* 1997, **19**(3):257-262.

336. O'Mahony RJ, Burns ATH, Millam S, Hooley P, Fincham DA: **Isotropic growth of spores and salt tolerance in *Aspergillus nidulans***. *Mycol Res* 2002, **106**(12):1480-1486.

337. Trinci AP: **A kinetic study of the growth of *Aspergillus nidulans* and other fungi**. *J Gen Microbiol* 1969, **57**(1):11-24.

338. Dantigny P, Bensoussan M, Vasseur V, Lebrihi A, Buchet C, Ismaili-Alaoui M, Devlieghere F, Roussos S: **Standardisation of methods for assessing mould germination: A workshop report**. *Int J Food Microbiol* 2006, **108**(2):286-291.

339. Judet D, Bensoussan M, Perrier-Cornet J-M, Dantigny P: **Distributions of the growth rate of the germ tubes and germination time of *Penicillium chrysogenum* conidia depend on water activity**. *Food Microbiol* 2008, **25**(7):902-907.

340. Araujo R, Rodrigues AG: **Variability of Germinative Potential among Pathogenic Species of *Aspergillus***. *J Clin Microbiol* 2004, **42**(9):4335-4337.

341. Barrios-González J, Martínez C, Aguilera A, Raimbault M: **Germination of concentrated suspensions of spores from *Aspergillus niger***. *Biotechnol Lett* 1989, **11**(8):551-554.

342. Hobot JA, Gull K: **The identification of a self-inhibitor from *Syncephalastrum racemosum* and its effect upon sporangiospore germination**. *Antonie van Leeuwenhoek* 1980, **46**(5):435-441.

343. Chitarra GS, Abee T, Rombouts FM, Posthumus MA, Dijksterhuis J: **Germination of *Penicillium paneum* Conidia Is Regulated by 1-Octen-3-ol, a Volatile Self-Inhibitor**. *Appl Environ Microbiol* 2004, **70**(5):2823-2829.

344. Lu X, Sun J, Nimtz M, Wissing J, Zeng A-P, Rinas U: **The intra- and extracellular proteome of *Aspergillus niger* growing on defined medium with xylose or maltose as carbon substrate**. *Microb Cell Fact* 2010, **9**(1):23.

345. Mitard A, Riba JP: **Rheological properties of *Aspergillus niger* pellet suspensions**. *Appl Microbiol Biotechnol* 1986, **25**(3):245-249.

346. Schügerl K, Gerlach SR, Siedenberg D: **Influence of the process parameters on the morphology and enzyme production of *Aspergilli***. *Adv Biochem Eng/Biotechnol* 1998, **60**:195-266.

347. Kolewe M: **Development of Plant Cell Culture Processes to Produce Natural Product Pharmaceuticals: Characterization, Analysis, and Modeling of Plant Cell Aggregation**. Amherst: University of Massachusetts; 2011.

348. Pépin M, Smith M, Reid J: **Application of imaging tools to plant cell culture: Relationship between plant cell aggregation and flavonoid production**. *In Vitro Cell Dev-Pl* 1999, **35**(4):290-295.

349. Ryu DDY, Lee SO, Romani RJ: **Determination of growth rate for plant cell cultures: Comparative studies**. *Biotechnol Bioeng* 1990, **35**(3):305-311.

350. Wilson JD, Bechtel DB, Todd TC, Seib PA: **Measurement of Wheat Starch Granule Size Distribution Using Image Analysis and Laser Diffraction Technology**. *Cereal Chem* 2006, **83**(3):259-268.

351. Rawle A: **Basic principles of particle size analysis**. *Surface coatings international Part A, Coatings journal* 2003, **86**(2):58-65.

352. Matsuyama T, Yamamoto H, Scarlett B: **Transformation of Diffraction Pattern due to Ellipsoids into Equivalent Diameter Distribution for Spheres**. *Part Part Syst Char* 2000, **17**(2):41-46.

353. O'Brien J, Wilson I, Orton T, Pognan F: **Investigation of the Alamar Blue (resazurin) fluorescent dye for the assessment of mammalian cell cytotoxicity**. *Eur J Biochem* 2000, **267**(17):5421-5426.

354. DeBaun RM, de Stevens G: **On the mechanism of enzyme action. XLIV. Codetermination of resazurin and resorufin in enzymatic dehydrogenation experiments**. *Arch Biochem Biophys* 1951, **31**(2):300-308.

355. Byth H-A, McHunu BI, Dubery IA, Bornman L: **Assessment of a simple, non-toxic alamar blue cell survival assay to monitor tomato cell viability**. *Phytochemical Anal* 2001, **12**(5):340-346.

356. Kalina M, Palmer JM: **The reduction of tetrazolium salts by plant mitochondria**. *Histochemistry and Cell Biology* 1968, **14**(4):366-374.

357. Nociari MM, Shalev A, Benias P, Russo C: **A novel one-step, highly sensitive fluorometric assay to evaluate cell-mediated cytotoxicity**. *J Immunol Methods* 1998, **213**(2):157-167.

358. Baker C, Banerjee S, Tenover F: **Evaluation of Alamar colorimetric MIC method for antimicrobial susceptibility testing of gram-negative bacteria.** *J Clin Microbiol* 1994, **32**(5):1261–1267.

359. Collins L, Franzblau S: **Microplate Alamarblue assay versus BACTEC 460 system for high-throughput screening of compounds against *Mycobacterium tuberculosis* and *Mycobacterium avium***. *Antimicrob Agents Chemother* 1997, **41**(5):1004-1009.

360. Larson EM, Doughman DJ, Gregerson DS, Obritsch WF: **A new, simple, nonradioactive, nontoxic in vitro assay to monitor corneal endothelial cell viability**. *Investigative Ophthalmology & Visual Science* 1997, **38**(10):1929-1933.

361. Pfaller M, Grant C, Morthland V, Rhine-Chalborg J: **Comparative evaluation of alternative methods for broth dilution susceptibility testing of fluconazole against *Candida albicans***. *J Clin Microbiol* 1994, **32**(2):506-509.

362. White M, DiCaprio M, Greenberg D: **Assessment of neuronal viability with Alamar blue in cortical and granule cell cultures.** *J Neurosci Methods* 1996, **70**(2).

363. Ibaraki Y, Kenji K: **Application of image analysis to plant cell suspension cultures**. *Comput Electron Agr* 2001, **30**(1-3):193-203.

364. Remotti PC, Löffler HJM: **Callus induction and plant regeneration from gladiolus**. *Plant Cell Tiss Org* 1995, **42**(2):171-178.

365. Smith MAL, Reid JF, Hansen AC, Li Z, Madhavi DL: **Non-destructive machine vision analysis of pigment-producing cell cultures**. *J Biotechnol* 1995, **40**(1):1-11.

366. Gibson D, Ketchum R, Vance N, Christen A: **Initiation and growth of cell lines of *Taxus brevifolia* (Pacific yew)**. *Plant Cell Rep* 1993, **12**(9):479-482.

367. Bruňáková K, Babincová Z, Čellárová E: **Selection of Callus Cultures of *Taxus baccata* L. as a Potential Source of Paclitaxel Production**. *Eng Life Sci* 2004, **4**(5):465-469.

368. Bruňáková K, Babincová Z, Čellárová E: **Production of taxanes in callus and suspension cultures of *Taxus baccata L***. In: *Liquid Culture Systems for in vitro Plant Propagation.* Edited by Hvoslef-Eide A, Preil W: Springer Netherlands; 2005: 567-574.

369. Wickremesinhe ERM, Arteea RN: **Taxus callus cultures: Initiation, growth optimization, characterization and taxol production**. *Plant Cell Tiss Org* 1993, **35**(2):181-193.

370.   Fett-Neto AG, Zhang WY, Dicosmo F: **Kinetics of taxol production, growth, and nutrient uptake in cell suspensions of *Taxus cuspidata***. *Biotechnol Bioeng* 1994, **44**(2):205-210.

371.   Kolewe ME, Gaurav V, Roberts SC: **Pharmaceutically Active Natural Product Synthesis and Supply via Plant Cell Culture Technology**. *Molecular Pharmaceutics* 2008, **5**(2):243-256.

372.   Eslahpazir Esfandabadi M, Wucherpfennig T, Krull R: **Agitation Induced Mechanical Stress in Stirred Tank Bioreactors-Linking CFD Simulations to Fungal Morphology**. *J Chem Eng Jpn* 2012, **45**(9):742-748.

373.   Mahnke EU, Büscher K, Hempel DC: **A Novel Approach for the Determination of Mechanical Stresses in Gas-Liquid Reactors**. *Chem Eng Technol* 2000, **23**(6):509-513.

374.   Pilz RD, Hempel DC: **Mechanical stress on suspended particles in two- and three-phase airlift loop reactors and bubble columns**. *Chem Eng Sci* 2005, **60**(22):6004-6012.

# Nomenclature

| | |
|---|---|
| A | projected area |
| AB | Alamar Blue |
| BDW | bio dry weight |
| BDWI | bio dry weight integral |
| C | morphological parameter compactness |
| D | fractal dimension |
| $D_F$ | Feret's diameter |
| d | maximal diameter |
| $D_{BM}$ | box mass dimension |
| $D_{BM}/D_{BS}$ | fractal quotient |
| $D_{BS}$ | box surface dimension |
| E | elongation or aspect ratio of a particle |
| ε | grid width |
| FOS | fructooligosaccharides |
| g | location of a box (Box counting method) |
| K | consistency index (Ostwald–de Waele model) |
| $K_{BDW}$ | biomass independent consistency coefficient |
| Λ | lacunarity |
| λ | wave length |
| $L_{HGU}$ | mean length of hyphal growth unit [μm] |
| MN | Morphology number |
| μ | mean pixels per box |

n                    flow behavior index (Ostwald–de Waele model)

$n_{BDW}$                    biomass independent flow behavior coefficient

$N(\varepsilon)$                    number of overlapping boxes (fractal analysis, box counting method)

R                    morphological parameter roughness

S                    solidity

$\sigma$                    standard deviation of pixels per box

SMD                    Sauter mean diameter

$\gamma$                    shear rate

$\varepsilon$                    width of the grid (fractal analysis, box counting method)

$\eta_{app}$                    apparent viscosity

$\tau$                    shear stress

**Band 1**  **Sunder, Matthias**: Oxidation grundwasserrelevanter Spurenverunreinigungen mit Ozon und Wasserstoffperoxid im Rohrreaktor. 1996. FIT-Verlag · Paderborn, ISBN 3-932252-00-4

**Band 2**  **Pack, Hubertus**: Schwermetalle in Abwasserströmen: Biosorption und Auswirkung auf eine schadstoffabbauende Bakterienkultur. 1996. FIT-Verlag · Paderborn, ISBN 3-932252-01-2

**Band 3**  **Brüggenthies, Antje**: Biologische Reinigung EDTA-haltiger Abwässer. 1996. FIT-Verlag · Paderborn, ISBN 3-932252-02-0

**Band 4**  **Liebelt, Uwe**: Anaerobe Teilstrombehandlung von Restflotten der Reaktivfärberei. 1997. FIT-Verlag · Paderborn, ISBN 3-932252-03-9

**Band 5**  **Mann, Volker G.**: Optimierung und Scale up eines Suspensionsreaktorverfahrens zur biologischen Reinigung feinkörniger, kontaminierter Böden. 1997. FIT-Verlag · Paderborn, ISBN 3-932252-04-7

**Band 6**  **Boll Marco**: Einsatz von Fuzzy-Control zur Regelung verfahrenstechnischer Prozesse. 1997. FIT-Verlag · Paderborn, ISBN 3-932252-06-3

**Band 7**  **Büscher, Klaus**: Bestimmung von mechanischen Beanspruchungen in Zweiphasenreaktoren. 1997. FIT-Verlag · Paderborn, ISBN 3-932252-07-1

**Band 8**  **Burghardt, Rudolf**: Alkalische Hydrolyse – Charakterisierung und Anwendung einer Aufschlußmethode für industrielle Belebtschlämme. 1998. FIT-Verlag · Paderborn, ISBN 3-932252-13-6

**Band 9**  **Hemmi, Martin**: Biologisch-chemische Behandlung von Färbereiabwässern in einem Sequencing Batch Process. 1999. FIT-Verlag · Paderborn, ISBN 3-932252-14-4

**Band 10**  **Dziallas, Holger**: Lokale Phasengehalte in zwei- und dreiphasig betriebenen Blasensäulenreaktoren. 2000. FIT-Verlag · Paderborn, ISBN 3-932252-15-2

**Band 11**  **Scheminski, Anke**: Teiloxidation von Faulschlämmen mit Ozon. 2001. FIT-Verlag · Paderborn, ISBN 3-932252-16-0

**Band 12**  **Mahnke, Eike Ulf**: Fluiddynamisch induzierte Partikelbeanspruchung in pneumatisch gerührten Mehrphasenreaktoren. 2002. FIT-Verlag · Paderborn, ISBN 3-932252-17-9

**Band 13**  **Michele, Volker**: CDF modeling and measurement of liquid flow structure and phase holdup in two- and three-phase bubble columns. 2002. FIT-Verlag · Paderborn, ISBN 3-932252-18-7

**Band 14**  **Wäsche, Stefan**: Einfluss der Wachstumsbedingungen auf Stoffübergang und Struktur von Biofilmsystemen. 2003. FIT-Verlag ·Paderborn, ISBN3-932252-19-5

**Band 15**  **Krull Rainer**: Produktionsintegrierte Behandlung industrieller Abwässer zur Schließung von Stoffkreisläuren.2003.FIT-Verlag·Paderborn, ISBN3-932252-20-9

**Band 16**  **Otto, Peter**: Entwicklung eines chemisch-biologischen Verfahrens zur Reinigung EDTA enthaltender Abwässer. 2003. FIT-Verlag ·Paderborn, ISBN3-932252-21-7

**Band 17**  **Horn, Harald**: Modellierung von Stoffumsatz und Stofftransport in Biofilmsystemen. 2003. FIT-Verlag · Paderborn, ISBN 3-932252-22-5

**Band 18**  **Mora Naranjo, Nelson**: Analyse und Modellierung anaerober Abbauprozesse in Deponien. 2004. FIT-Verlag · Paderborn, ISBN 3-932252-23-3

**Band 19**  **Döpkens, Eckart**: Abwasserbehandlung und Prozesswasserrecycling in der Textilindustrie. 2004. FIT-Verlag · Paderborn, ISBN 3-932252-24-1

**Band 20**  **Haarstrick, Andreas**: Modellierung millieugesteuerter biologischer Abbauprozesse in heterogenen problembelasteten Systemen. 2005. FIT-Verlag · Paderborn, ISBN 3-932252-27-6

**Band 21**  **Baaß, Anne-Christina**: Mikrobieller Abbau der Polyaminopolycarbonsäuren Propylendiamintetraacetat (PDTA) und Diethylentriaminpentaacetat (DTPA). 2004. FIT-Verlag · Paderborn, ISBN 3-932252-26-8

**Band 22**  **Staudt, Christian**: Entwicklung der Struktur von Biofilmen. 2006. FIT-Verlag · Paderborn, ISBN 3-932252-28-4

**Band 23**  **Pilz, Roman Daniel**: Partikelbeanspruchung in mehrphasig betriebenen Airlift-Reaktoren. 2006. FIT-Verlag · Paderborn, ISBN 3-932252-29-2

**Band 24**  **Schallenberg, Jörg**: Modellierung von zwei- und dreiphasigen Strömungen in Blasensäulenreaktoren. 2006. FIT-Verlag · Paderborn, ISBN 3-932252-30-6

**Band 25**  **Enß, Jan Hendrik**: Einfluss der Viskosität auf Blasensäulenströmungen. 2006. FIT-Verlag · Paderborn, ISBN 3-932252-31-4

**Band 26**  **Kelly, Sven**: Fluiddynamischer Einfluss auf die Morphogenese von Biopellets filamentöser Pilze. 2006. FIT-Verlag · Paderborn, ISBN 3-932252-32-2

**Band 27**  **Grimm, Luis Hermann**: Sporenaggregationsmodell für die submerse Kultivierung koagulativer Myzelbildner. 2006. FIT-Verlag · Paderborn, ISBN 3-932252-33-0

**Band 28**  **León Ohl, Andrés**: Wechselwirkungen von Stofftransport und Wachstum in Biofilsystemen. 2007. FIT-Verlag · Paderborn, ISBN 3-932252-34-9

**Band 29**  **Emmler, Markus**: Freisetzung von Glucoamylase in Kultivierungen mit *Aspergillus niger*. 2007. FIT-Verlag · Paderborn, ISBN 3-932252-35-7

**Band 30**  **Leonhäuser, Johannes**: Biotechnologische Verfahren zur Reinigung von quecksilberhaltigem Abwasser. 2007. FIT-Verlag · Paderborn, ISBN 3-932252-36-5

**Band 31**   **Jungebloud, Anke**: Untersuchung der Genexpression in *Aspergillus niger* mittels Echtzeit-PCR. 1996. FIT-Verlag · Paderborn, ISBN 978-3-932252-37-2

**Band 32**   **Hille, Andrea**: Stofftransport und Stoffumsatz in filamentösen Pilzpellets. 2008. FIT-Verlag · Paderborn, ISBN 978-3-932252-38-9

**Band 33**   **Fürch, Tobias**: Metabolic characterization of recombinant protein production in *Bacillus megaterium*. 2008. FIT-Verlag · Paderborn, ISBN 978-3-932252-39-6

**Band 34**   **Grote, Andreas Georg**: Datenbanksysteme und bioinformatische Werkzeuge zur Optimierung biotechnologischer Prozesse mit Pilzen. 2008. FIT-Verlag · Paderborn, ISBN 978-3-932252-40-120

**Band 35**   **Möhle, Roland Bernhard**: An Analytic-Synthetic Approach Combining Mathematical Modeling and Experiments – Towards an Understanding of Biofilm Systems. 2008. FIT-Verlag · Paderborn, ISBN 978-3-932252-41-9

**Band 36**   **Reichel, Thomas**: Modelle für die Beschreibung das Emissionsverhaltens von Siedlungsabfällen. 2008. FIT-Verlag · Paderborn, ISBN 978-3-932252-42-6

**Band 37**   **Schultheiss, Ellen**: Charakterisierung des Exopolysaccharids PS-EDIV von *Sphingomonas pituitosa*. 2008. FIT-Verlag · Paderborn, ISBN 978-3-932252-43-3

**Band 38**   **Dreger, Michael Andreas**: Produktion und Aufarbeitung des Exopolysaccharids PS-EDIV aus *Sphingomonas pituitosa*. 1996. FIT-Verlag · Paderborn, ISBN 978-3-932252-44-0

**Band 39**   **Wiebels, Cornelia**: A Novel Bubble Size Measuring Technique for High Bubble Density Flows. 2009. FIT-Verlag · Paderborn, ISBN 978-3-932252-45-7

**Band 40**   **Bohle, Kathrin**: Morphologie- und produktionsrelevante Gen- und Proteinexpression in submersen Kultivierungen von *Aspergillus niger*. 2009. FIT-Verlag · Paderborn, ISBN 978-3-932252-46-2

**Band 41**   **Fallet, Claas**: Reaktionstechnische Untersuchungen der mikrobiellen Stressantwort und ihrer biotechnologischen Anwendungen. 2009. FIT-Verlag · Paderborn, ISBN 978-3-932252-47-1

**Band 42**   **Vetter, Andreas**: Sequential Co-simulation as Method to Couple CFD and Biological Growth in a Yeast. 2009. FIT-Verlag · Paderborn, ISBN 978-3-932252-48-8

**Band 43**   **Jung, Thomas**:  Einsatz chemischer Oxidationsverfahren zur Behandlung industrieller Abwässer. 2010. FIT-Verlag· Paderborn, ISBN 978-3-932252-49-5

**Band 45**   **Herrmann, Tim**: Transport von Proteinen in Partikeln der Hydrophoben Interaktions Chromatographie. 2010. FIT-Verlag · Paderborn, ISBN 978-3-932252-51-8

**Band 46** **Becker, Judith**: Systems Metabolic Engineering of *Corynebacterium glutamicum* towards improved Lysine Prodction. 2010. Cuvillier-Verlag · Göttingen, ISBN 978-3-86955-426-6

**Band 47** **Melzer, Guido**: Metabolic Network Analysis of the Cell Factory *Aspergillus niger*. 2010. Cuvillier-Verlag · Göttingen, ISBN 978-3-86955-456-3

**Band 48** **Bolten J., Christoph**: Bio-based Production of L-Methionine in *Corynebacterium glutamicum*. 2010. Cuvillier-Verlag · Göttingen, ISBN 978-3-86955-486-0

**Band 49** **Lüders, Svenja**: Prozess- und Proteomanalyse gestresster Mikroorganismen. 2010. Cuvillier-Verlag · Göttingen, ISBN 978-3-86955-435-8

**Band 50** **Wittmann, Christoph**: Entwicklung und Einsatz neuer Tools zur metabolischen Netzwerkanalyse des industriellen Aminosäure-Produzenten *Corynebacterium glutamicum*. 2010. Cuvillier-Verlag · Göttingen, ISBN 978-3-86955-445-7

**Band 51** **Edlich, Astrid**: Entwicklung eines Mikroreaktors als Screening-Instrument für biologische Prozesse. 2010. Cuvillier-Verlag · Göttingen, ISBN 978-3-86955-470-9

**Band 52** **Hage, Kerstin**: Bioprozessoptimierung und Metabolomanalyse zur Proteinproduktion in *Bacillus licheniformis*. 2010. Cuvillier-Verlag · Göttingen, ISBN 978-3-86955-578-2

**Band 53** **Kiep, Katina Andrea**: Einfluss von Kultivierungsparametern auf die Morphologie und Produktbildung von *Aspergillus niger*. 2010. Cuvillier-Verlag · Göttingen, ISBN 978-3-86955-632-1

**Band 54** **Fischer, Nicole**: Experimental investigations on the influence of physico-chemical parameters on anaerobic degradation in MBT residual waste. 2011. Cuvillier-Verlag · Göttingen, ISBN 978-3-86955-679-6

**Band 55** **Schädel, Friederike**: Stressantwort von Mikroorganismen. 2011. Cuvillier-Verlag · Göttingen, ISBN 978-3-86955-746-5

**Band 56** **Wichter, Johannes**: Untersuchung der L-Cystein-Biosynthese in *Escherichia coli* mit Techniken der Metabolom- und $^{13}$C-Stoffflussanalyse. 2011. Cuvillier-Verlag · Göttingen, ISBN 978-3-86955-750-2

**Band 57** **Knappik, Irena Isabell**: Charakterisierung der biologischen und chemischen Reaktionsprozesse in Siedlungsabfällen. 2011. Cuvillier-Verlag · Göttingen, ISBN 978-3-86955-760-1

**Band 58** **Driouch, Habib**: Systems biotechnology of recombinant protein production in *Aspergillus niger*. 2011. Cuvillier-Verlag Göttingen, ISBN 978-3-86955-808-0

**Band 59** **Gehder, Matthias:** Development and Validation of Indicators for the Production and Quality of Seed Cultures. 2011. Cuvillier-Verlag Göttingen, ISBN 978-3-86955-847-9

**Band 60** **Sommer, Becky:** Methodenentwicklung zur Charakterisierung sporenbildender Pilz-Seedingkulturen. 2011. Cuvillier-Verlag Göttingen, ISBN 978-3-86955-851-6

**Band 61** **Dohnt, Katrin:** Charakterisierung von *Pseudomonas aeruginosa*-Biofilmen in einem *in vitro*-Harnwegskathetersystem. 2011. Cuvillier-Verlag Göttingen, ISBN 978-3-86955-852-3

**Band 62** **Greis, Tillman:** Modelling the risk of chlorinated hydrocarbons in urban groundwater. 2011. Cuvillier-Verlag Göttingen, ISBN 978-3-86955-970-4

**Band 63** **David, Florian:** Holistic bioprocess engineering of antibody fragment secreting *Bacillus megaterium*. 2012. Cuvillier-Verlag Göttingen, ISBN 978-3-95404-115-2

**Band 64** **Palme, Wiebke:** Taxonomische Einordnung des Polyaminopolycarbonsäure-abbauenden Stammes BNC1 und Untersuchungen zum Abbau von 1,3 Propylendiamintetraacetat. 2012. Cuvillier-Verlag Göttingen, ISBN 978-3-95404-158-9

**Band 65** **Lin, Pey-Jin:** Effect of fluid dynamics on pellet morphology and product formation of *Aspergillus niger*. 2012. Cuvillier-Verlag Göttingen, ISBN 978-3-95404-181-7

**Band 66** **Kind, Stefanie:** Synthetic Metabolic Engineering of *Corynebacterium glutamicum* for Bio-based Production of 1,5-Diaminopentane. 2012. Cuvillier-Verlag Göttingen, ISBN 978-3-95404-264-7

**Band 67** **Wilk, Franziska:** Charakterisierung von Stoffströmen vorbehandelter Siedlungsabfälle in Deponiebioreaktoren. 2012. Cuvillier-Verlag Göttingen, ISBN 978-3-95404-281-4

**Band 68** **Korneli, Claudia:** Target-oriented Bioprocess Optimization for Recombinant Protein Production in *Bacillus megaterium*. 2012. Cuvillier-Verlag Göttingen, ISBN 978-3-95404-289-0

**Band 69** **Eslahpazir Esfandabadi, Manely:** Numerical Characterization of Mechanical Stress and Flow Patterns in Stirred Tank Bioreactors. 2013. Cuvillier-Verlag Göttingen, ISBN 978-3-95404-449-8